2016

DESIGN AND SIMULATION OF A RESIDENTIAL PV-BATTERY SYSTEM

Sevket Burak Ovali
Michigan Technological University, sbovali@mtu.edu

DESIGN AND SIMULATION OF A RESIDENTIAL PV-BATTERY SYSTEM

By

Sevket Burak Ovali

A THESIS

Submitted in partial fulfillment of the requirements for the degree of

MASTER OF SCIENCE

In Electrical Engineering

MICHIGAN TECHNOLOGICAL UNIVERSITY

2016

This thesis has been approved in partial fulfillment of the requirements for the Degree of MASTER OF SCIENCE in Electrical Engineering.

Department of Electrical and Computer Engineering

Thesis Advisor: *Assistant Professor Lucia Gauchia*

Committee Member: *Assistant Professor Sumit Paudyal*

Committee Member: *Associate Professor Joshua M. Pearce*

Department Chair: *Professor Daniel R. Fuhrmann*

Table of Contents

List of Figures

List of Tables

Acknowledgement

I would particularly like to appreciate my thesis advisor Assistant Professor Lucia Gauchia. Her office door was always opened whenever I met a problem or had a question about my research. She consistently provided guidance me in the right direction whenever she thought I needed it. During my research, she always stands behind me whenever I ran into not only trouble about my research but also a problem about my life. I will always remember her unforgettable assistances and remain grateful forever.

Also, I want to thank the moral support from my wife throughout my research of period. We always support each other against all negative conditions. My wife and I completed each other in this research as usual.

Finally, I would like to appreciate prayers from my parents. Even if they are not with me in here, I always feel their prayers behind me during my life and master education.

Abstract

This thesis provides the design and simulation of a stand-alone photovoltaic (PV) system to ensure the load demands for a single residential in Houghton (MI) and Tucson (AZ). The fundamental activities of this study aim to model for particular stand-alone photovoltaic of components. Entire stand-alone design stages for used load data sets are carried out. Daily irradiance and load data are taken into consideration throughout the design stages. The Simulink program is developed to obtain simulation results to observe PV system and battery behaviors regarding various months which have most various irradiances throughout 30 days. Sizing of PV systems is conducted for Tucson and Houghton separately.

1 Introduction

Solar energy is a commonly used renewable energy since it is free, plentiful, and pollution free during operation [1]. Renewable Energy resources are attractive among electrical power resources because they bring a more advantages in terms of environment. In addition, residential PV system installation are increasing day-by-day (Figure 1). It is approximated that 80% of all photovoltaic systems (PV) are used in off grid (stand-alone) implementation [2]. Many countries have a roadmap to rise renewable energy and decrease global warming effects against the increasing energy demand. For instance, Austria, Finland, Sweden and Australia have targets to reach 34%, 38%, 49 % and 20 % of overall energy usage from renewables by 2020 [3]. Moreover, solar panel prices have been decreasing during last 35 years. The solar panel prices dropped from \$75/Watt to almost \$0.75/Watt [4]. In contrast, fossil fuel such as the cost of coal has increased a 13% since 2008. So PV installations are recently becoming more popular, with data showing they have increased a 50% annually during the last five years. This percentage will get to 80% in the following years. [4]

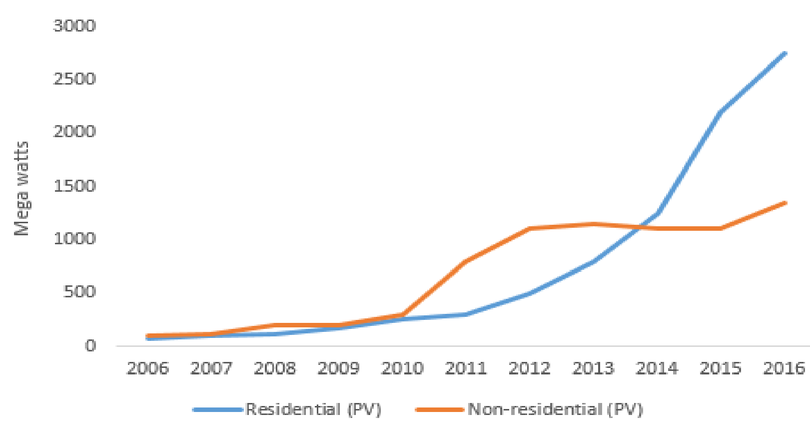

Figure 1-Yearly U.S Photovoltaic PV installation[5]

Furthermore, generated power from a PV system depends on weather conditions, as it does not produce electricity during the night or during highly cloudy period [6]. Therefore, energy storage (in particular in this Thesis batteries), is needed to power the load when PV does not generate enough electricity. A conventional stand-alone PV system usually comprises of PV arrays, energy storage (batteries) that is a very significant part of stand-alone PV systems, power conversion system (DC/DC converter and AC/DC inverter), and an energy management system.

2 Methodology

Relevant power components related to the off-grid PV/storage residential system such as, PV, electrical storage (battery banks), maximum power point tracking (MPPT), and battery charge controller have been modeled by using MATLAB® /Simulink. The fundamental structure of PV a system is given below (Figure 2).

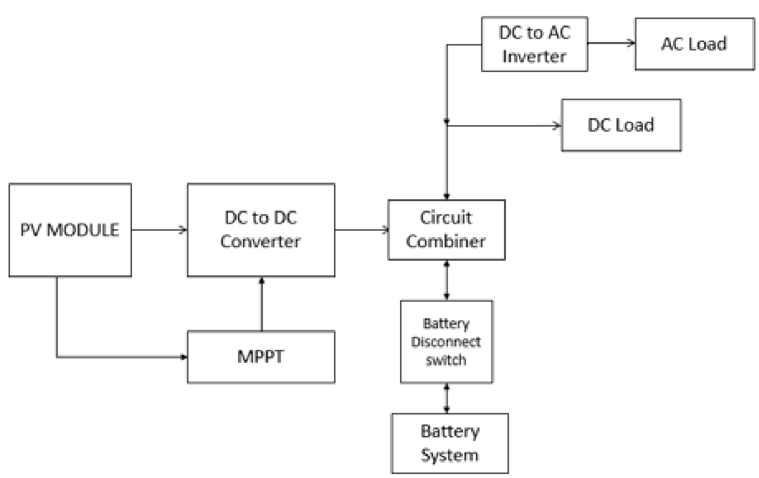

Figure 2-Structure of PV Residential System

The model does not take into considering DC to AC inverter influence because the efficiency of inverters varies between 80% and 95% [7]. If we use the most efficient inverter, there is almost no loss [8]. Therefore, the inverter efficiency was ignored in this study. Two cities were selected by looking to the best and worst insolation areas in the United States [9]. Two cities residential load and irradiance data are collected and analyzed in this study. [10] A stand-alone PV system was sized by determining load requirement for each city [8]. Then, the battery and array sizing were committed to the meet load demand [11]. The stand-alone PV system was analyzed to size it correctly and the battery, PV, and load behavior during the most variable and critical month for two cities (Houghton MI, Tucson AZ) in the United States.

3 Photovoltaic System (PV)

Photovoltaic (PV) systems are used to convert solar energy to electricity. Photovoltaic tools produce electricity directly from sunlight through an electronics process that occurs naturally in semiconductor materials. PV devices can be found in applications such as a calculator, road signs, transportation, home and commercial. Solar cell efficiency is still challenging due to the reflected light and, losses in the conversion process. [12]. The basic structure of a photovoltaic cell is shown below in Figure 3.

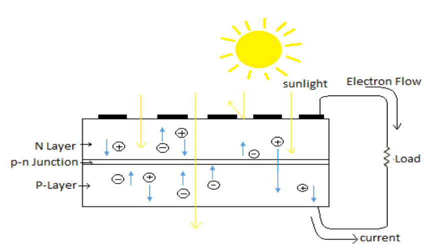

Figure 3-PV cell

3.1 PV Modelling

The ideal solar cell circuit includes a current source that models the solar irradiance, a diode in antiparallel models the p-n junction, as observed in Figure 4 [14]. When the photovoltaic cells are exposed to the sunlight, the direct current produced changes with the solar irradiance. The model is improved with shunt resistance and series resistance to represent the losses. [[15]- [16]]

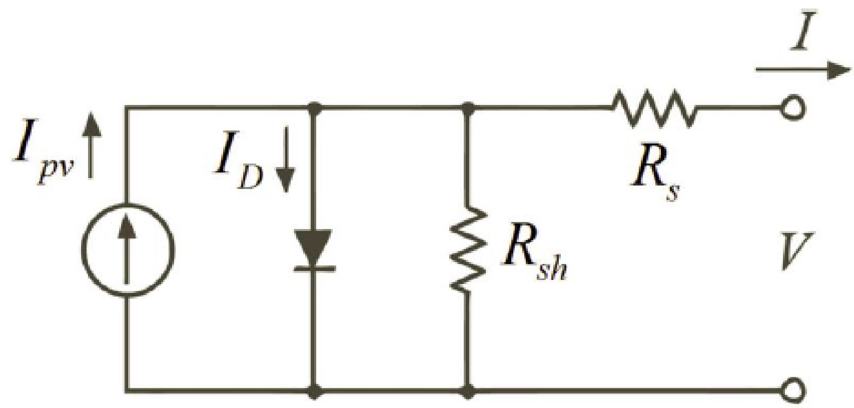

Figure 4-Photovoltaic equivalent circuit cell based on single diode model

The PV output current can be obtained from Kirchhoff's law. The equation is given below [17]

$$I_{pv} = I_{ph} - I_d - I_P \tag{1}$$

Where I_{pv} is the cell current, I_{ph} is the photocurrent, I_d is the diode current, I_P is the parallel current.

$$I_d = I_0 \left[e^{\frac{V+I.R_S}{V_T}} - 1 \right] \tag{2}$$

$\boldsymbol{I_0}$ is saturation current, $\boldsymbol{R_s}$ is serial resistance, $\boldsymbol{V_T}$ is thermal voltage, $\boldsymbol{q}$ is electron charge constant, $\boldsymbol{T_c}$ is actual cell temperature

$$V_T = k\,.T_c/q \tag{3}$$

$$I_{ph} = \frac{G}{G_{ref}}\left(I_{ph,ref} + \mu_{sc}.\Delta T\right) \tag{4}$$

where $\boldsymbol{G}$ is the irradiance, $\boldsymbol{G_{ref}}$ is the irradiance at standard test condition(STC) (1000 $W/_{m^2}$), $\boldsymbol{I_{ph,ref}}$ is the photo current at STC, $\mu_{\boldsymbol{sc}}$ is the coefficient temperature of short circuit current and $\Delta T = T_c - T_{c,ref}$ where the $\boldsymbol{T_{c,ref}}$ is the cell temperature at STC. I_{ph} depends on the temperature and irradiance.

$$I_P = \frac{V + R_s.I}{R_p} \tag{5}$$

Where $\boldsymbol{R_p}$ is the parallel resistance in the equivalent circuit. The final equation for the PV system can be seen below.

$$I = \frac{G}{G_{ref}}\left(I_{ph,ref} + \mu_{sc}.\Delta T\right) - I_0\left[e^{\frac{V+I.R_S}{a}} - 1\right] - \frac{V + R_s.I}{R_p} \tag{6}$$

This equivalent circuit is for a single cell and therefore requires adjustment in N_p (number of parallel cells) and N_s (number of series cells) , so then array current is given below:

$$I_{pv} = N_p I_{ph} - I_0 \left[e^{\left(\frac{q(\frac{V_d}{R1} + \frac{R_s I}{R_p}}{N_s K F T_{pv}} \right)} - 1 \right] - \frac{N_p V_d / N_s}{R_p} \quad (7)$$

3.2 PV Simulation

Without considering other losses, theoretically, there is maximum power point anticipated from the PV array, and that value can be calculated from the short circuit current (I_{sc}) and open circuit voltage (V_{oc}). The PV simulation is obtained by using the PV equations given above. The module created has 36 cells in series, and one cell produce 0.6 V [18]. The Simulink model is depicted in Figure 5.

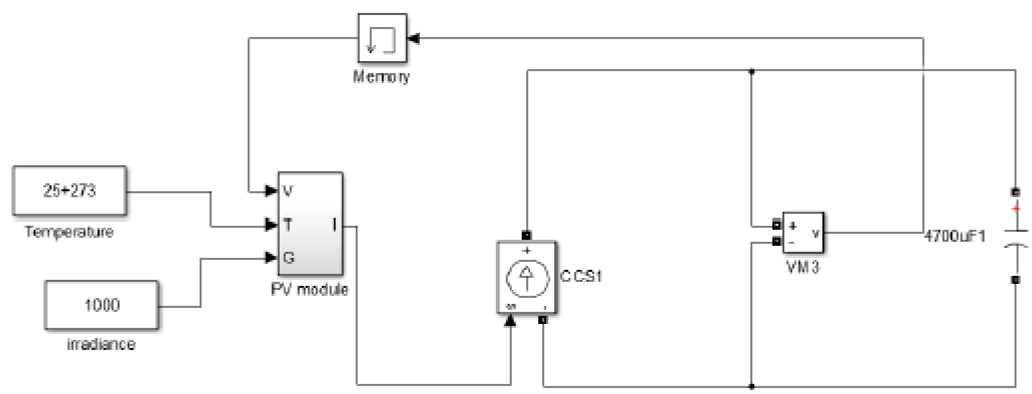

Figure 5-Simulink model

The PV module consists of three subsystems that are shunt current, diode current, and phase current. There are two inputs that are irradiance and temperature and one output which is the current generated by the PV array. Moreover, a number of parallel module and number of the series module can be arranged easily inside of

the PV module subsystem to adjust it to the sizing needed. By using this system, a typical I-V and P-V curves were obtained below.

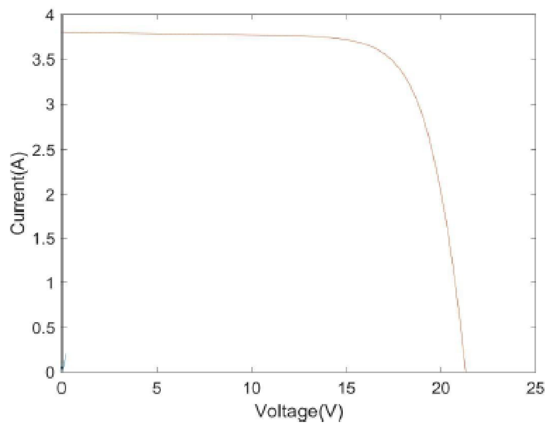

Figure 6- I-V Curve

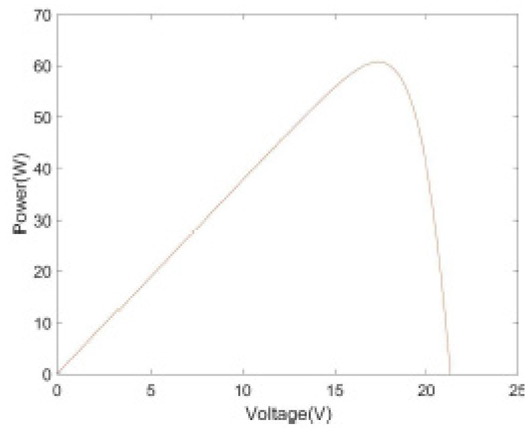

Figure 7- P-V Curve

In this study, the sizing for the PV module was done by changing number of parallel and series cells in the PV model subsytem. When the number of the series cells increases, the voltage of the module produced also increases. While the number of the parallel modules are increased, current of the module generated is raised evenly [19].

Table 1-The key specification of PV module

Open Circuit Voltage	V_{oc}	21.1 V
Short Circuit Current	I_{sc}	3.74 A
Voltage, Maximum Power	V_m	3.479 V
Current, Maximum Power	I_m	17.45 A
Maximum Power	P_m	60.7 W

The most relevant values are calculated and given Table 1.

3.3 Maximum Power Point Tracking (MPPT)

Maximum power point tracking (MPPT) operates the photovoltaic arrays in a way that maximizes their power output [20]. The major basis of MPPT is to receive the highest suitable power from PV arrays by controlling at the maximum efficient voltage. Which means that, MPPT controls the output of PV array, compares it against the battery voltage, and fixes the available power that PV array can generate to charge the battery and converts them for the most suitable voltage to obtain the highest current into battery [21]. MPPT increases the solar energy output efficiency around 30% or more compare to non-MPPT systems (Figure 8Figure 8-Advantage of MPPT) [22]- [23]

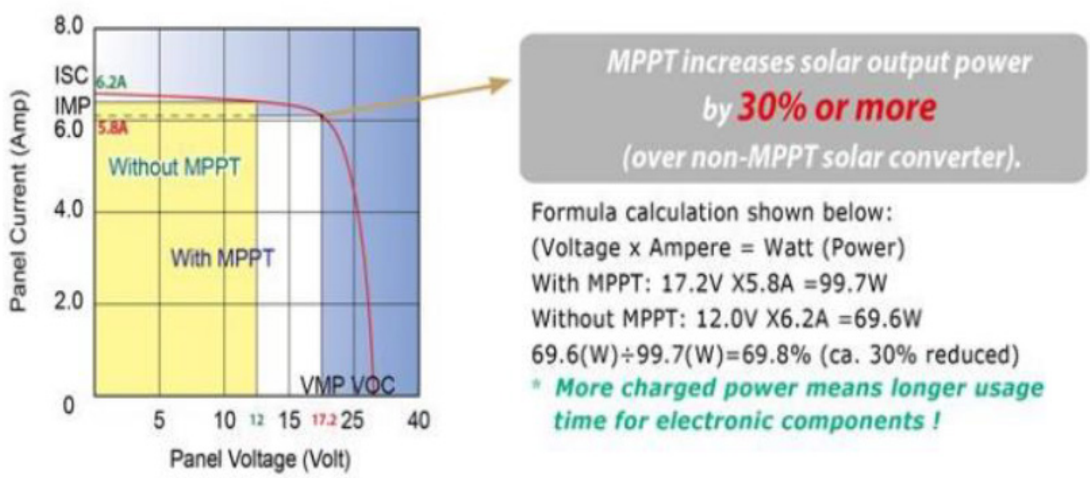

Figure 8-Advantage of MPPT

In this study, MPPT is used in MATLAB®/Simulink embedded function Figure 9. It generates a suitable duty cycle that depends on the PV array voltage and current.

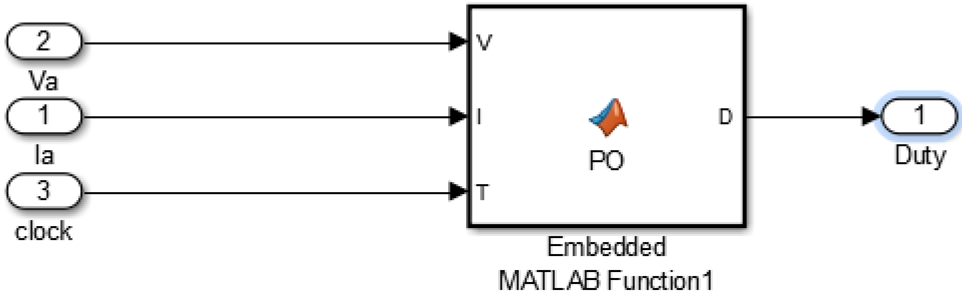

Figure 9-Embedded MATLAB® Function

3.4 DC-DC Converter

DC-DC converters are widely utilized for photovoltaic systems between the load and PV array. The converters chosen for PV system should be matched to the PV array maximum power point [24]. In this study, a dc-dc converter was created by considering on equation given below

$$\mathrm{V_{BAT}.D = V_{PV}} \tag{8}$$

$$I_{PV}.D = I_{DCDC} \tag{9}$$

The aim of the dc-dc converter is to change a dc voltage from one range to another range by varying the duty cycle [25]. The dc-dc converter includes switches and magnetic and electric storage components (inductance and capacitors) [26]. The dc-dc converter used is depicted in Figure 10

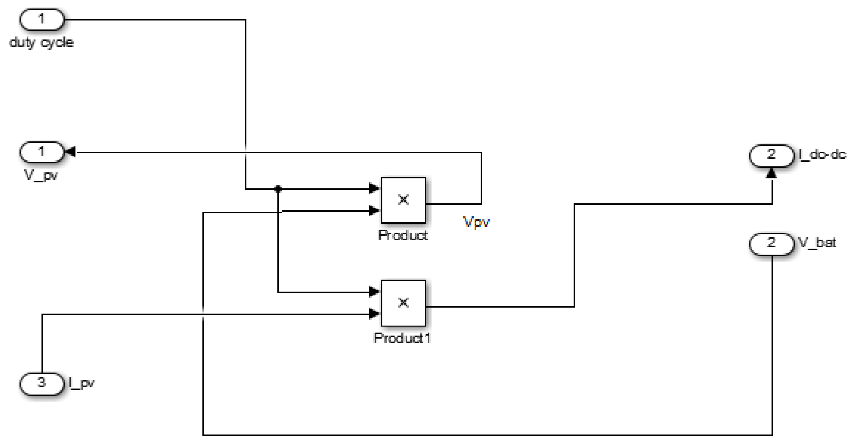

Figure 10-DC-DC Converter in Simulink

Generally, the PV system design need DC/AC (inverter) system, however this thesis focused on DC side. Aforementioned before, the efficiency of the inverter is quiet high because of this inverter is neglected in this system.

4 Battery System

4.1 Battery Model

Electrochemical batteries have a very significant role in the electrical system. Recently, electrochemical batteries have become an irreplaceable tool in human life such laptops, mobile phones and many other portable devices [22]. Batteries are utilized to store chemical energy, and then they convert this energy stored from chemical to electrical in a controllable manner to satisfy the generation load mix it is connected to [27]. In this study, a lithium-ion (Li-ion) battery which has been embraced widely is used. Li-ion battery has a important advantages in comparison to other batteries such as higher

energy density; it manages higher voltages, and it also has lower self-discharge rate [22]. The eequivalent circuit battery is given in Figure 11.

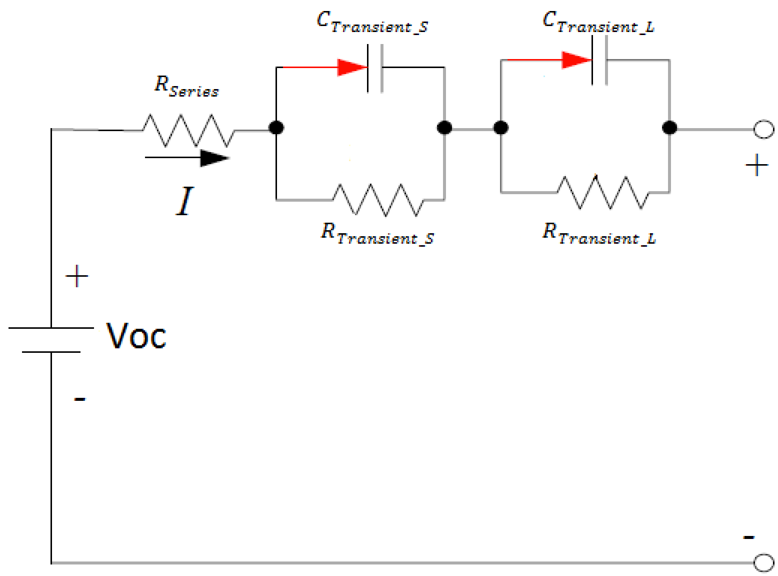

Figure 11-Battery equivalent circuit model

This battery model consists of three parts: open-circuit voltage (OCV), (R_{Series}) ohmic resistance and two resistor-capacitor (RC) parallel network. The voltage of resistor-capacitor parallel system yields the transient battery voltage response and represents the dynamic in the electrode-electrolyte interface. The voltage of each RC circuit is calculated by using the equation given below [28],

$$I = V/R + Scv \tag{10}$$

$$I/sC = V/sCR + V \tag{11}$$

$$V = (1/s)/[\frac{1}{C} - \frac{V}{RC}] \tag{12}$$

4.2 SOC and OCV Calculation

The state of charge (SOC) of the battery is as the ratio of its current capacity to nominal capacity. The nominal capacity is the maximum amount of charge that can be stored in the battery [29]. The relationship between SOC and OCV should be established to include it as part of the battery equivalent circuit [30]. A typical representation of this relationship between SOC and OCV for Li-ion battery is given in Figure 12 [30]. This relationship is detected from implementing a pulse load in battery at each SOC level, and after allowing the battery to reach equilibrium in open circuit. The OCV simulation model created is also given Figure 13.

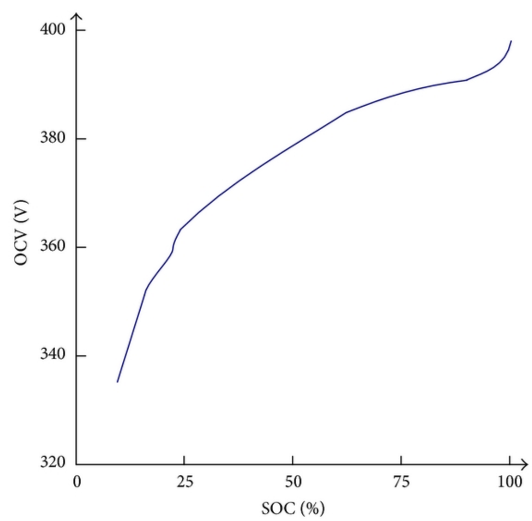

Figure 12-Typical relationship between OCV and SOC

$$OCV(SoC) = K_0 + K_1 e^{-\alpha.SoC} + K_2.SoC + K_3.SoC^2 + K_4.SoC^3 \qquad (13)$$

Where, α, K_0, K_1, K_2, K_3, K_4 are the constant values, SOC is the state of charge. The SOC equation is also given below.

$$SOC_{(t)} = SOC_{(t-1)} + \frac{I_c(t)}{Q_n}\Delta t \tag{14}$$

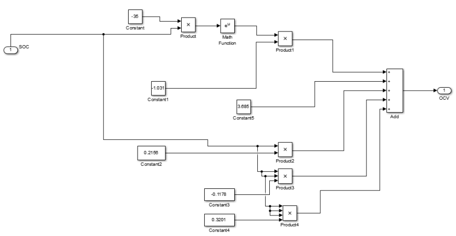

Figure 13-OCV Simulation model

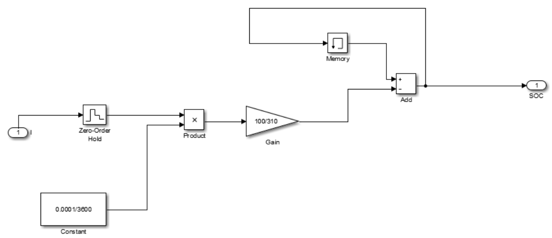

Figure 14-SOC Simulation model

4.3 Battery Simulation

In this study, the battery model is designed in MATLAB® Simulink by using following equations [22]

$$R_{Series}(SOC) = 0.1562.\, e^{-24.37.SOC} + 0.07446 \tag{15}$$

$$R_{Transient\_S}(SOC) = 0.3208.\, e^{-29.14.SOC} + 0.04669 \tag{16}$$

$$C_{Transient\_S}(SOC) = -752.9.\, e^{-13.51.SOC} + 703.6 \tag{17}$$

$$R_{Transient\_L}(SOC) = 6.603.\, e^{-155.2.SOC} + 0.04984 \tag{18}$$

$$C_{Transient\_L}(SOC) = -6056.\, e^{-27.12.SOC} + 4475 \tag{19}$$

The battery model is represented by one cell with nominal voltage and capacity values 4V and 360 Ah capacity. By increasing the number of cells in series, the battery voltage can be increased. Also, by increasing the number of the parallel cells, the battery capacity can be improved.

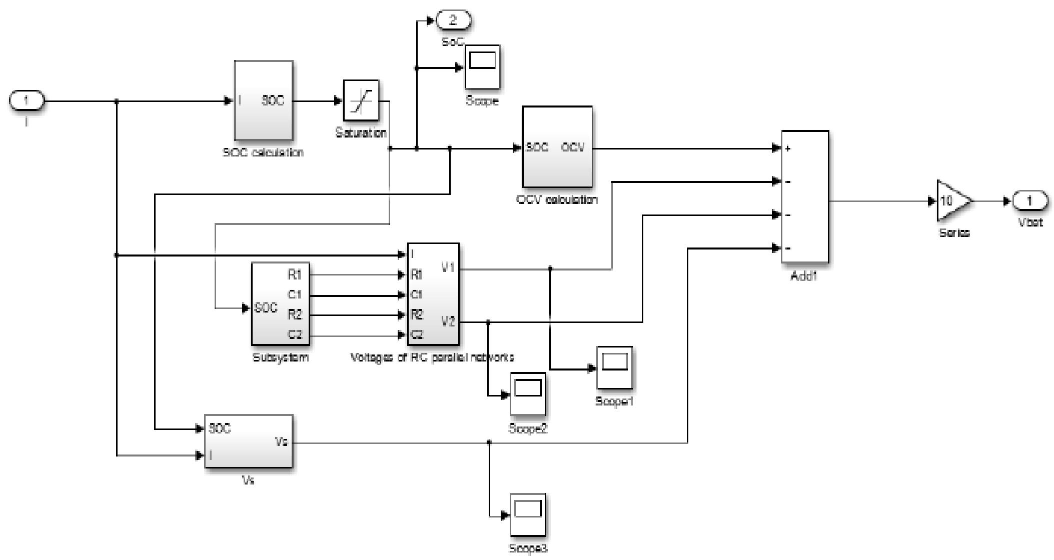

Figure 15-Battery Model in Simulink

5 Charge Controller

The battery charge controller system is placed in PV systems to control the battery charging procedures. This control unit protects the battery from overcharge and deep charge. Thanks to this unit, the battery SOC is kept between 20% and 90% to protect the battery against the over discharge and gassing process. Typical charge graph depicted below Figure 16.

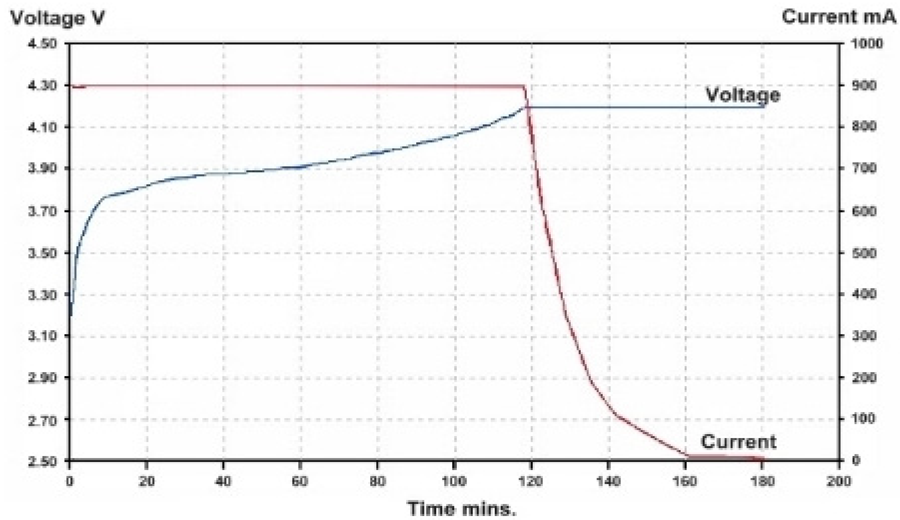

Figure 16-Typical charge graph (Li-ion)

6 System Sizing

When sizing the photovoltaic system, the logical first step is to consider the energy demand. Thus, a primarily stand-alone PV system sizing begins at the load side and proceeds backward to the PV arrays [12]. See Figure 17.

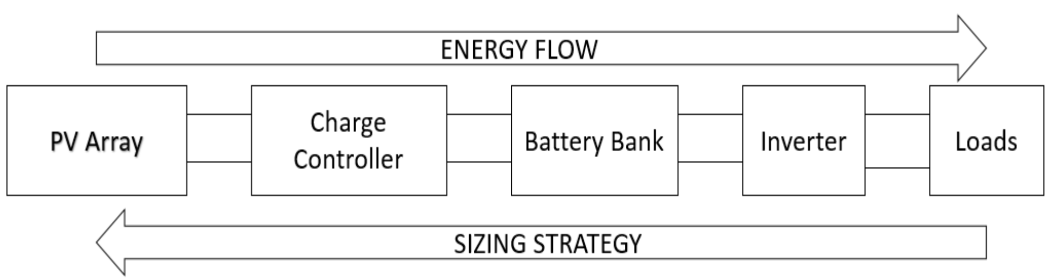

Figure 17-Sizing strategy for stand-alone system

The purpose is first to decide the system loads needed and then to decide the size of the PV module, converter, and battery that are required to meet the energy demand from load side.

6.1 Sizing Calculation

The sizing stand-alone PV system is based on four fundamental calculations. First, a load analysis decides the energy demand requirements on the load side. Second, monthly load requirements are compared to the insolation of the availability city data to determine the critical design month. Then, the battery bank should be sized appropriately to produce enough energy for loads to a certain length of time such as if PV arrays reduce outputs during cloudy days. Finally, the PV arrays should be sized to generate enough power for both load requirements and battery.

6.1.1 Load Analysis

The load analysis is the most significant part in stand-alone PV sizing. [32] The energy utilized necessitates the amount of electricity that must be generated. In this study, residential loads were used for Tucson(AZ) and Houghton(MI). These data sets were collected from the OpenEI website. [11]. This website provides free data that users can download, edit and add new data. This website particularly focuses on energy efficiency and renewable energy to analyze them.

6.1.2 Critical Design Month

Stand-alone PV systems must generate sufficient electricity in order to meet load demand during each month. Thus, the PV system must be sized according to a worst-case scenario of the lowest insolation rate and highest load. This worst-case scenario is used to determine the critical design month that has a critical design ratio. The critical design ratio is calculated by dividing the average daily consumption by the insolation. This ratio is calculated for each month separately and the critical month is detected.

After the critical design month is identified, the lowest ratio selects the optimal orientation [8].

Table 2- Critical design month for Houghton

Month	Average Daily DC Energy Consumption (Wh/day)	Array Orientation 1 Latitude -15		Array Orientation 2 Latitude		Array Orientation 3 Latitude +15	
		Insolation (PSH/day)	Design Ratio	Insolation (PSH/day)	Design Ratio	Insolation (PSH/day)	Design Ratio
January	15375	2.1	7321	2.3	6685	2.5	6150
February	14803	3.2	4626	3.5	4229	3.6	4112
March	12618	4.5	2804	4.7	2685	4.7	2685
April	11915	5.2	2291	4.2	2837	4.8	2482
May	11110	5.6	1984	5.3	2096	4.7	2364
June	7647	5.9	1296	5.4	1416	4.7	1627
July	9960	6.0	1660	5.6	1779	4.8	2075
August	9994	5.5	1817	5.2	1922	4.7	2126
September	10669	4.4	2425	4.4	2425	4.2	2540
October	11839	3.2	3700	3.4	3482	3.4	3482
November	12667	1.9	6667	2.1	6032	2.1	6032
December	14707	1.6	**9192**	1.8	**8171**	1.9	7740.5

The critical design month is <u>December</u> for Houghton and, <u>July</u> for Tucson. Therefore, these months are used to size the PV arrays.

Table 3-Critical design month for Tucson

Month	Average Daily DC Energy Consumption (Wh/day)	Array Orientation 1 Latitude -15		Array Orientation 2 Latitude		Array Orientation 3 Latitude +15	
		Insolation (PSH/day)	Design Ratio	Insolation (PSH/day)	Design Ratio	Insolation (PSH/day)	Design Ratio
January	12120	4.6	2634.782609	5.4	2244	5.9	2054
February	11865	5.5	2157	6.2	1914	6.4	1854
March	10692	6.4	1671	6.7	1596	6.6	1620
April	10551	7.5	1407	7.3	1445	6.8	1552
May	13268	7.8	1701	7.3	1818	6.4	2073
June	18601	7.8	2385	7.1	2620	6.1	3049
July	20950	6.9	3036.2	6.4	3273	5.6	3741
August	19467	6.9	2821	6.6	2950	6.0	3245
September	17017	6.6	2578	6.8	2503	6.6	2578
October	13136	6.1	2153	6.6	1990	6.8	1932
November	10827	5.0	2165	5.8	1867	6.2	1746
December	12153	4.3	2826	5.1	2383	5.6	2170

6.1.3 Battery Sizing

Batteries are used to store the excess of energy generated by the PV array during sunny and high insolation of periods, and they provide power to the system during nighttime and low insolation of periods [12]. The required battery capacity for stand-alone PV system depends on load demands and desired autonomy. The autonomy day is the time during which a lonely battery provides power for load requirements, without any solar energy, beginning from a full state of charge [33]. Greater autonomy days are associated with larger and higher cost battery banks. However, it drops the average daily depth of charge (DOD), and it provides longer lifetime for battery in this manner. In Houghton, autonomy days are higher than Tucson as Houghton has a higher number of cloudier days and therefore needs more battery power to meet its load demands than Tucson. Autonomy day is assumed 3 days in Tucson and 15 days for Houghton in this study [34]. The required battery capacity is calculated by using following equation;

$$B_{out} = E_{crit} \cdot \frac{t_a}{V_{SDC}} \tag{20}$$

$$B_{rated} = \frac{B_{out}}{DOD_a \cdot V_{SDC}} \tag{21}$$

Where B_{out} is the required battery output(Ah) , E_{crit} is the daily energy demand during critical design month (Wh/day), t_a is autonomy days V_{SDC} is the nominal dc system voltage (V) and, DOD_a is the allowable depth of discharge which is assumed to be 80% in this study. Based on these equations, the number of battery cells in parallel is 19 and 6 for Houghton and Tucson respectively. The number of battery cells in series is 12 for both cities to reach a 48V standard. Considering the number of cells in parallel, with

each cell having a 310 Ah, the battery pack rated capacity(B_{rated}) were found to be 5745 Ah for Houghton and, 1637 Ah for Tucson by taking into account average daily dc energy consumption during the critical design month.

6.1.4 Array Sizing

The stand-alone PV system is sized to generate sufficient electrical power to meet the load demand during the critical design month. In this manner, the battery is always charged, and the system availability is high during the whole year. Firstly, the required PV array current is computed from the load demands and, and the nominal system voltage, and insolation of critical design month [12]. On the other hand, as the battery efficiency is of 0.85, more current must be provided to charge battery bank than is taken back on discharge. The following equation is used to calculate the required array current [[12]- [35]].

$$I_{array} = \frac{E_{crit}}{\eta_{bat}. V_{SDC}. t_{PSH}} \tag{22}$$

Where I_{array} the required array maximum-power current (A), η_{bat} is battery system charging efficiency, and t_{PSH} are the peak sun hours for the critical month (hr/day). The maximum current and output voltage generated by PV were already calculated above (Table 1). The final part of sizing process is to determine the number of PV cells and the array configuration based on the voltage and current parameters. The number of parallel modules are determined by dividing the rated array current output by the module current at maximum-power and rounding up to the next integer. The required number of series modules are determined by dividing the rated array voltage by the module

voltage at maximum-power and rounding up to the next integer. Then the rated PV array maximum power is computed by multiplying the maximum module power by the sum of module number [12]. When these equations are used, the actual array rated is 10015.5 W for Houghton, and 4006.2 W for Tucson.

7 System Simulation

In the system simulation all components (which are PV, MPPT, dc-dc converter, battery and battery controller) are put together, and the stand-alone PV/Battery MATLAB® /Simulink simulation is created. The simulation results are obtained by simulating for 24 hours in one critical month for each city. A general overview is given in Figure 18.

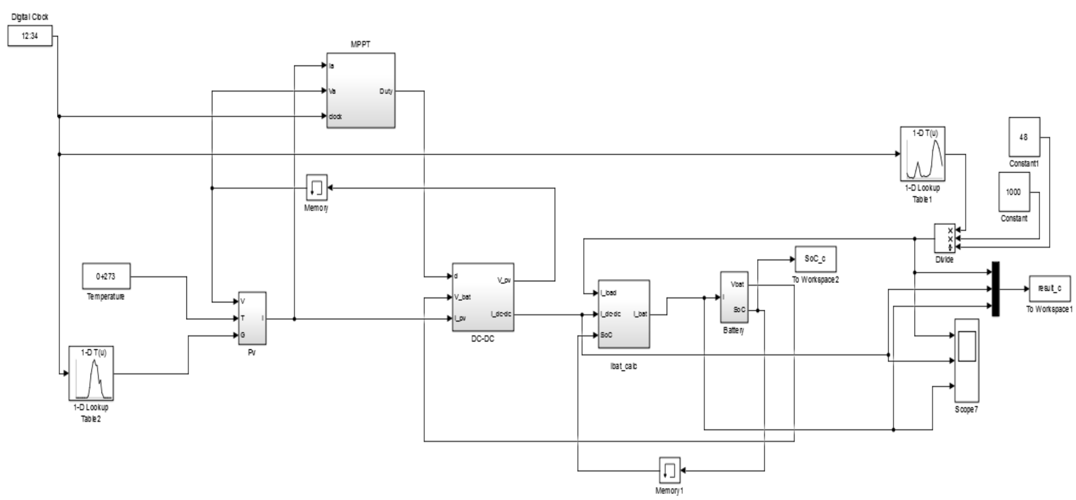

Figure 18-Stand-alone PV Simulink design

Look up tables are used to represent the irradiance and loads for 24 hours. In this manner, the daily, power generated by the PV and the battery behavior are easily observed.

8 Data Analysis

The solar irradiance and load data for Houghton and Tucson were analyzed to implement stand-alone PV design. The irradiance data was collected from the System Advisor Model (SAM) [36] and the load data was collected from the OpenEI website [11]. Each month was plotted for both cities during one year. The results for the PV generation can be consulted in the Appendix.

Table 4- Tucson Max, Min Irradiance Analysis for a year

TUCSON			
Month	Min Irradiance at noon	Max Irradiance at noon	Difference
January	263.314	669.636	406.322
February	144.907	799.512	654.605
March	627.55	962.313	334.763
April	660.766	1042.1	381.334
May	428.601	1040.59	611.989
June	407.668	1073.01	665.342
July	655.553	998.905	343.352
August	388.466	958.489	570.023
September	554.613	934.787	380.174
October	440.863	843.772	402.909
November	244.377	725.898	481.521
December	246.373	621.165	374.792

Firstly, the maximum difference between minimum irradiance and maximum irradiance are calculated. (Table 4, Table 5). According to these differences and monthly plots, the most variable month were determined for each location and are depicted in Figure 19-20.

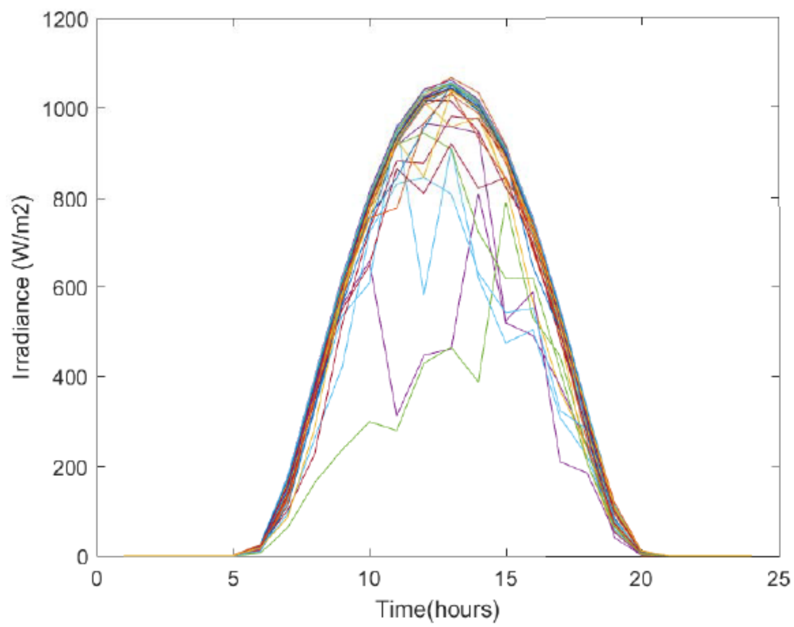

Figure 19-Tucson Most Variable Month (May)

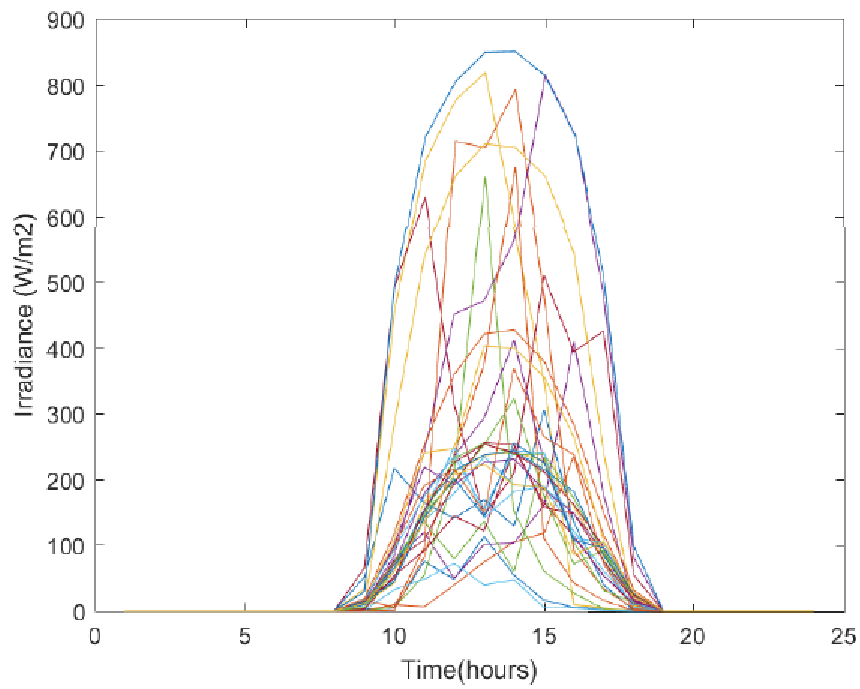

Figure 20-Houghton Most Variable Month (January)

Table 5-Houghton Max, Min Irradiance Analysis for a year

HOUGHTON			
Month	Min Irradiance at noon	Max Irradiance at noon	Difference
January	12.26	804.003	791.743
February	135.307	590.856	455.549
March	222.283	774.082	551.799
April	165	867.932	702.932
May	190.853	907.599	716.746
June	285.998	936.478	650.48
July	141	882.311	741.311
August	135	821.894	686.894
September	151.661	739.882	588.221
October	179.167	562.611	383.444
November	122.18	419.031	296.851
December	67.0612	335.24	268.1788

9 Simulation Results and Discussion

In this study, two cities were observed by the simulating most variable month which is May for Tucson and January for Houghton. At the beginning of the month, the SOC was assumed to be 100%. All the days of the month were simulated, and for each day, the SOC started at the value at which the simulation ended for the previous day. The objective for this was to simulate the full month and really consider the consequences of the irradiance variations and its impact in the final SOC at the end of the month. For the sake of space, the first day and last day of the month for both cities are shown below. The simulation results for the rest of days of the month are presented in the Appendix. In general, when the irradiation is increasing, the battery voltage and SOC are also

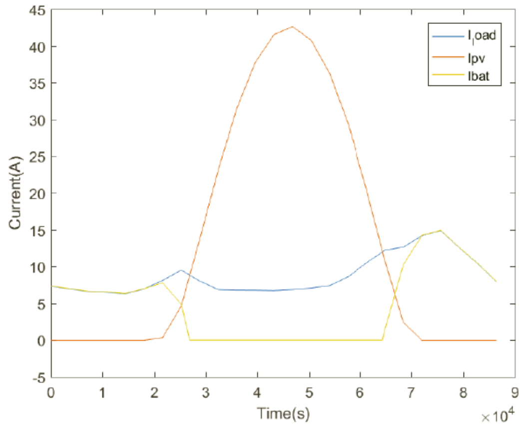

Figure 21-First day currents for Tucson(May 1)

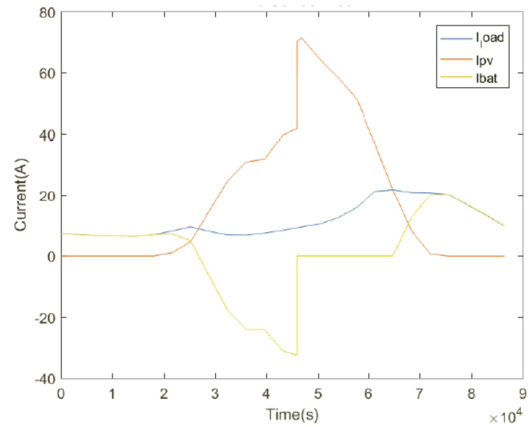

Figure 22- Last day currents for Tucson(May 30)

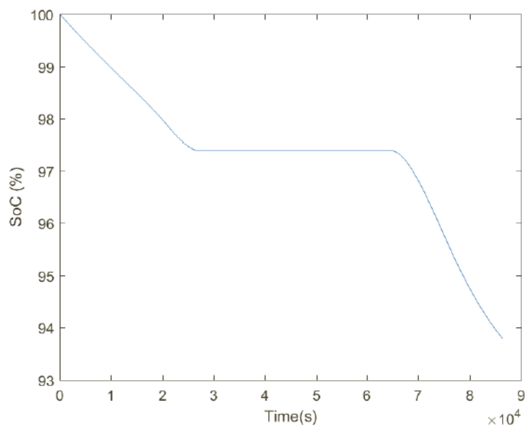

Figure 23-First day SoC for Tucson

(May 1)

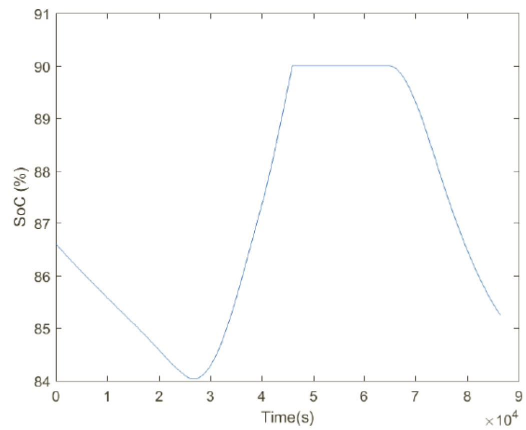

Figure 24-Last day SoC for Tucson

(May 30)

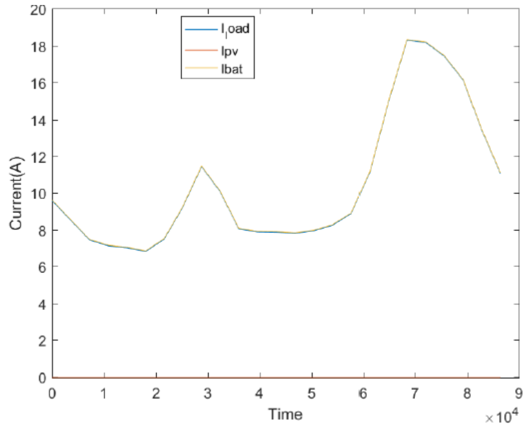

Figure 25--First day currents for Houghton (January 1)

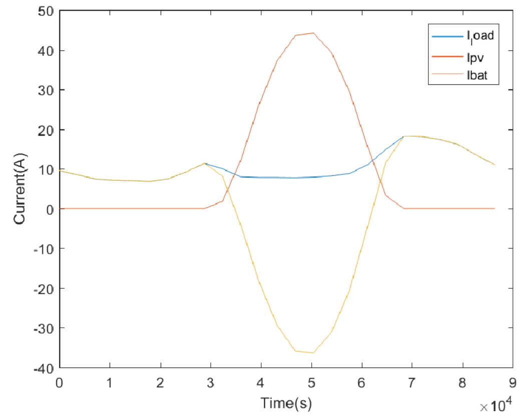

Figure 26-Last day currents for Houghton (January 30)

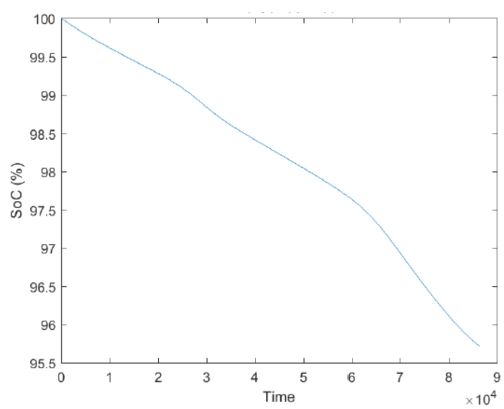

Figure 27-First day SoC for Houghton (January 1)

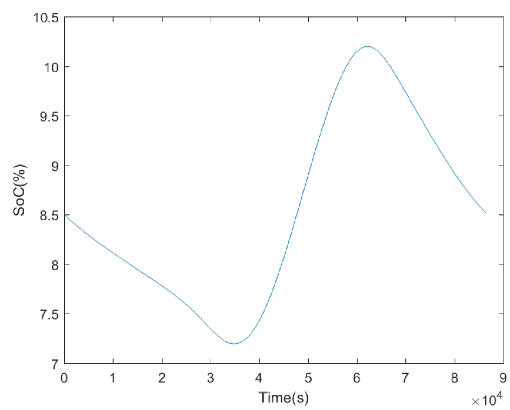

Figure 28-Last day SoC for Houghton (January 30)

The results show that PV generates enough power for both load demand and battery for the first day of May in Tucson(AZ) (Figure 21) and SOC graph indicates that it was decreasing but it is a stable throughout some time during day due to charge controller

(Figure 23) since the charge controller keeps the SOC between 20% and 90%. If there was no charge controller in design, SOC would reach 100% level again. For last day in Tucson when the battery current is negative side (Figure 22) the SOC increases as the battery starts to charge the battery. For Houghton (MI), the PV does not produce enough power for both load demand and battery in the first 18 days of January because of snow coverage (see appendices). The battery supply to meet the required load demands, and therefore the SOC is decreasing (Figure 27) during these days. For the Houghton case, although the PV supplies sufficient power for load demand and battery during the last day of the January (Figure 26), the simulation results show (Figure 28) that SOC is decreasing day by day and end of the month SOC reaches 8.5%, which is substantially smaller than the last day of the month for Tucson. increasing.

10 Conclusion

In this Thesis, an off-grid PV-storage residential system is sized and simulated for two different locations with very different solar irradiations (Houghton MI, Tucson AZ). When Tucson simulation results are analyzed, the system produces more power than the load demanded in some of the sunny day because the battery is fully charged with 90 % SOC during this period. On the other hand, autonomy day may be reduced 3 to 1 for Tucson case, seen the results; and battery capacity can be reduced in this way. However, when autonym days is reduced, depth of discharge rate is increased during the cloudy and insufficient irradiance days. Therefore, the battery lifetime is shorter because of the depth of discharge is larger. Thus, autonomy day and depth of discharge rate should be kept in balance in order to provide excellent efficiency for battery.

Final note on the models used in this Thesis: the PV was validated against the software SAM (System Advisor Model), and results showed a ***5.5%*** error in the PV production for Tucson. Comparisons can be made between Figures 29 and 30. However, error in Houghton was larger as the snowfall was not considered. Therefore, the PV model was adapted to reduce its power output during the winter period to match SAM, and simulations for Houghton were repeated for the month of January considered. Snowfall data is presented in Fig. 31 for the month of January. The load was used as an input for the Matlab/Simulink, but equally, it was checked again to show that the load dynamics were adequate. The battery model was experimentally obtained from reference [28]. Comparisons with SAM are shown in Figure 29-30.

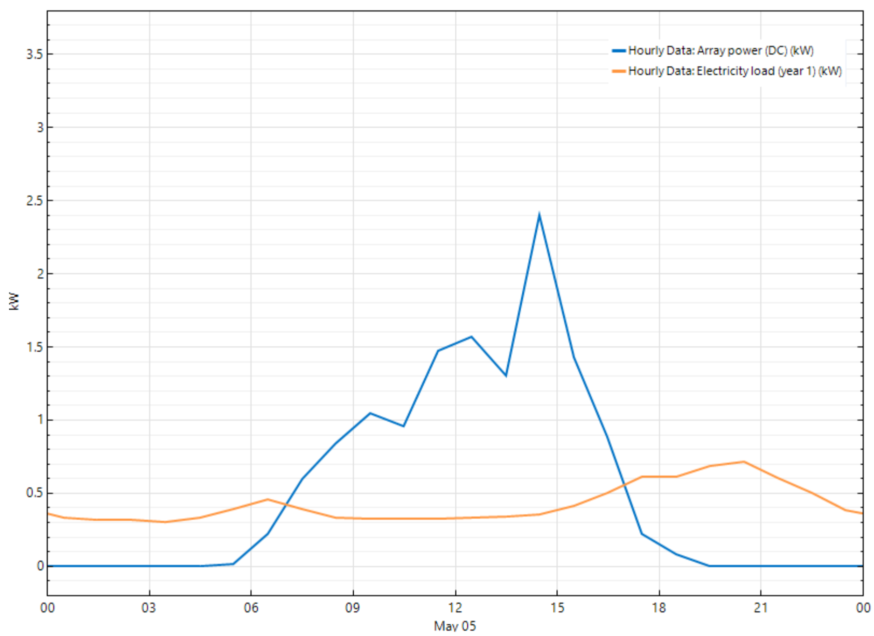

Figure 29-Result from SAM in May 5 for Tucson

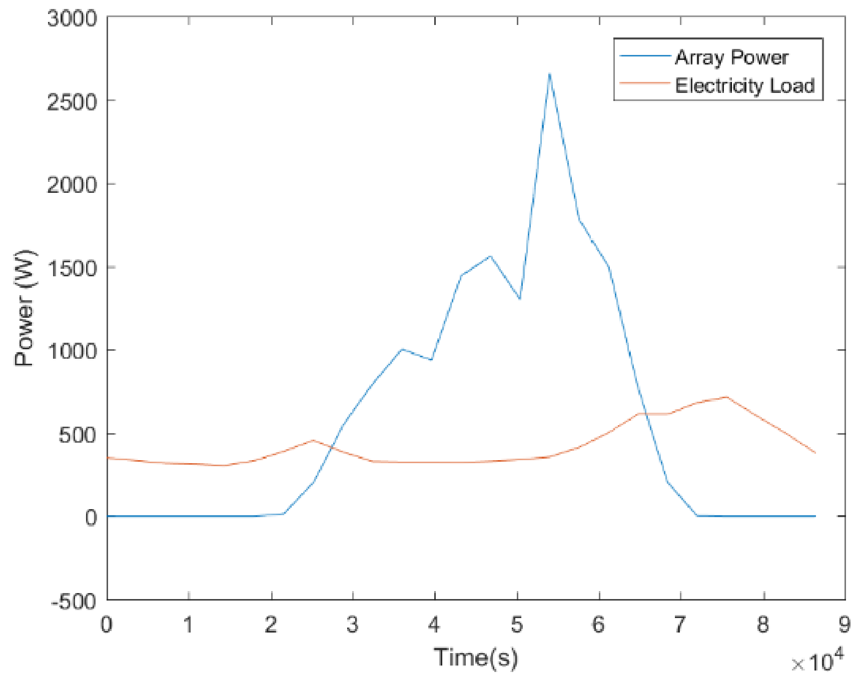

Figure 30-Result from MATLAB® in May 5 for Tucson

For the Houghton case, even if the battery capacity is larger in this case, the PV does not produce enough power during January. For Houghton, the grid-connected PV system would be more adequate because the combination of snowfall and lower irradiance reduces its power output so that it cannot produce enough electricity to meet the load demands during certain periods of the winter. A grid-connected system or other controllable source would be able to complement the PV system and battery throughout winter. On the other hand, when the irradiance graphs are analyzed in Houghton for the summer, there is enough irradiance to produce sufficient electricity for the residential system, and it can have a surplus as it generates more electricity than the load demand. When we compare our results with System Advisor Model (SAM), we obtain almost same result.

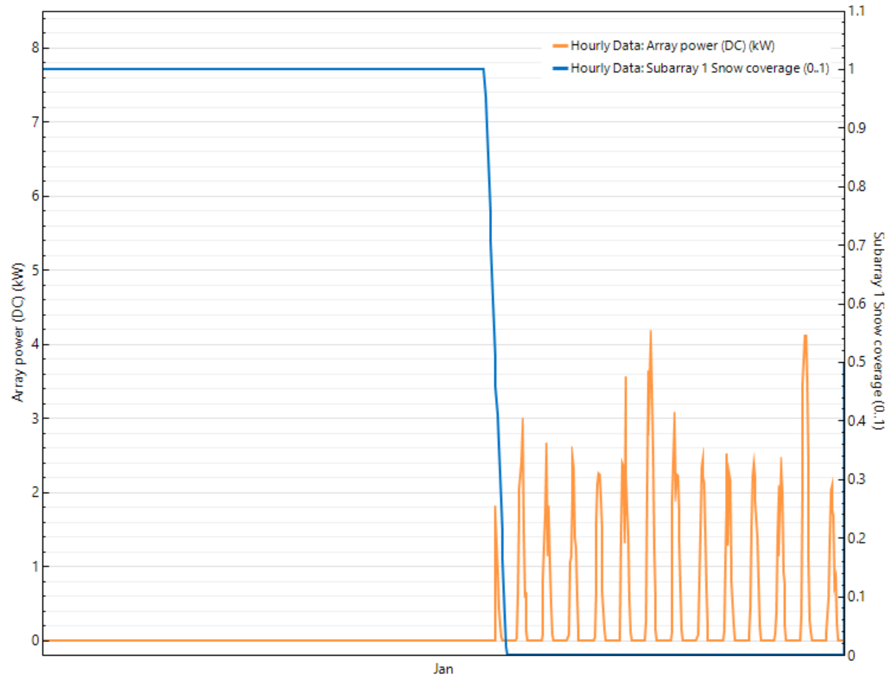

Figure 31-SAM Results for Snowfall (blue) and PV power (orange) for Houghton in January

The blue line represents snow coverage that varies between zero and one. There is no power produced by the PV until January 18th. The snow coverage rate decreases after that date and reached zero, meaning the PV panel surface was clear of snow. After January 18th the PV system produced enough power for the loads and battery.

11 Appendices

Monthly irradiance in Houghton

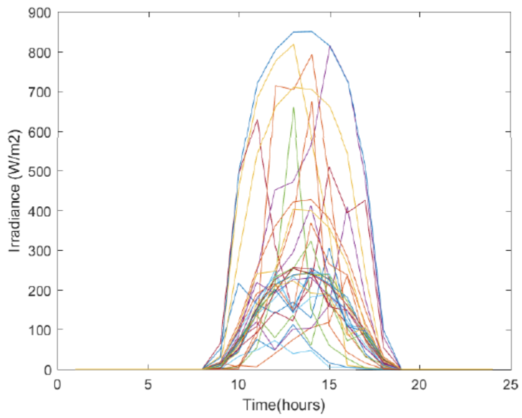

Figure 32-Irradiance January

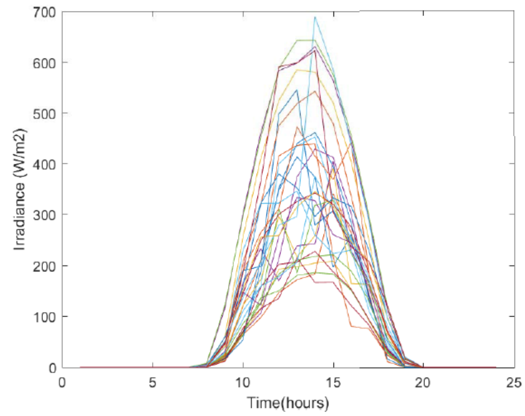

Figure 33-Irradiance February

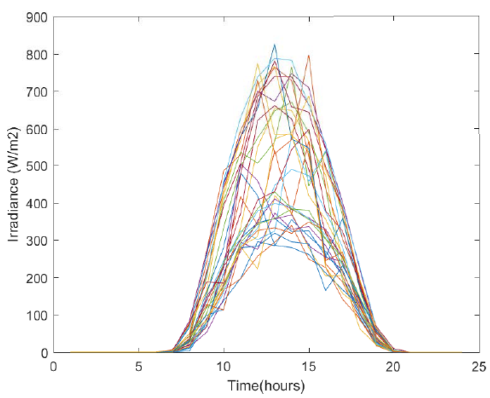

Figure 34-Irradiance March

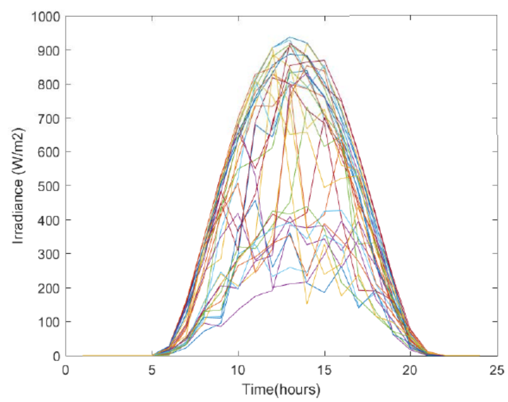

Figure 35-Irradiance May

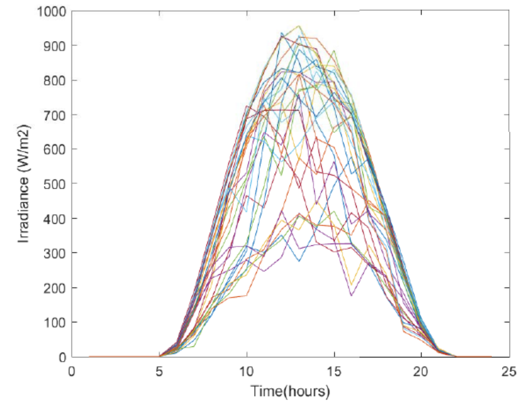

Figure 36-Irradiance June

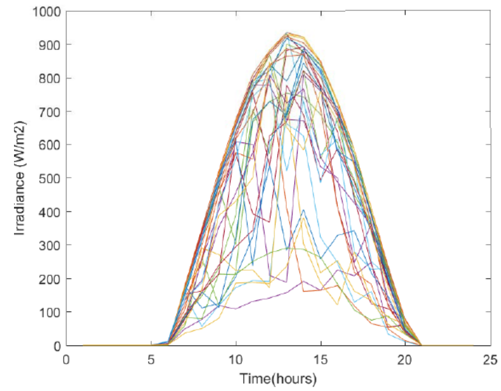

Figure 37-Irradiance July

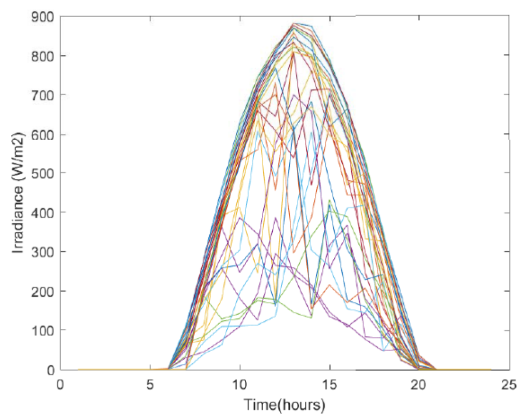

Figure 38-irradiance August

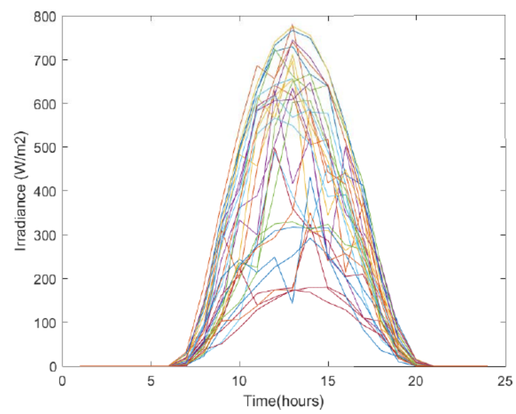

Figure 39-Irradiance September

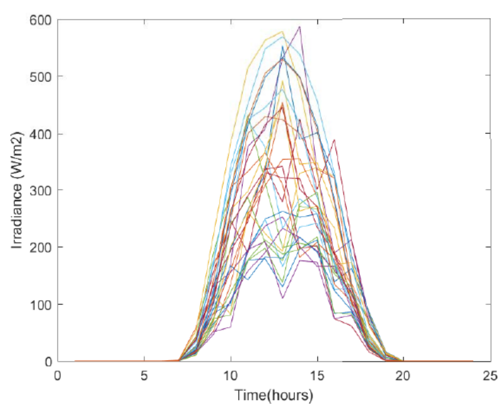

Figure 40-Irradiance October

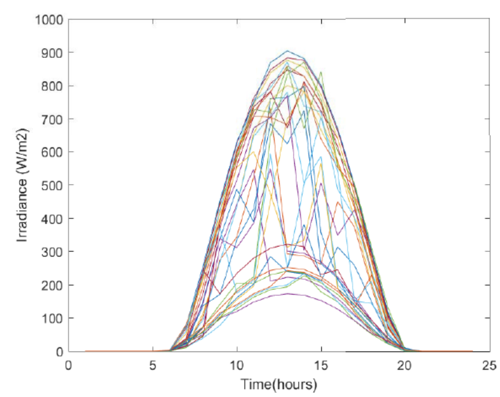

Figure 41-Irradiance April

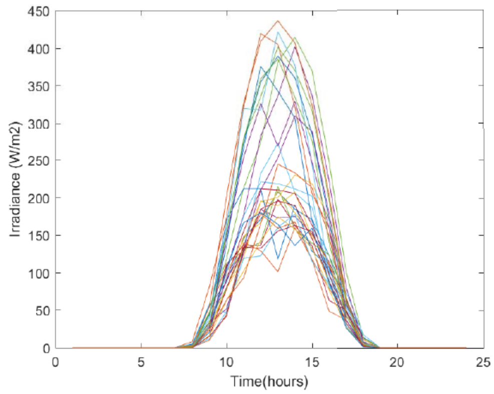

Figure 42-Irradiance November

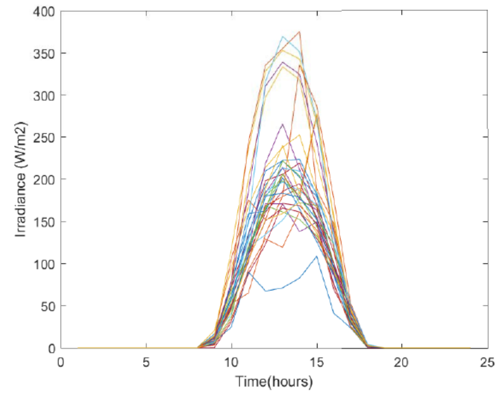

Figure 43-Irradiance December

Monthly irradiance in Tucson

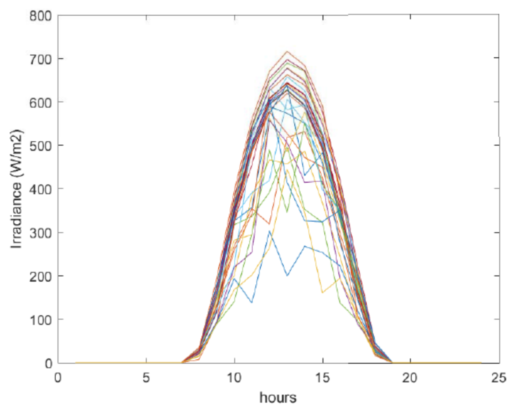

Figure 44-Irradiance January

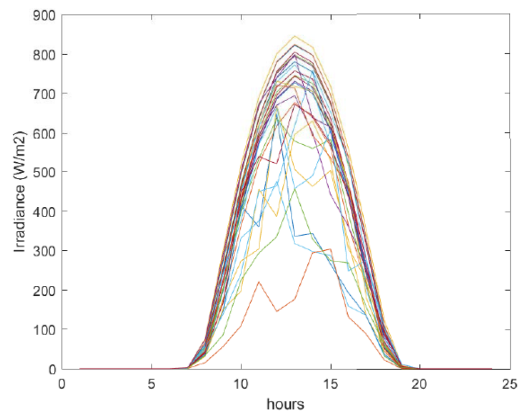

Figure 45-Irradiance February

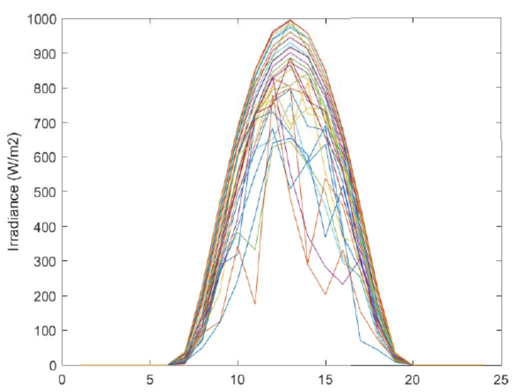

Figure 46-Irradiance March

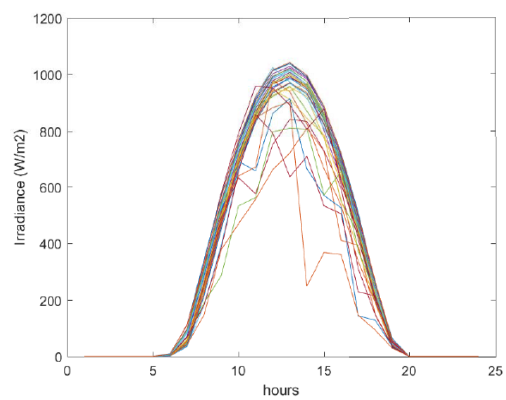

Figure 47-Irradiance April

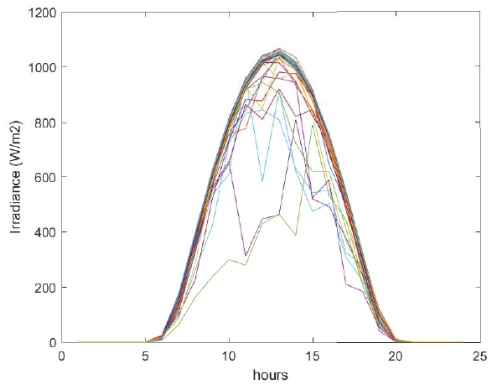

Figure 48-Irradiance May

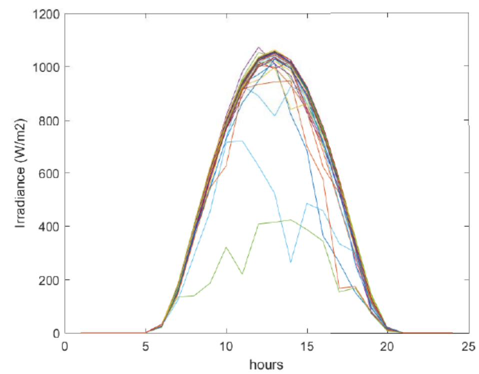

Figure 49-Irradiance June

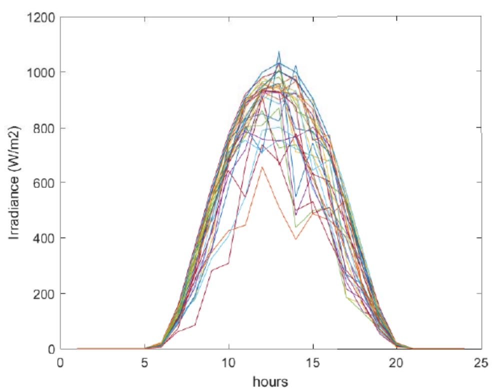

Figure 50-Irradiance July

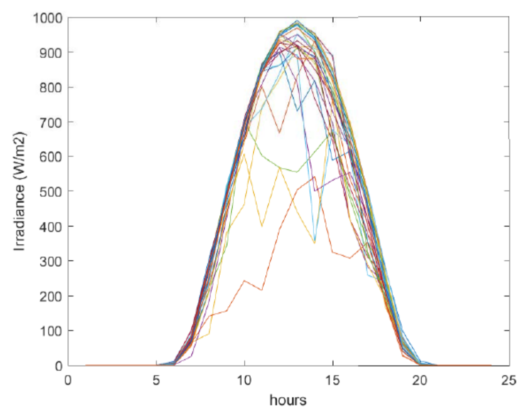

Figure 51-Irradiance August

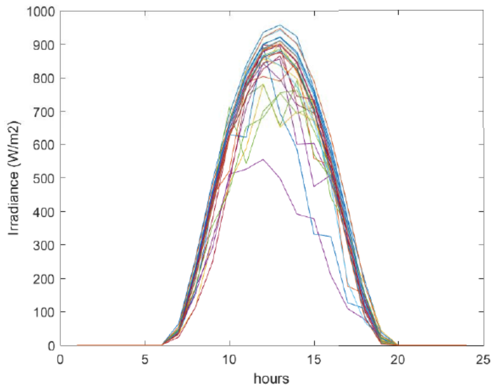

Figure 52-Irradiance September

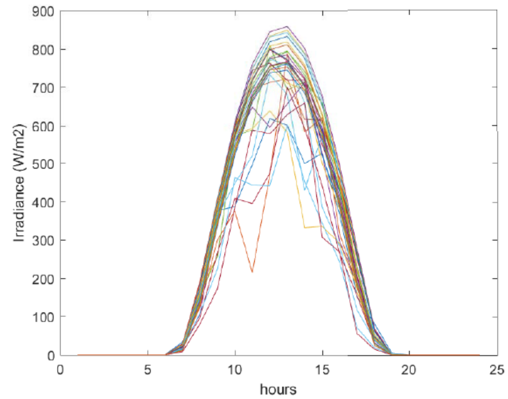

Figure 53-Irradiance October

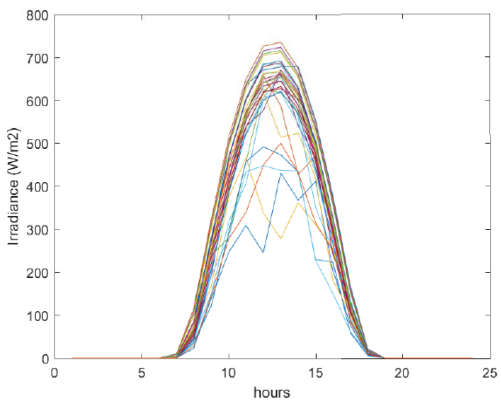

Figure 54-Irradiance November

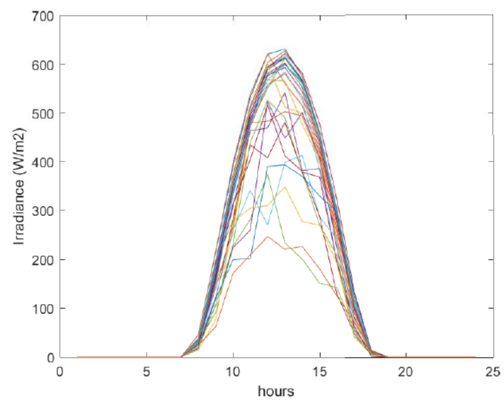

Figure 55-Irradiance December

Simulation Results for January in Houghton

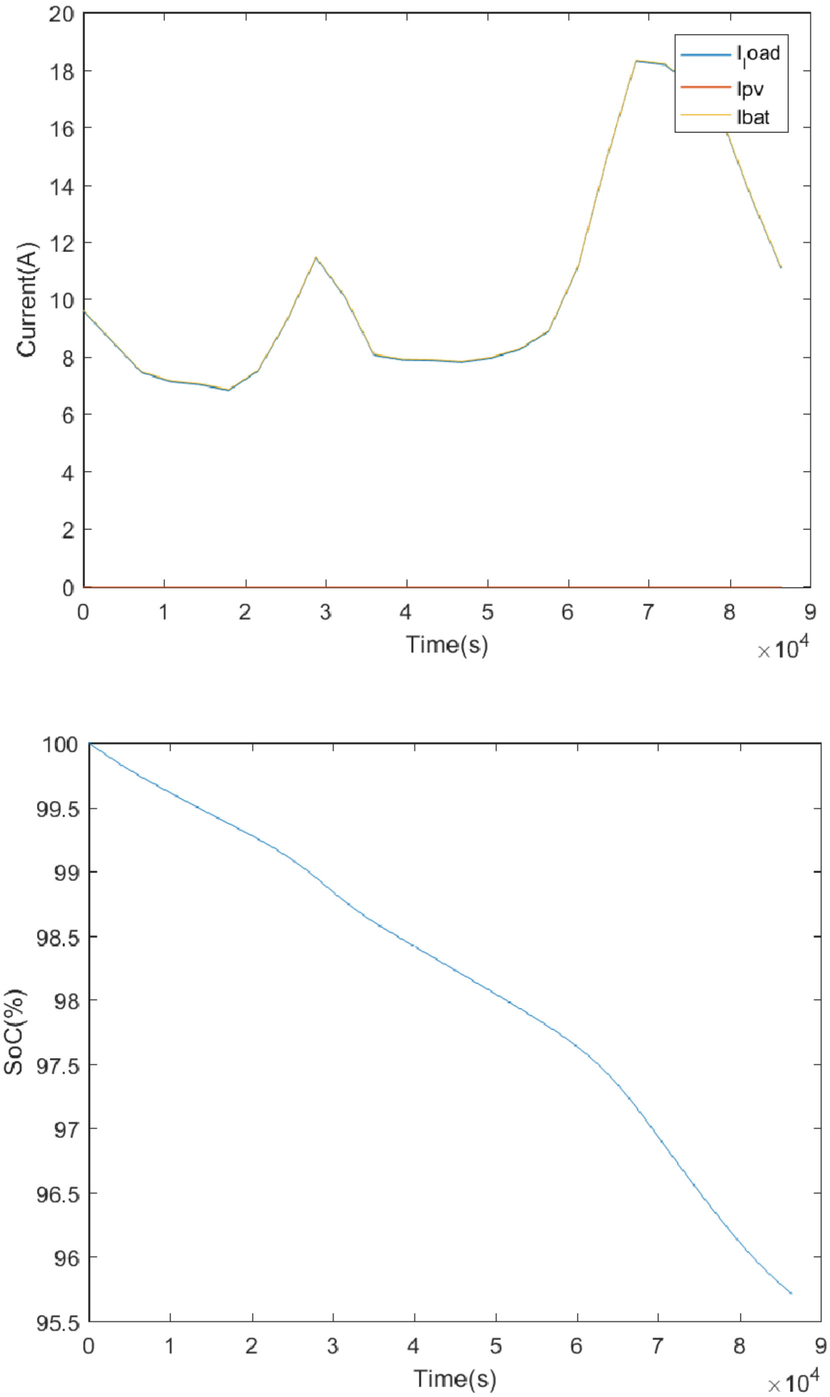

Figure 56-Current and SOC results for Houghton in January 1

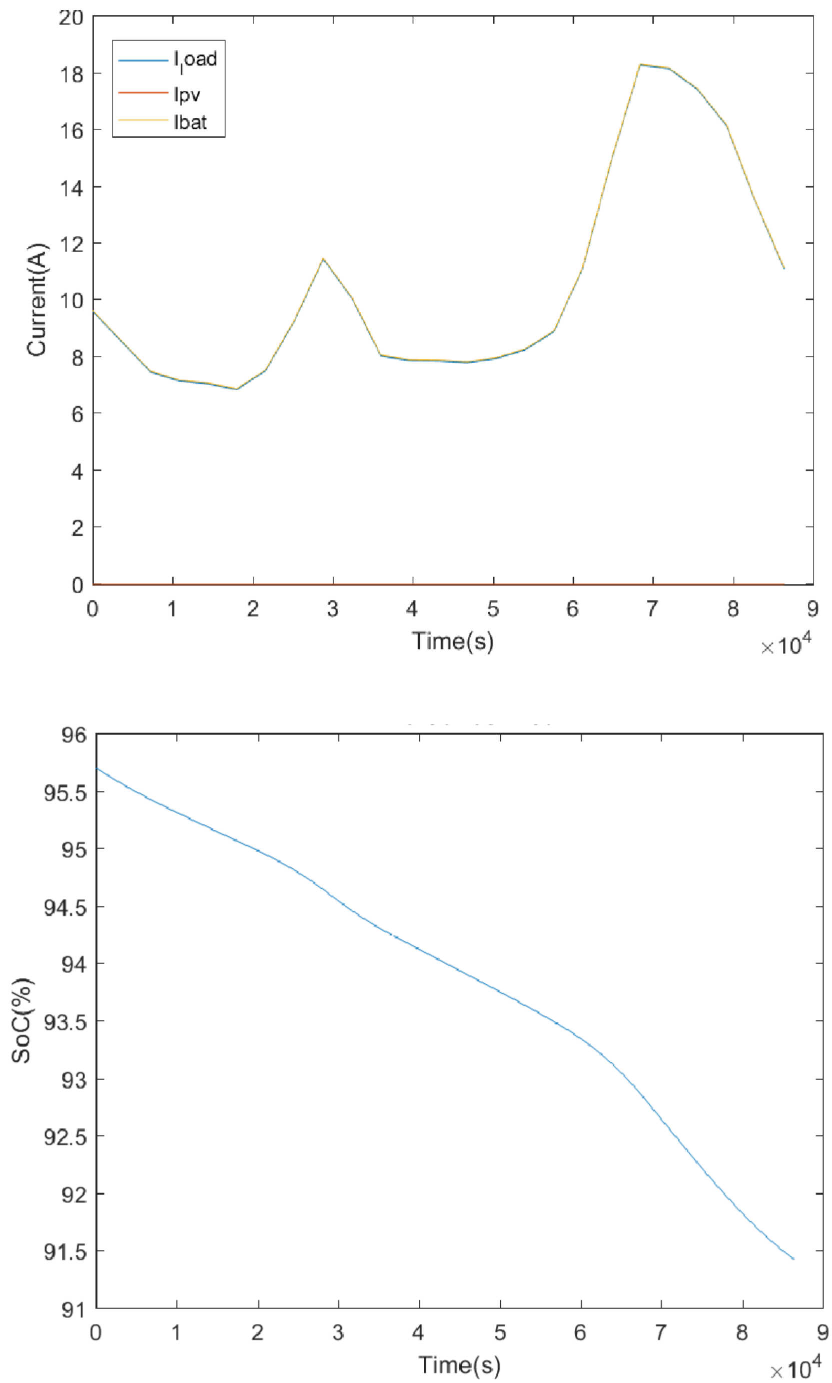

Figure 57-Current and SOC results for Houghton in January 2

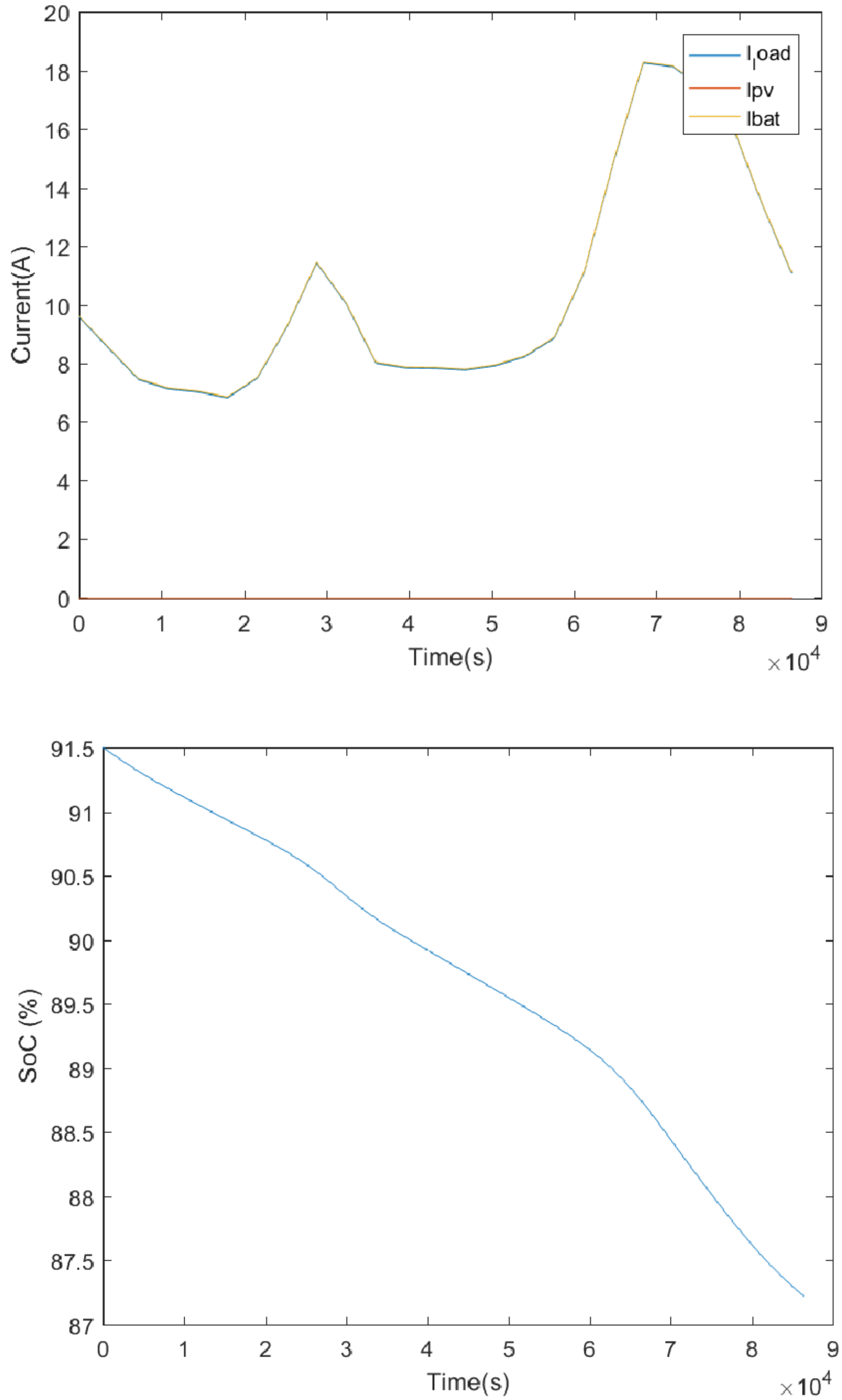

Figure 58-Current and SOC results for Houghton in January 3

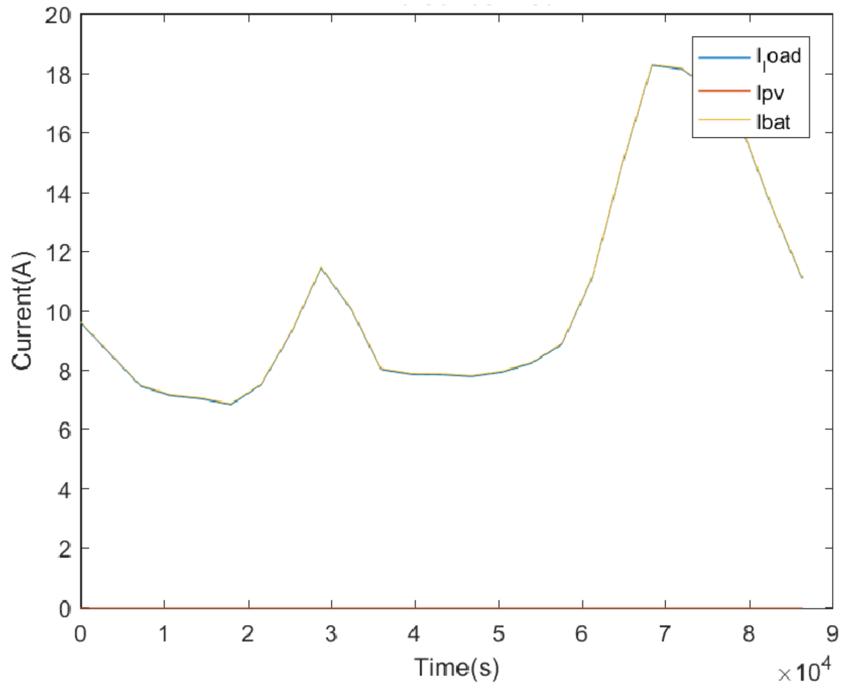

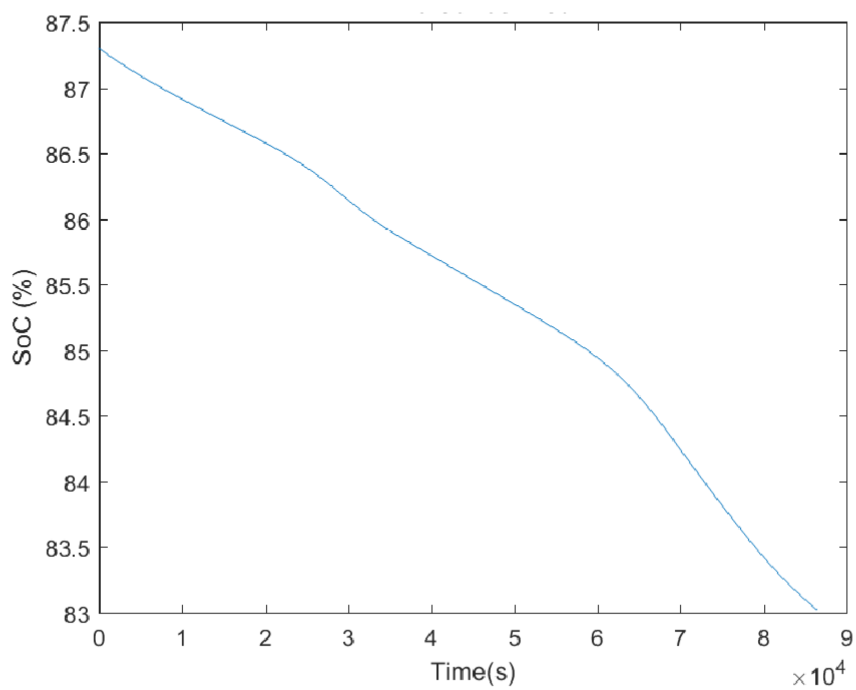

Figure 59-Current and SOC results for Houghton in January 4

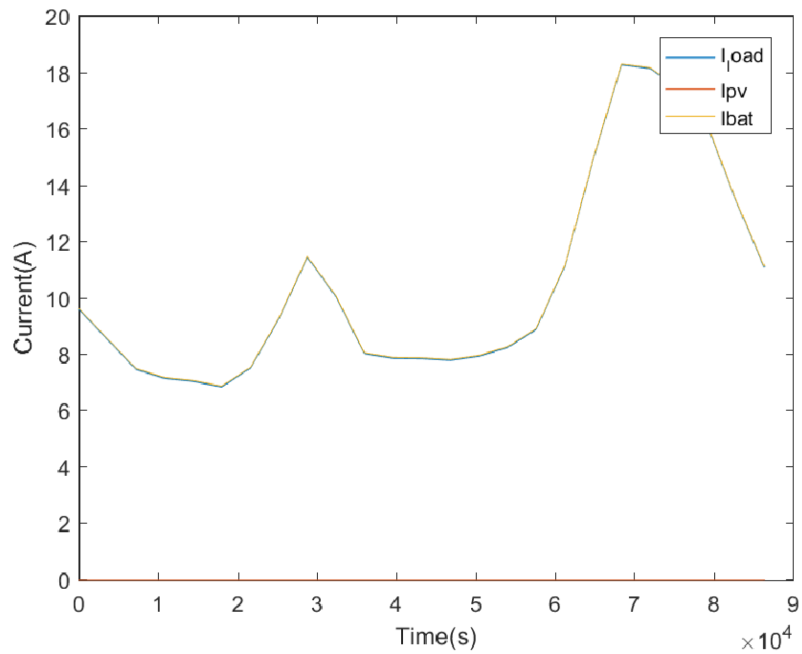

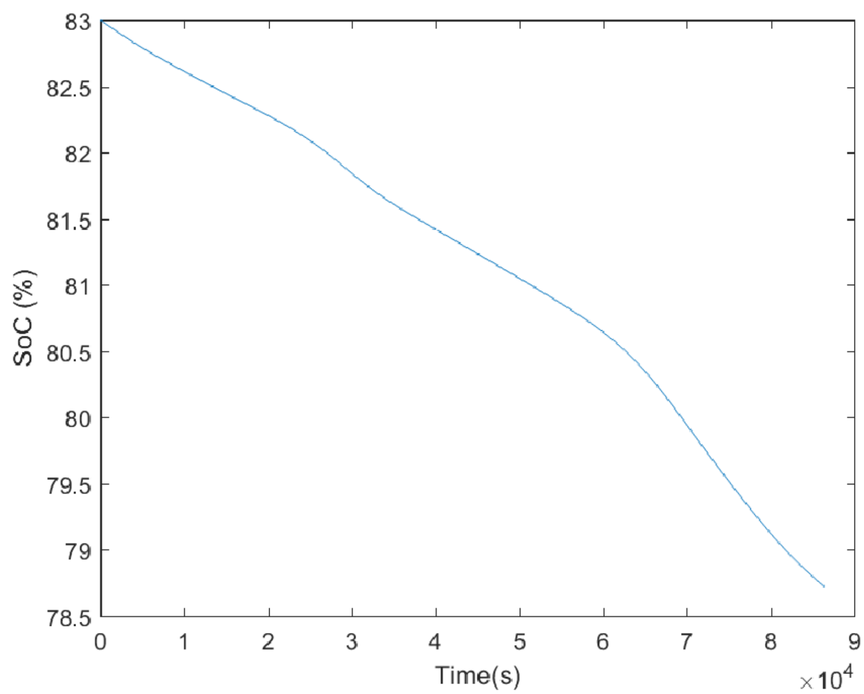

Figure 60-Current and SOC results for Houghton in January 5

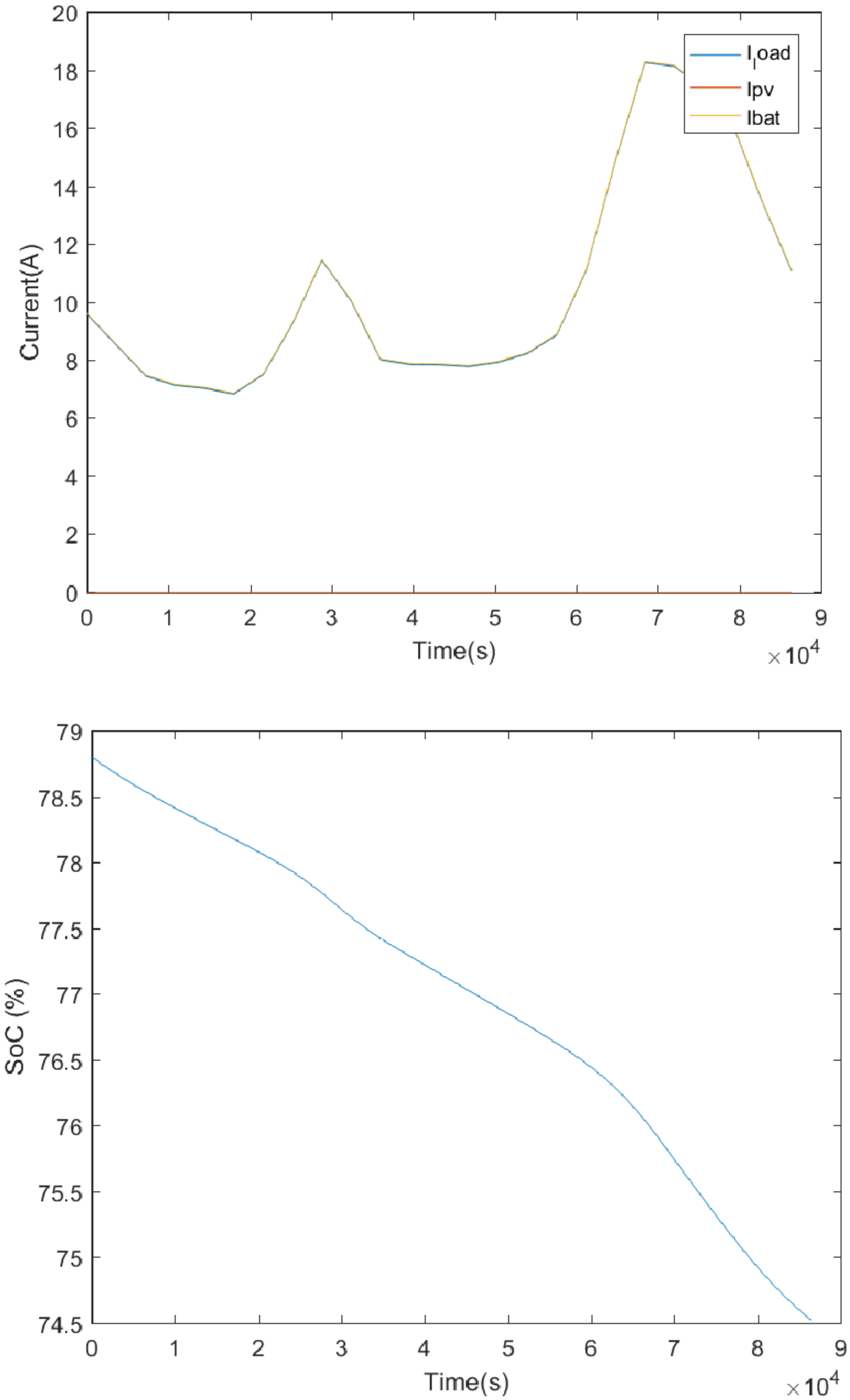

Figure 61-Current and SOC results for Houghton in January 6

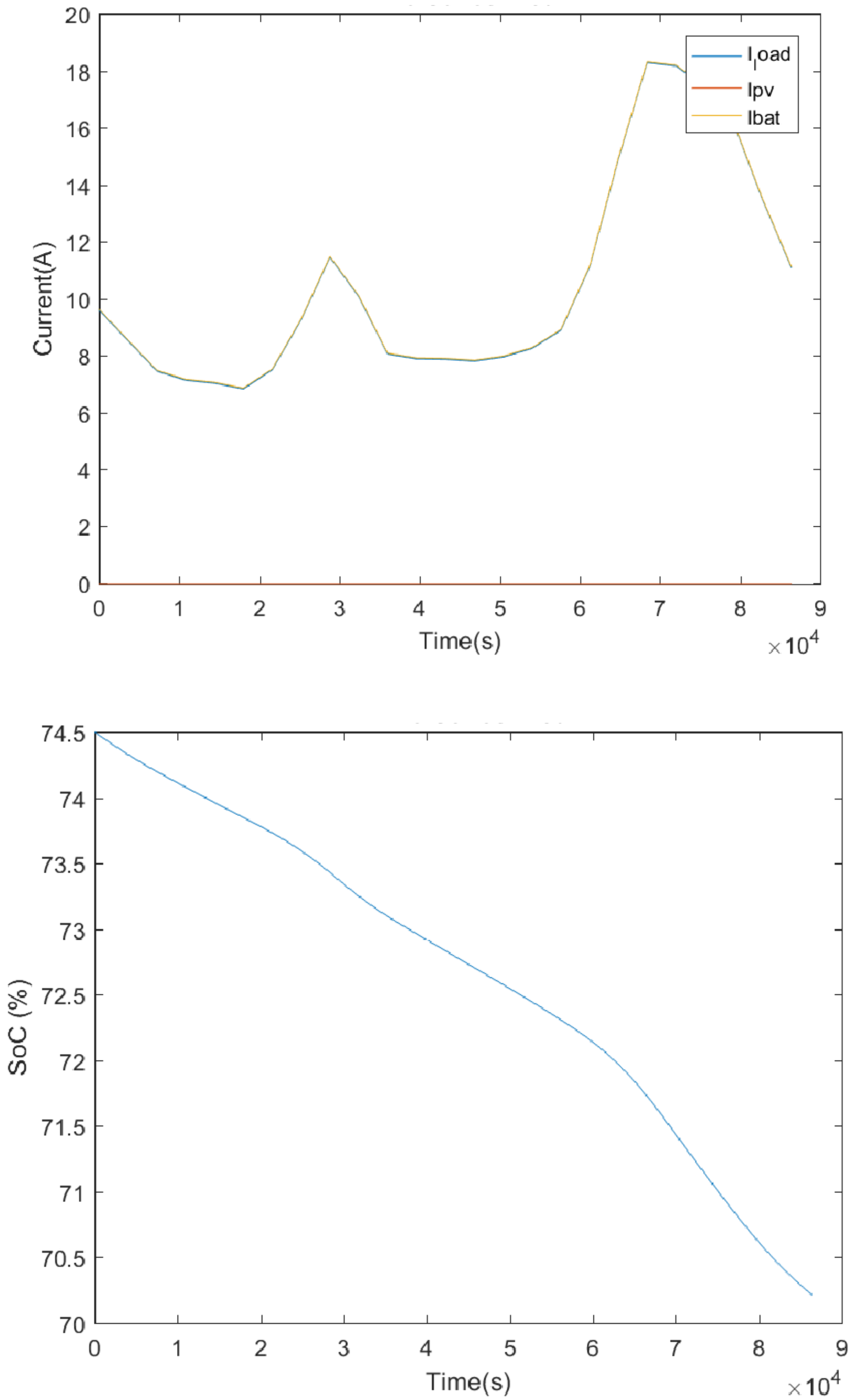

Figure 62-Current and SOC results for Houghton in January 7

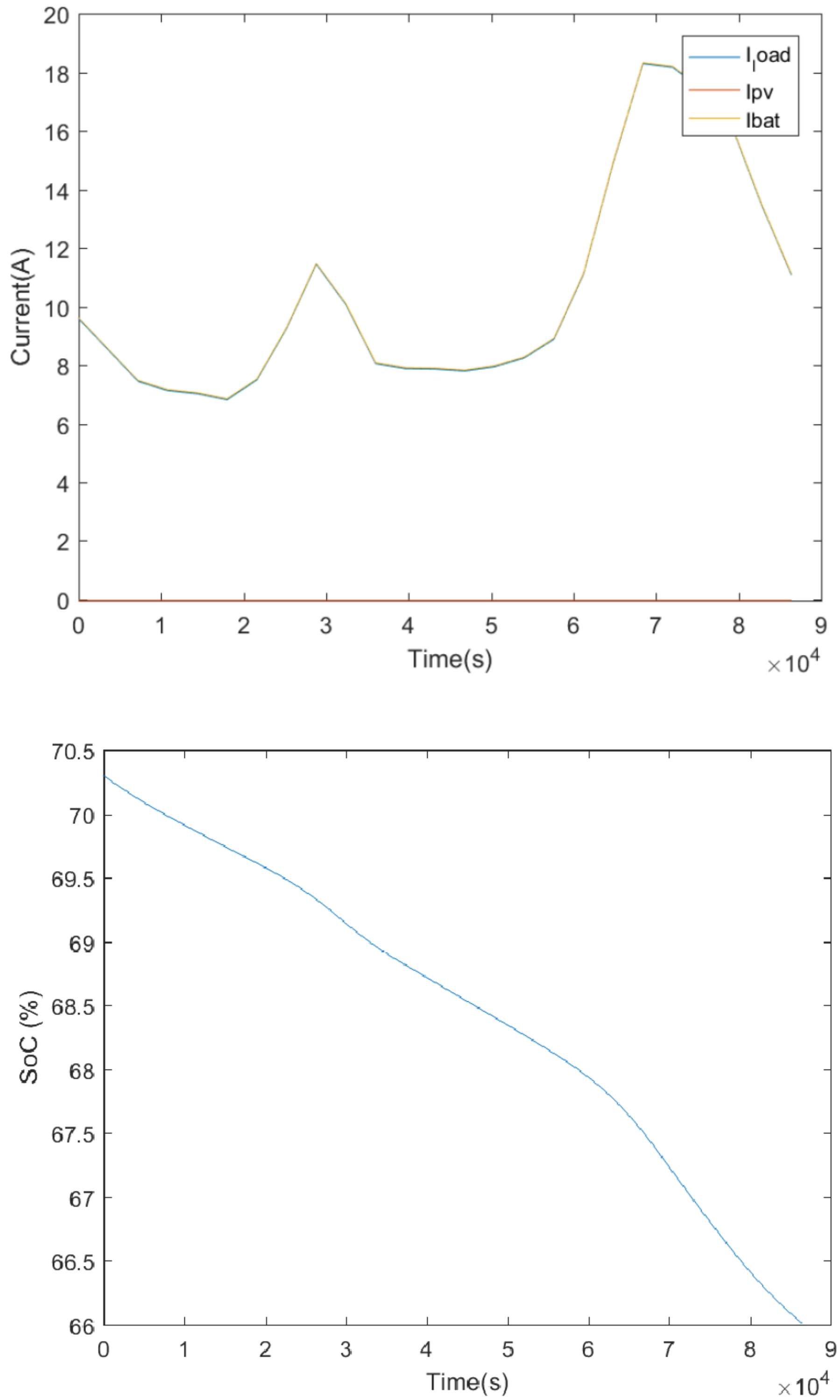

Figure 63-Current and SOC results for Houghton in January 8

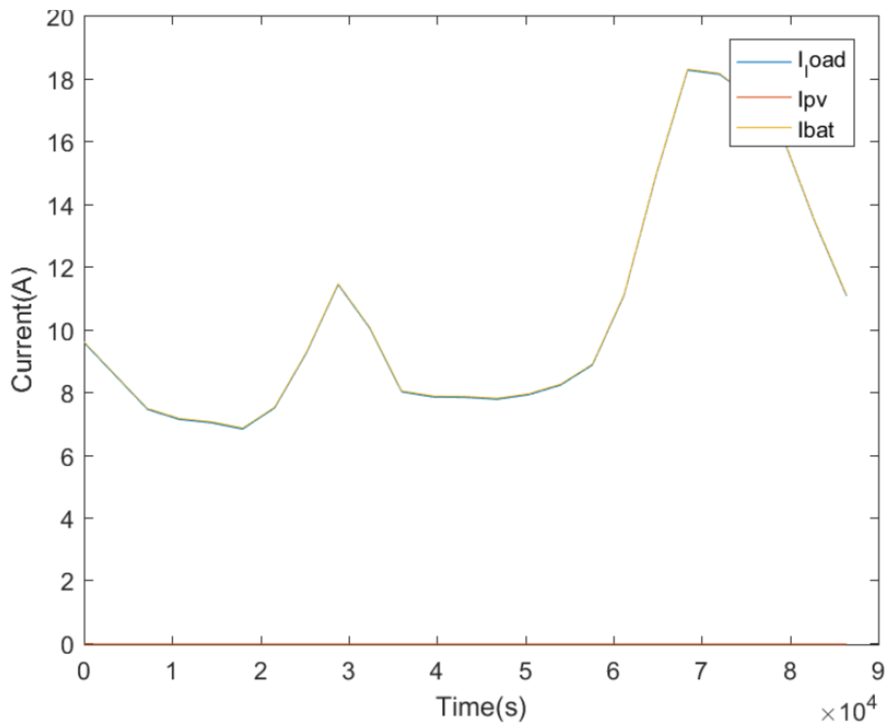

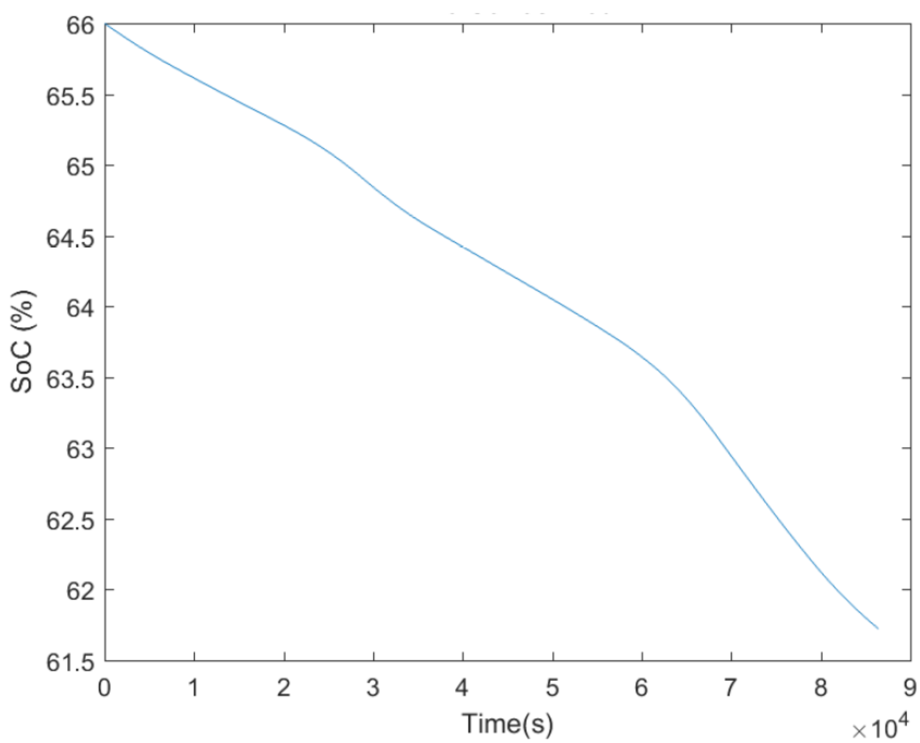

Figure 64-Current and SOC results for Houghton in January 9

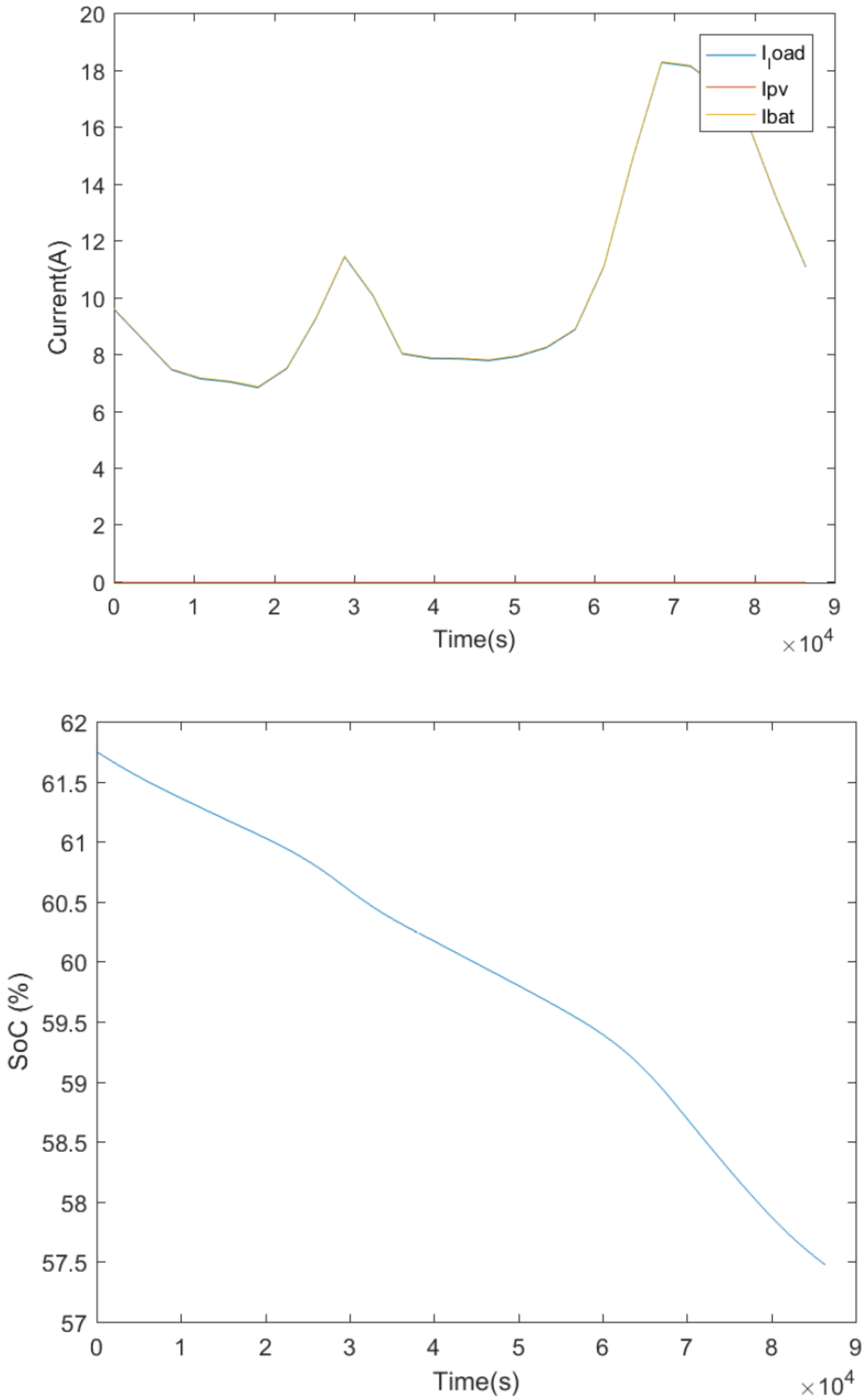

Figure 65-Current and SOC results for Houghton in January 10

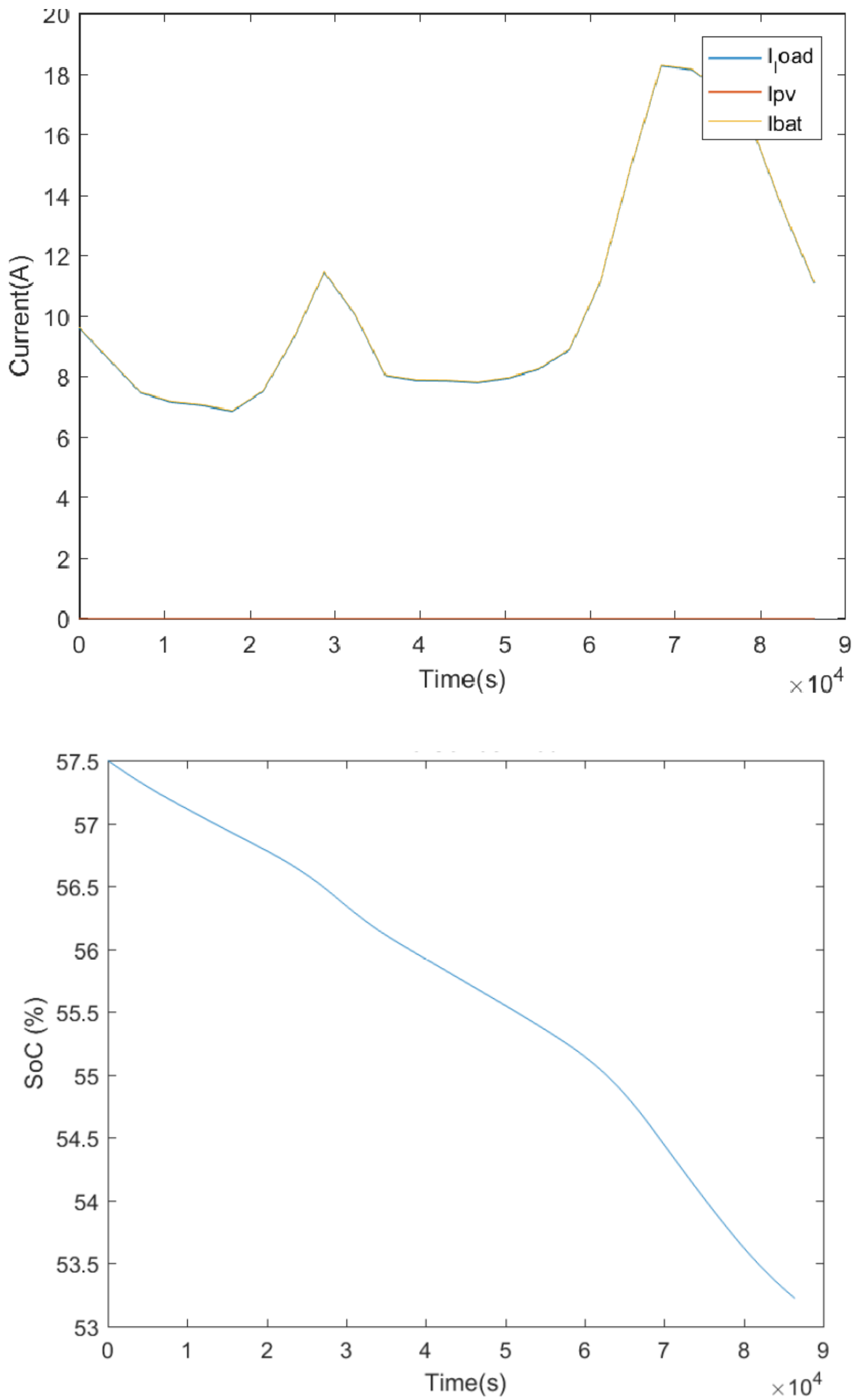

Figure 66-Current and SOC results for Houghton in January 11

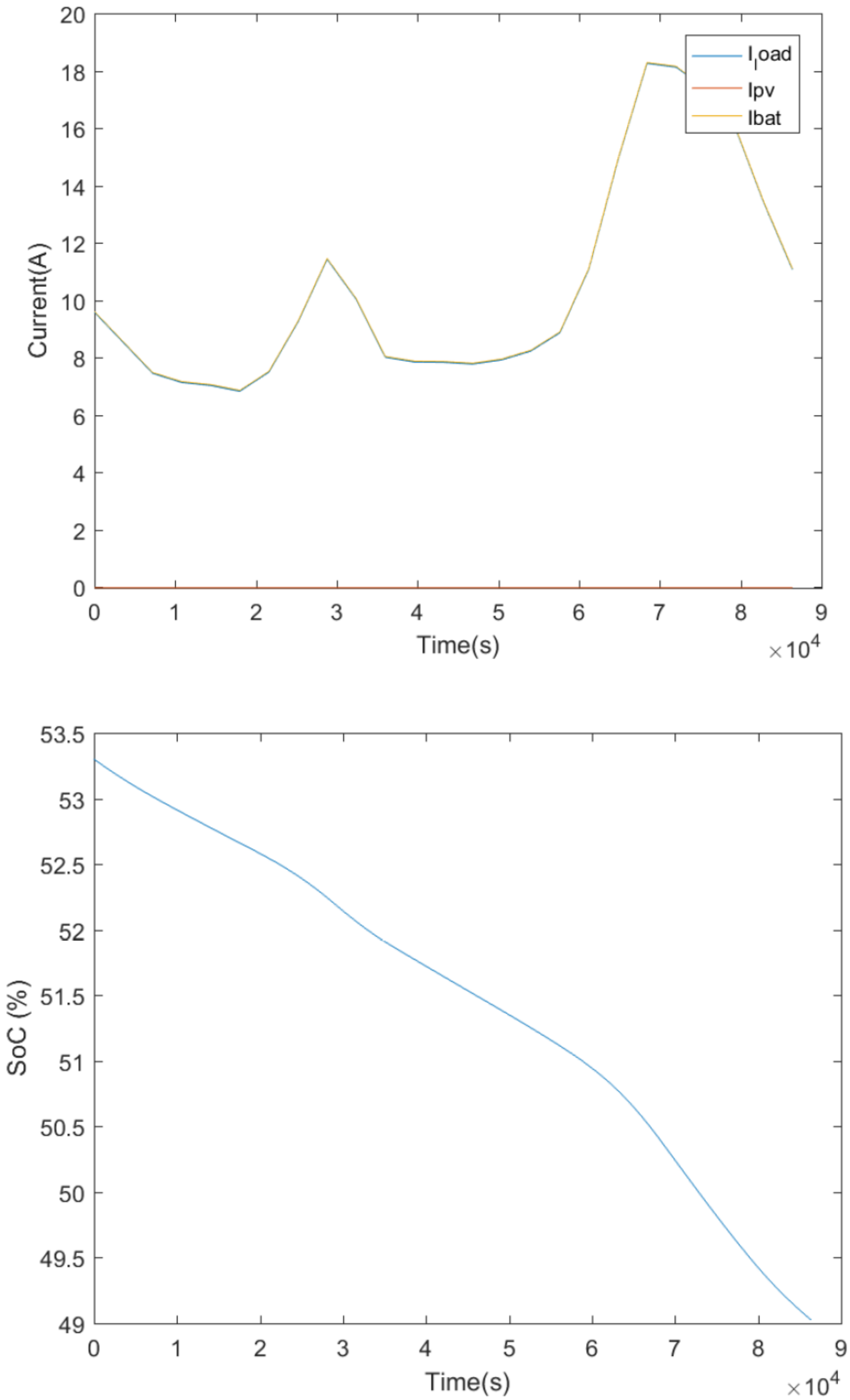

Figure 67-Current and SOC results for Houghton in January 12

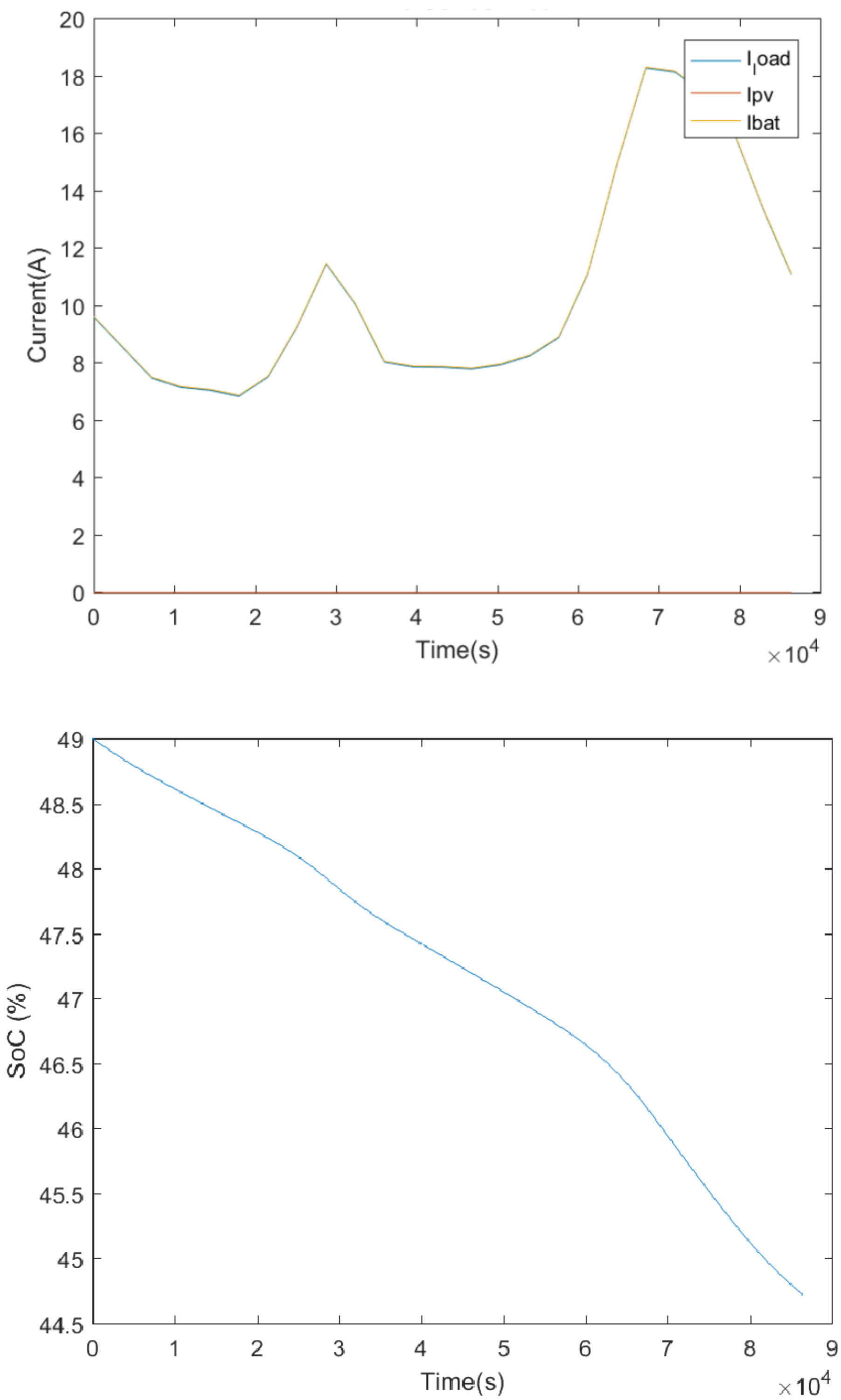

Figure 68-Current and SOC results for Houghton in January 13

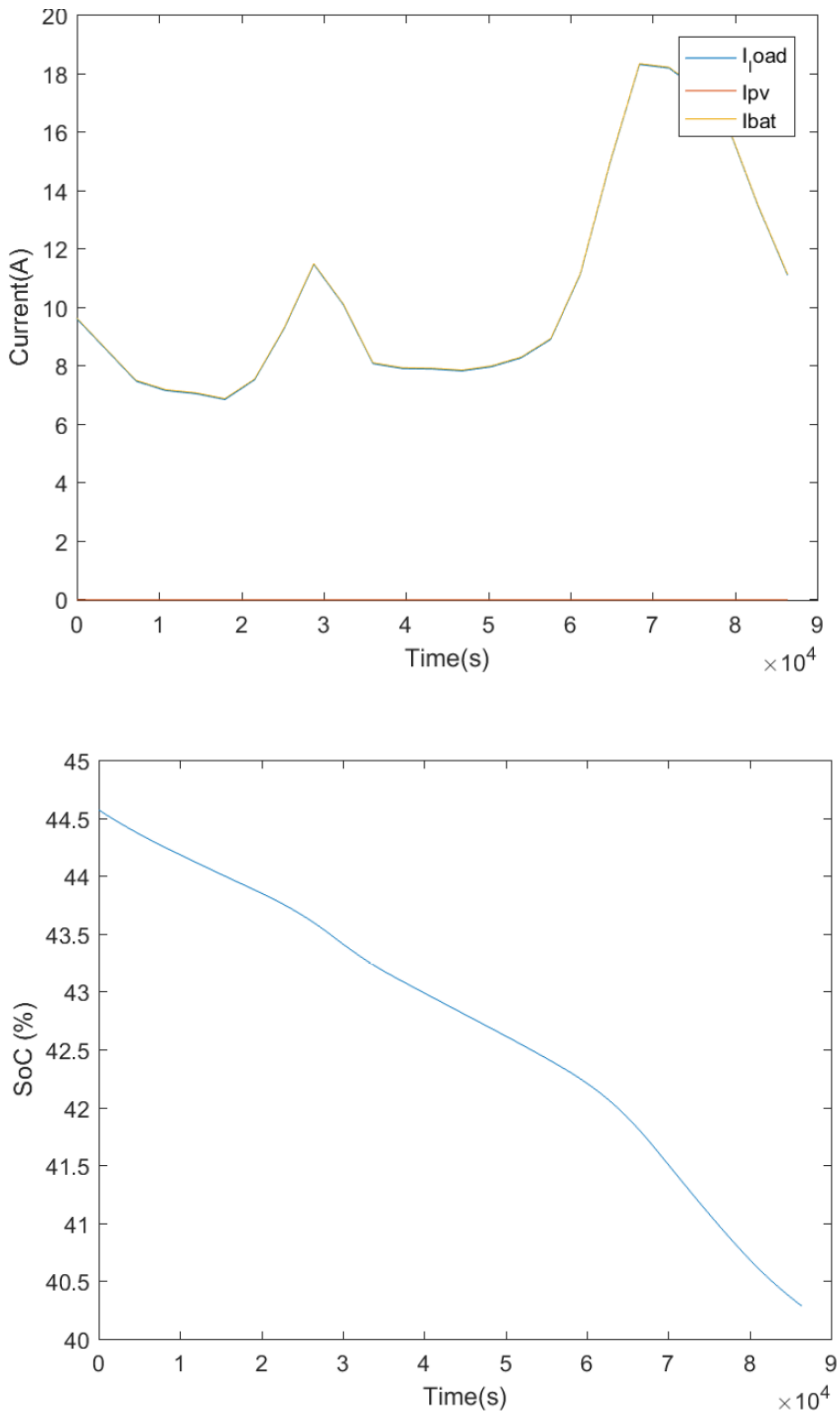

Figure 69-Current and SOC results for Houghton in January 14

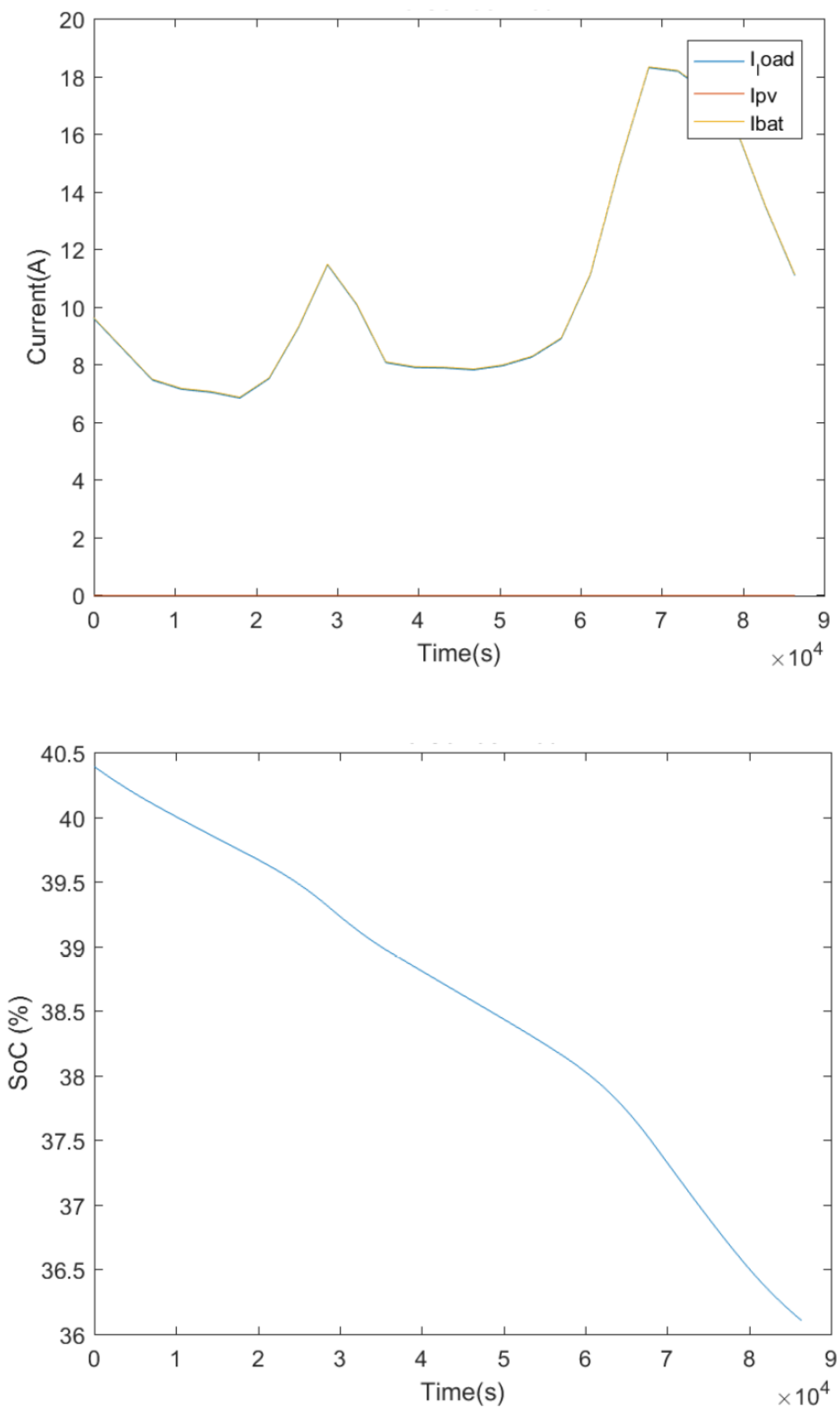

Figure 70-Current and SOC results for Houghton in January 15

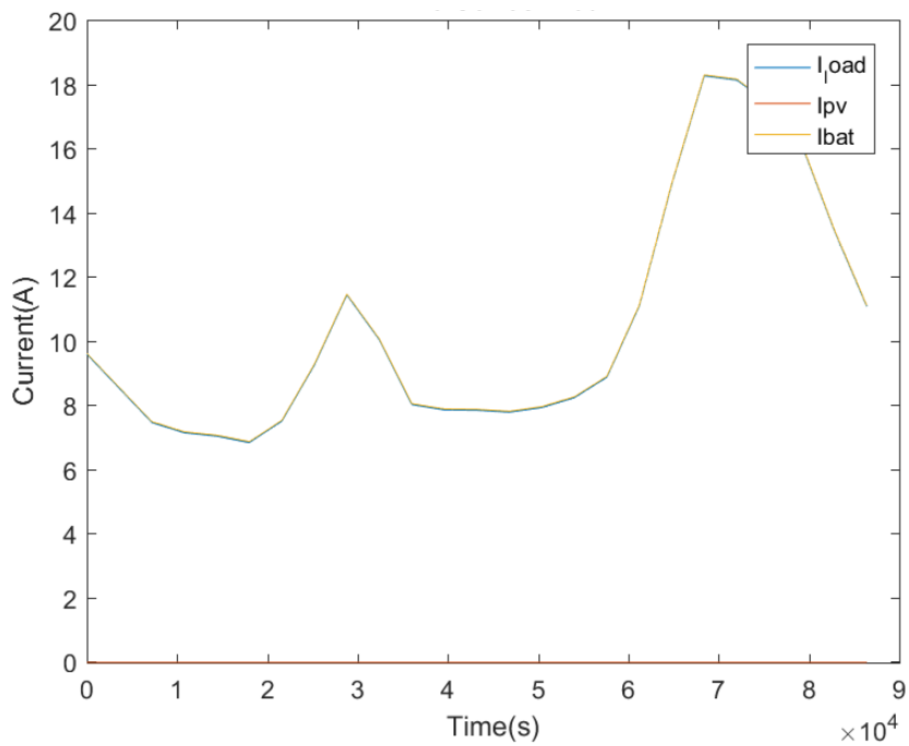

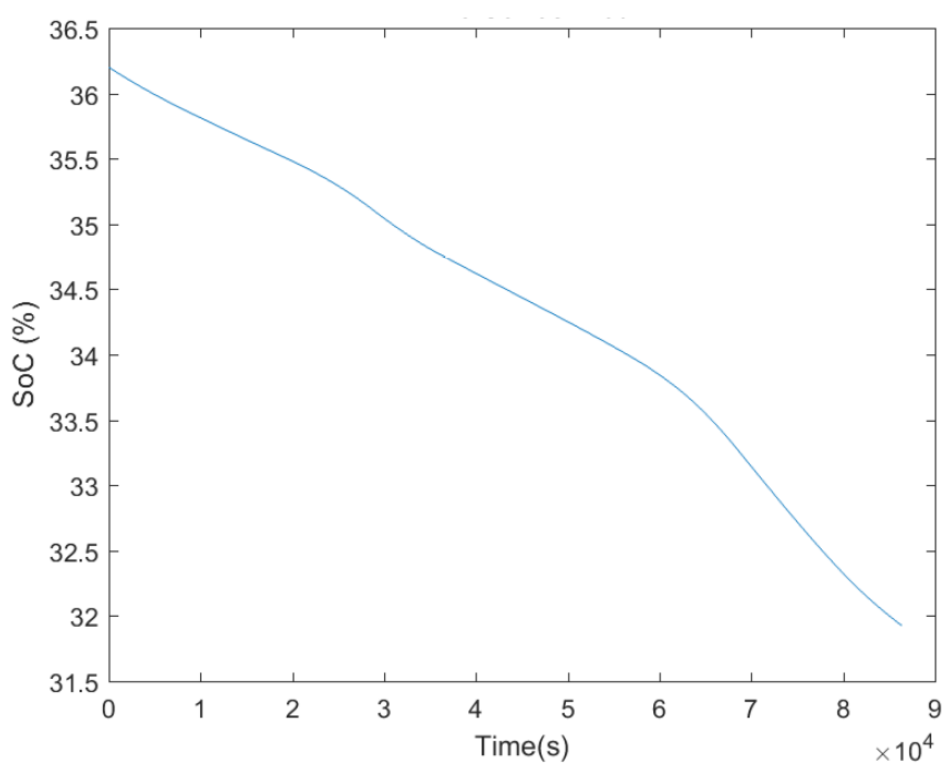

Figure 71-Current and SOC results for Houghton in January 16

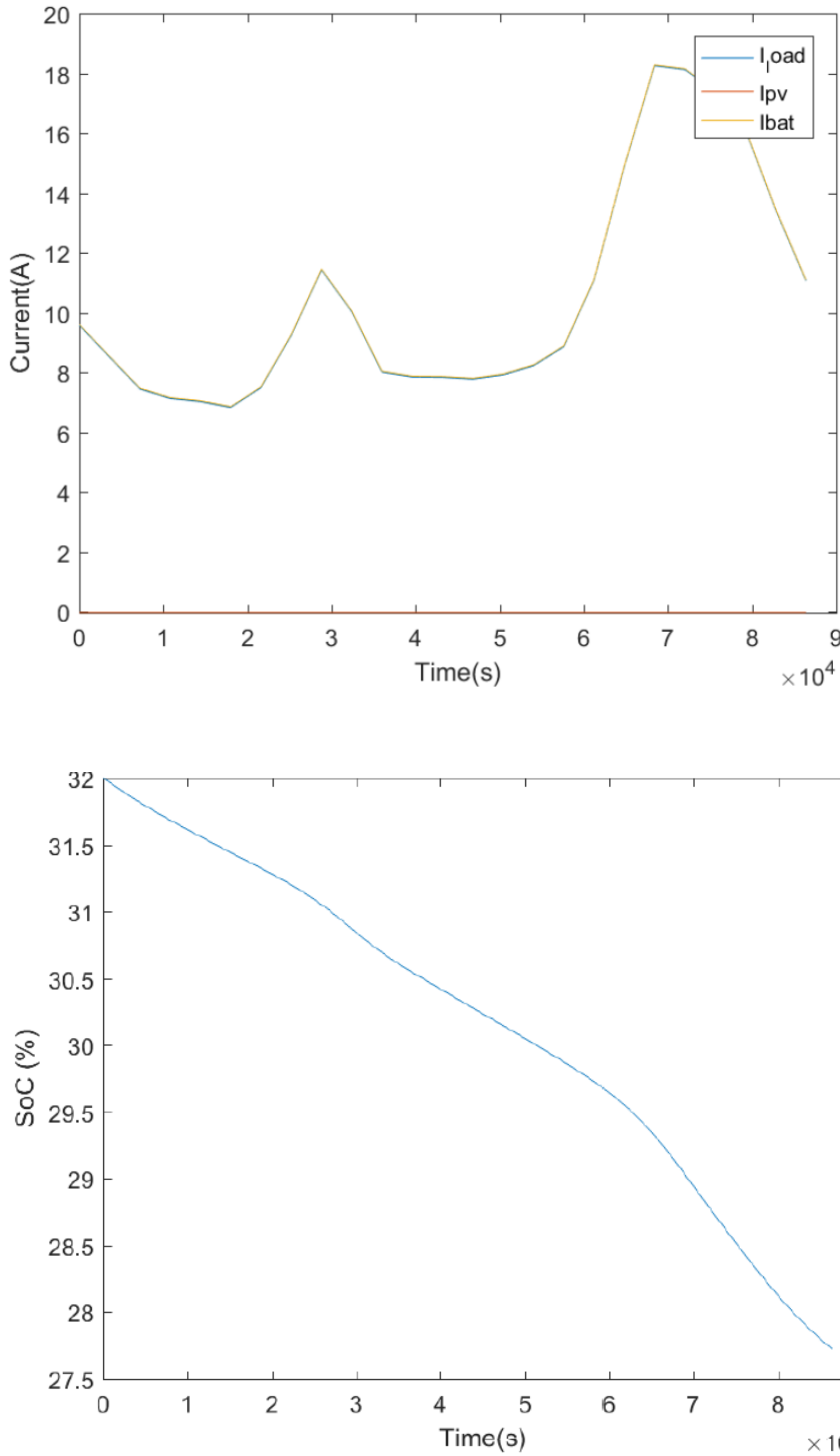

Figure 72-Current and SOC results for Houghton in January 17

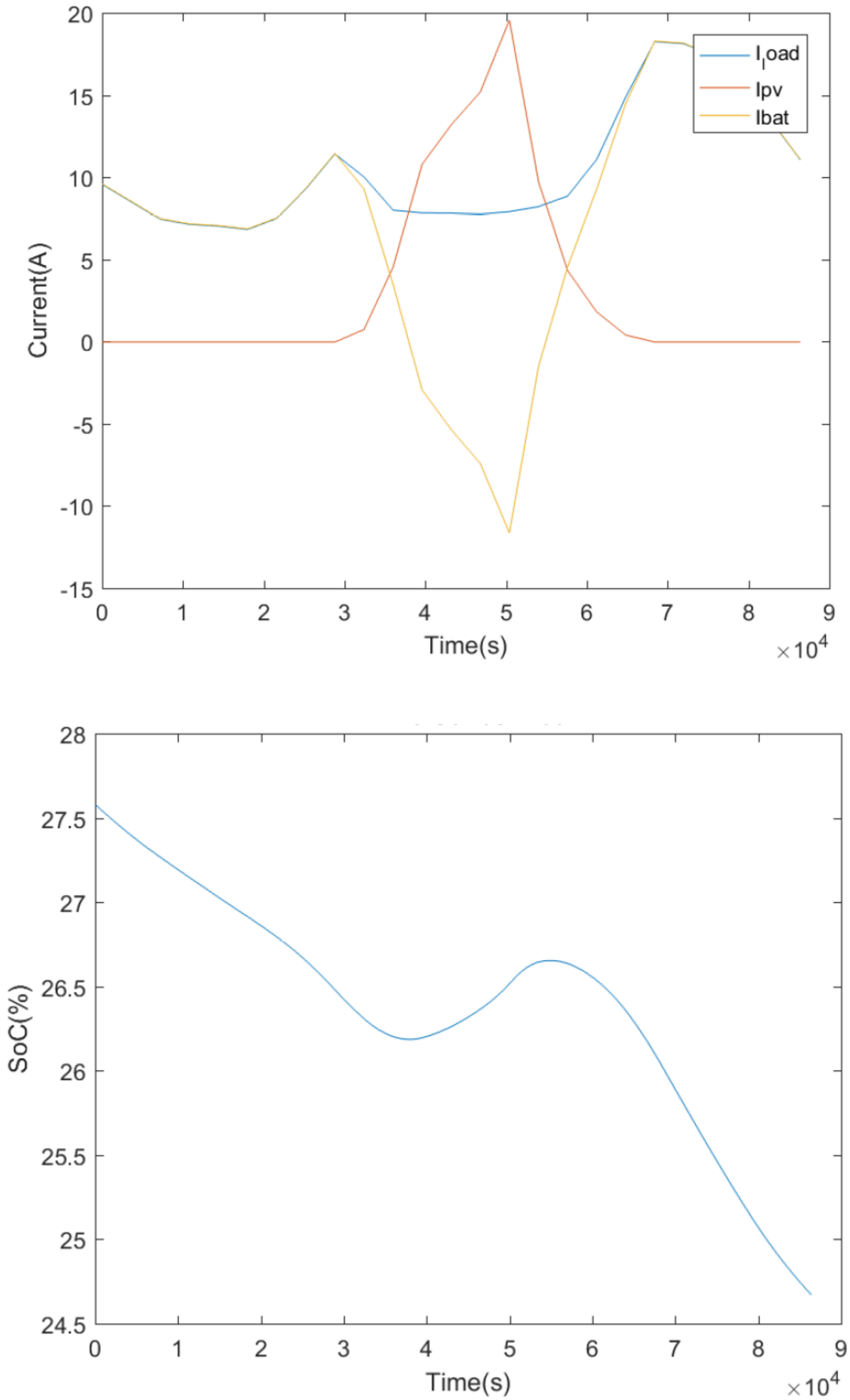

Figure 73-Current and SOC results for Houghton in January 18

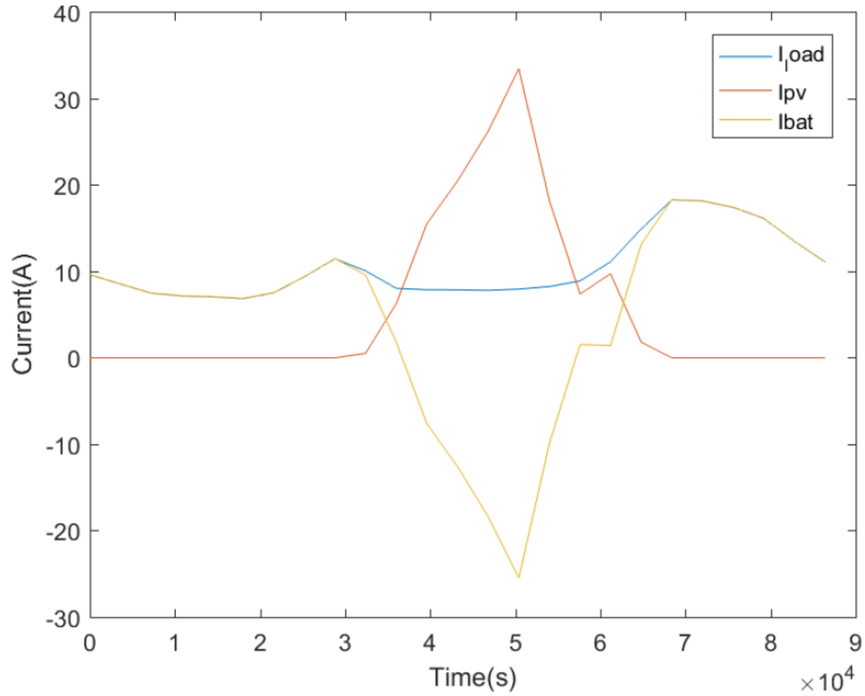

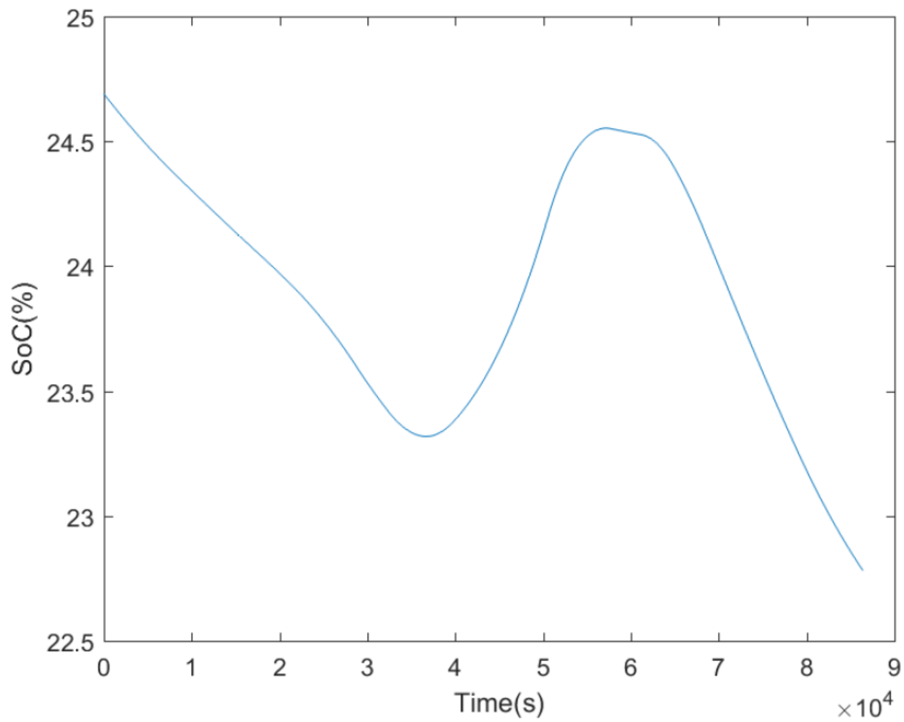

Figure 74-Current and SOC results for Houghton in January 19

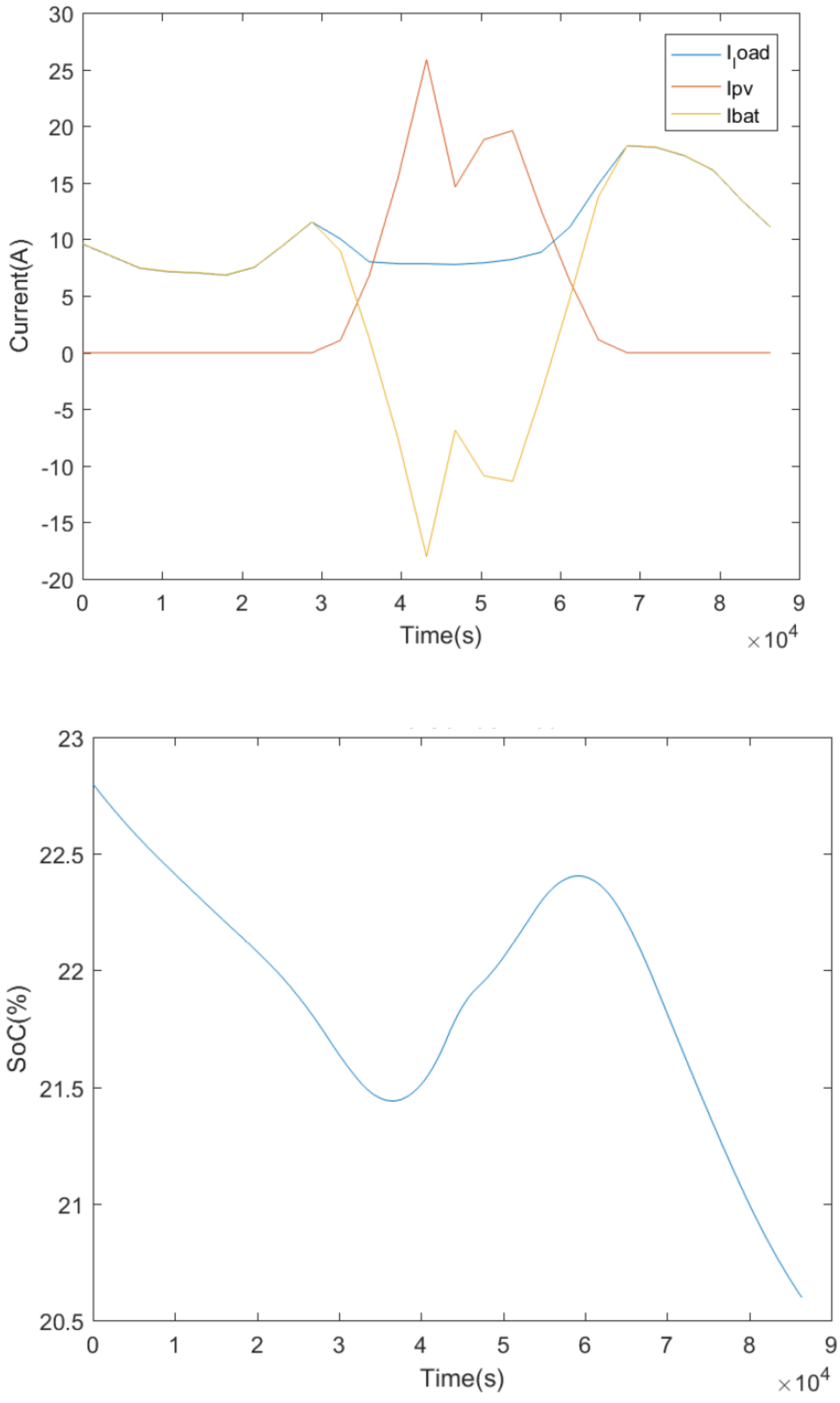

Figure 75-Current and SOC results for Houghton in January 20

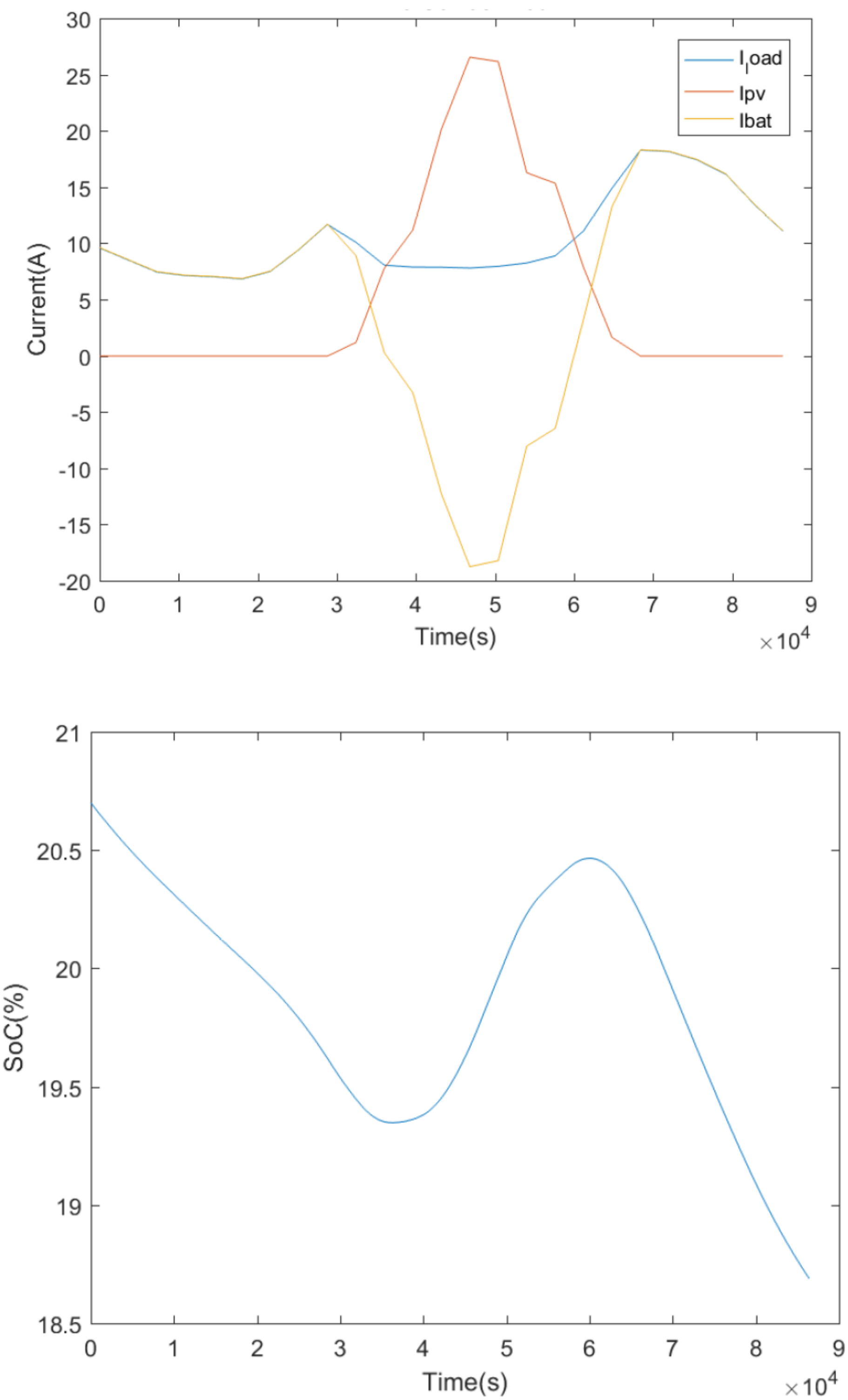

Figure 76-Current and SOC results for Houghton in January 21

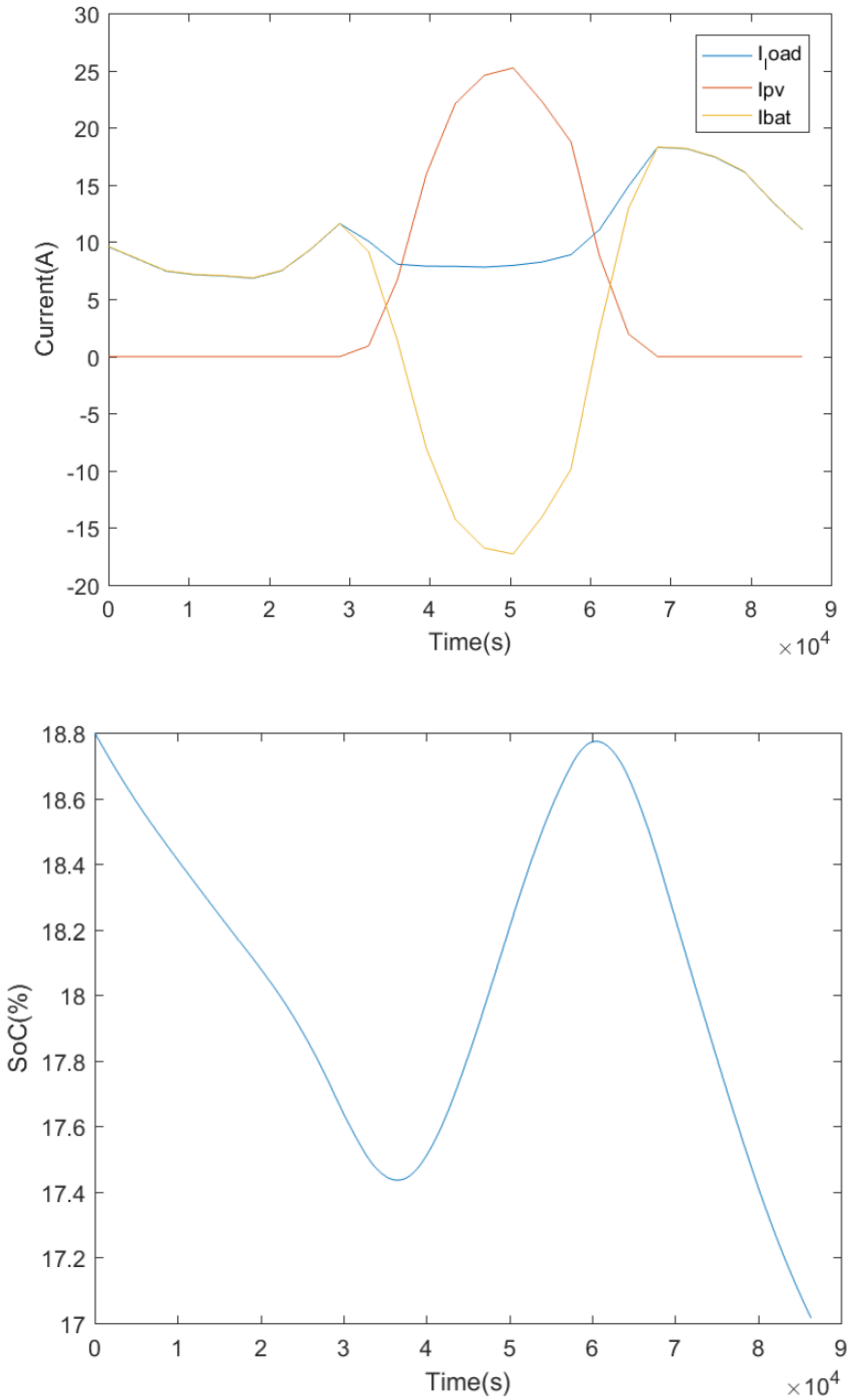

Figure 77-Current and SOC results for Houghton in January 22

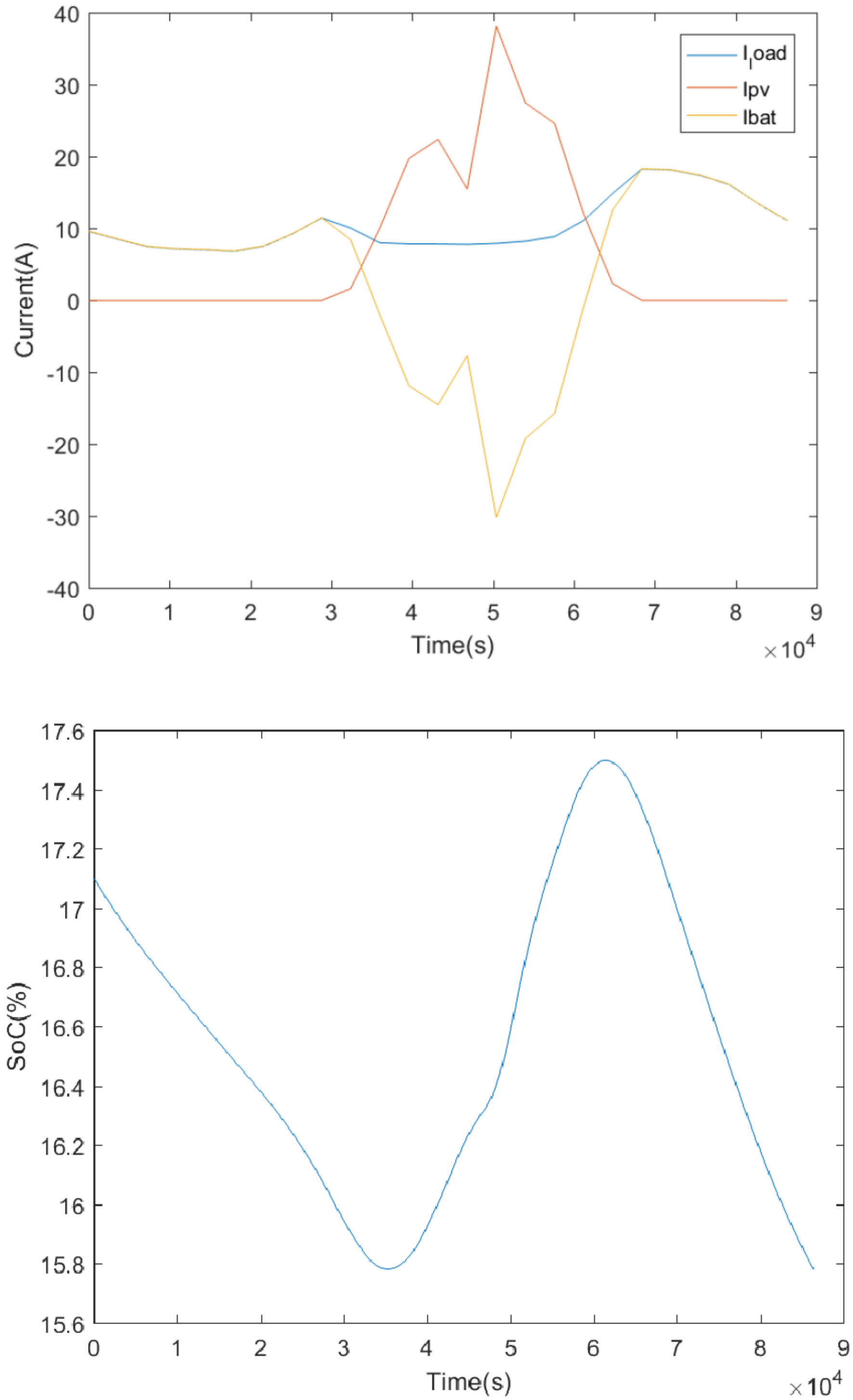

Figure 78-Current and SOC results for Houghton in January 23

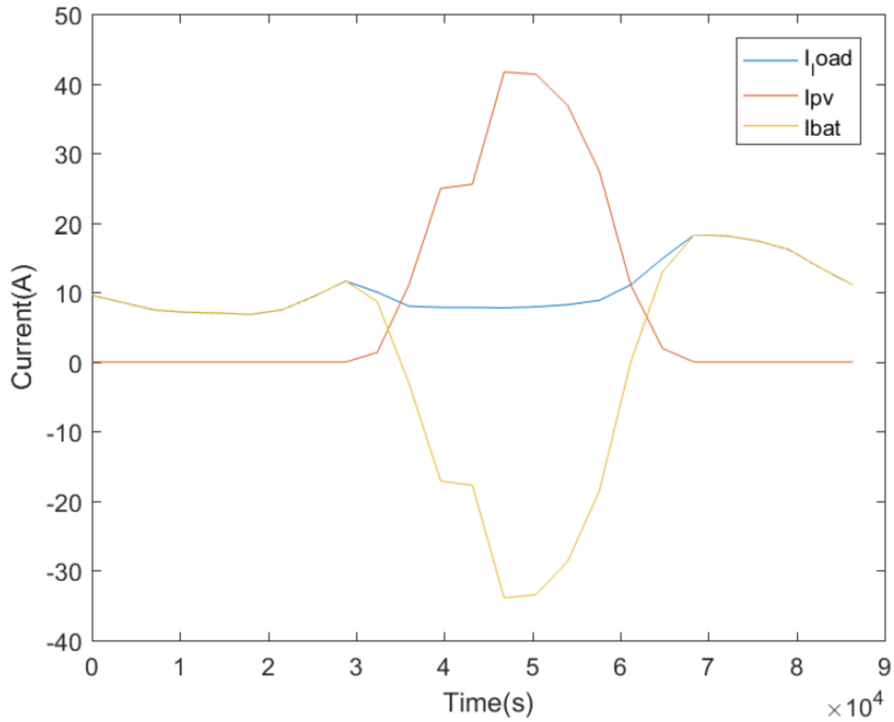

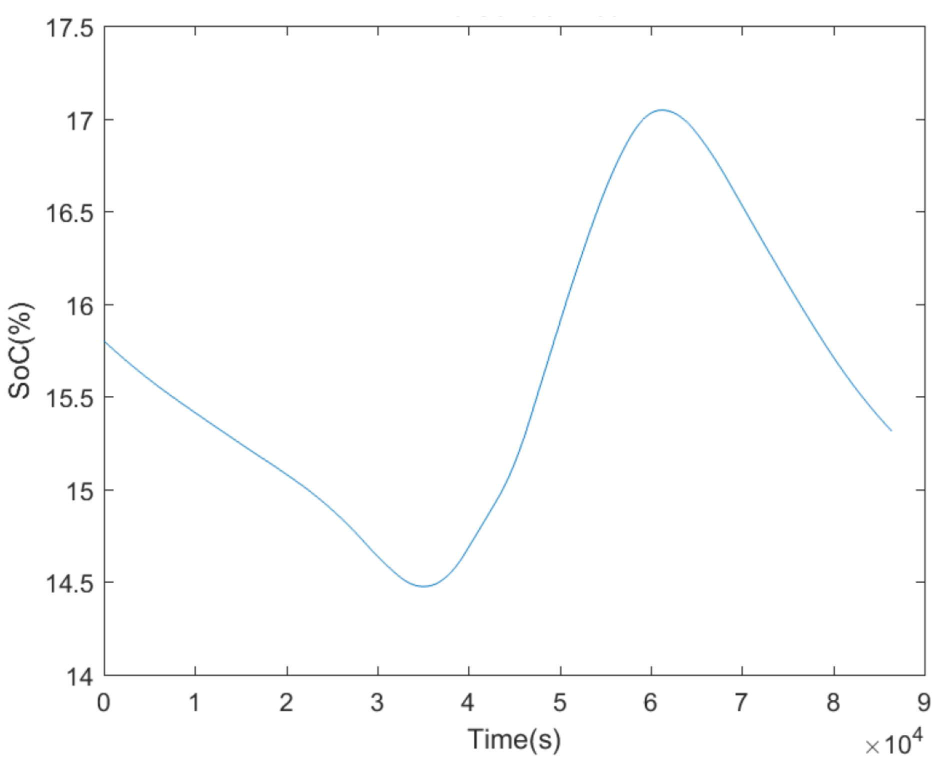

Figure 79-Current and SOC results for Houghton in January 24

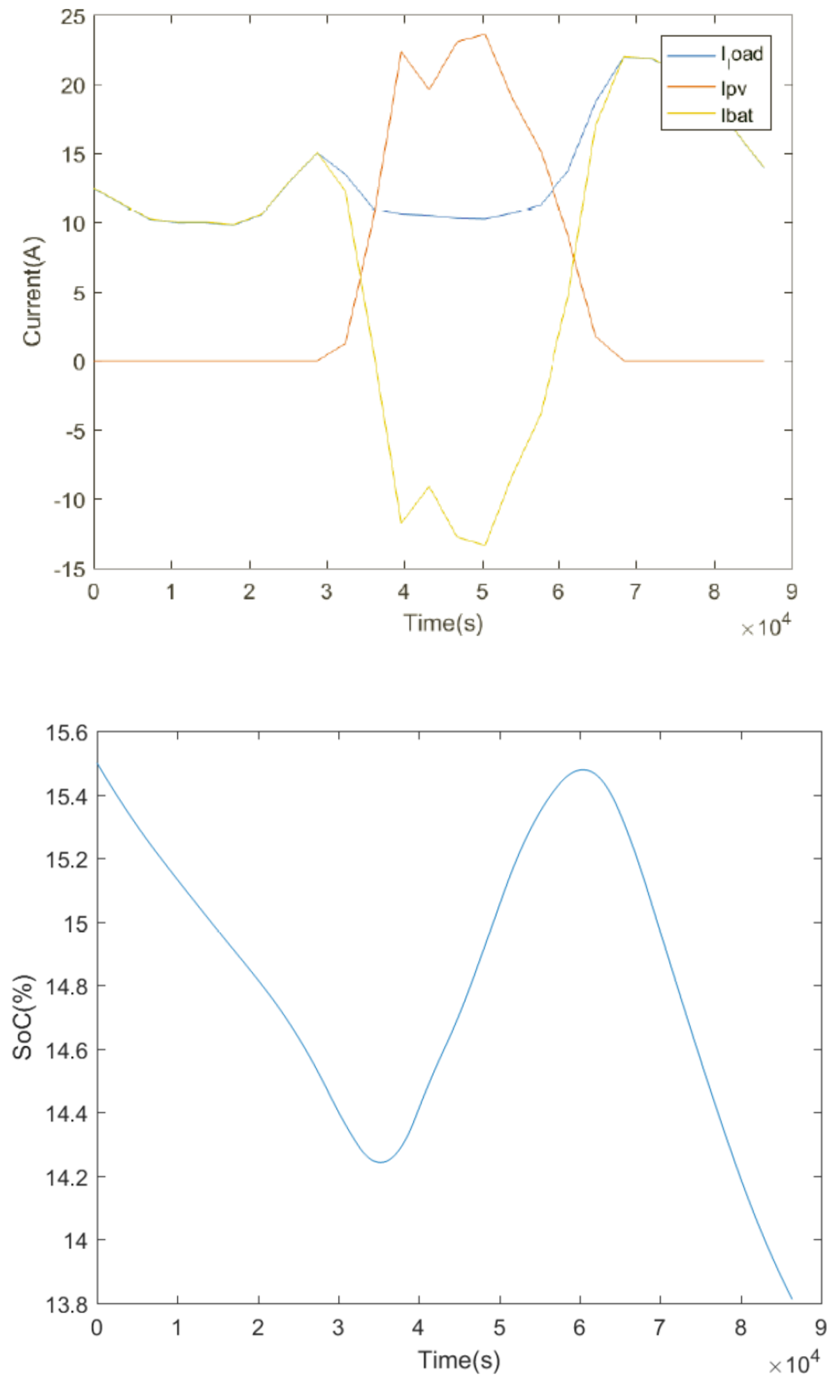

Figure 80-Current and SOC results for Houghton in January 25

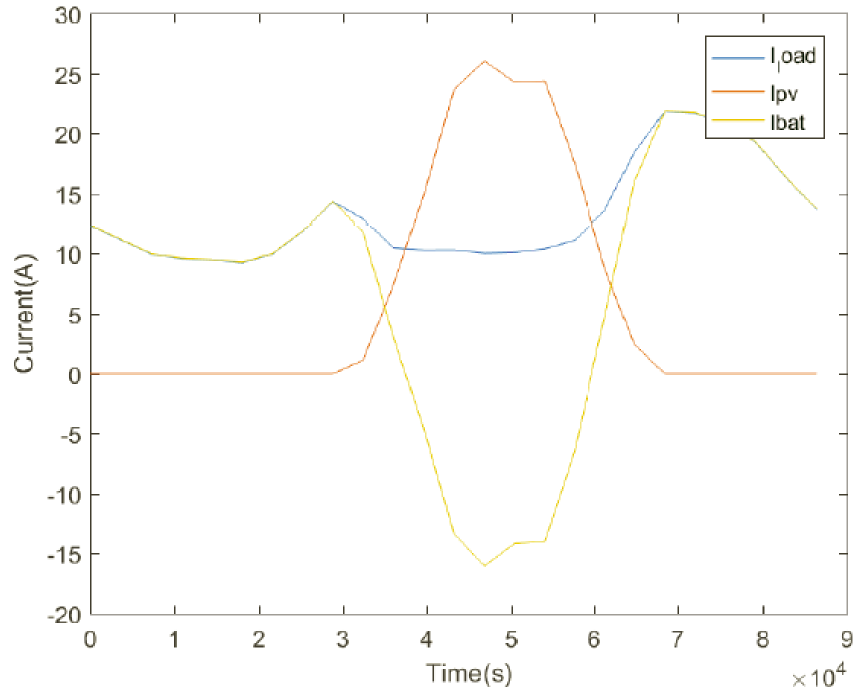

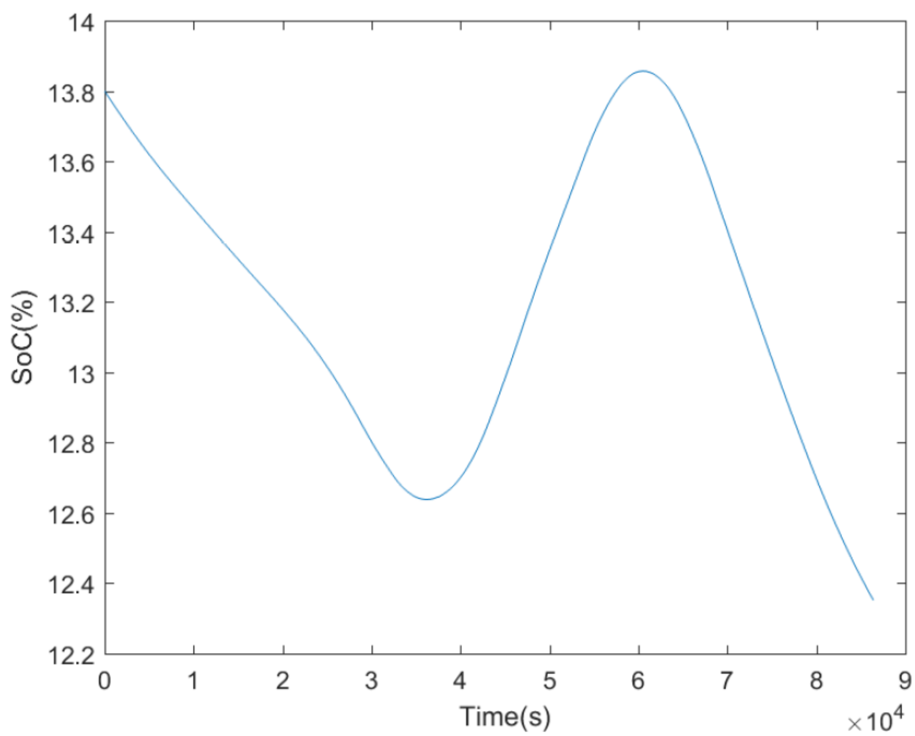

Figure 81-Current and SOC results for Houghton in January 26

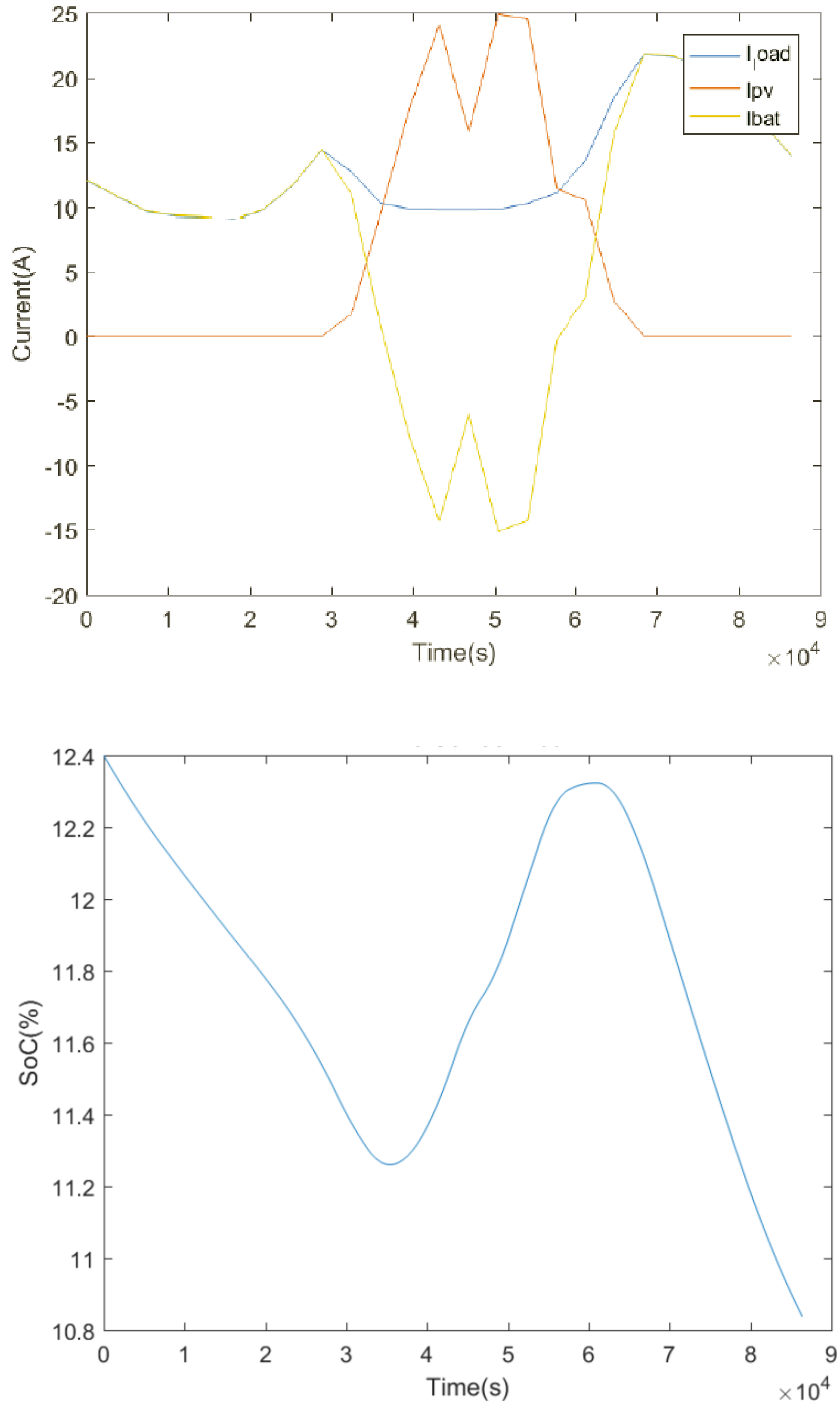

Figure 82-Current and SOC results for Houghton in January 27

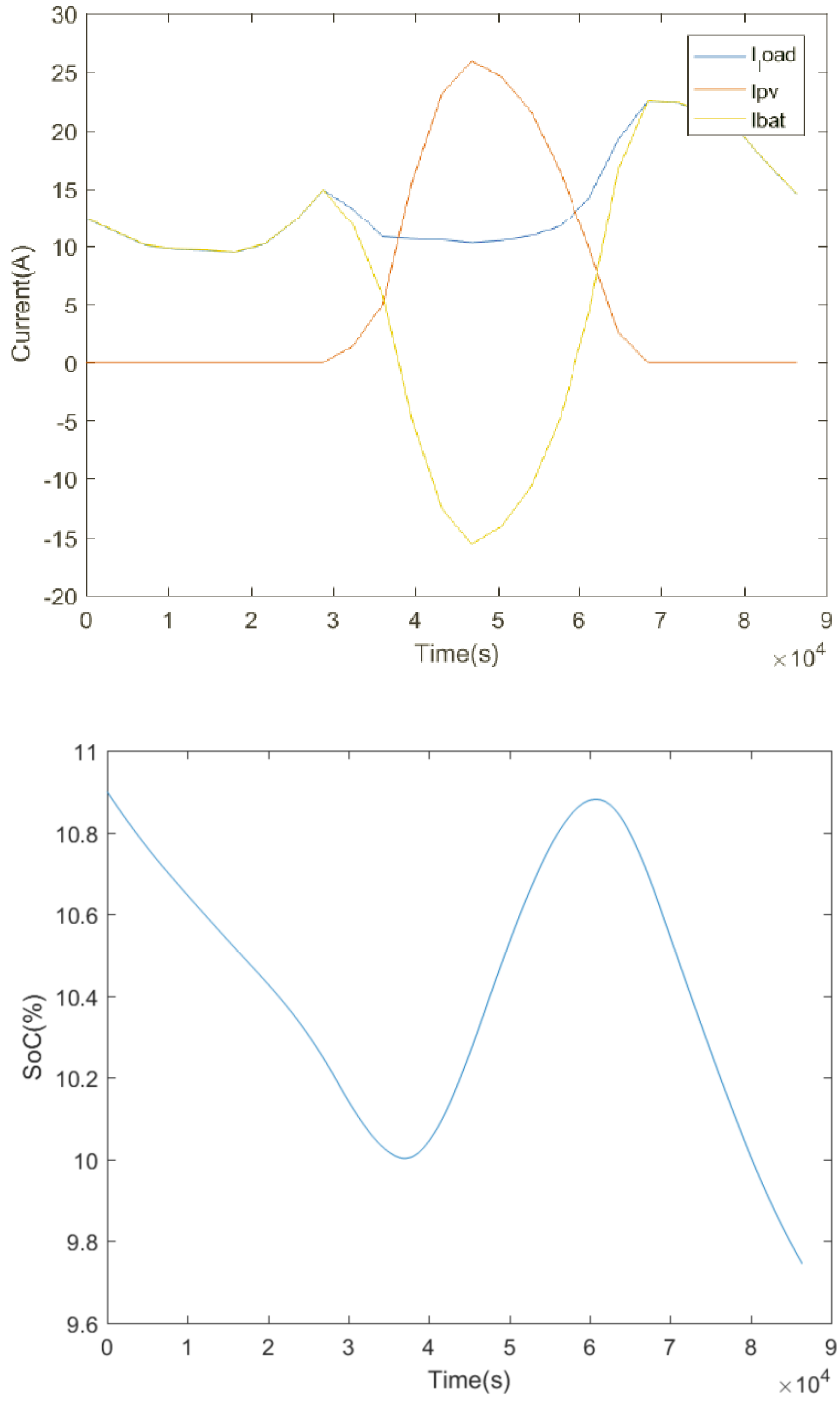

Figure 83-Current and SOC results for Houghton in January 28

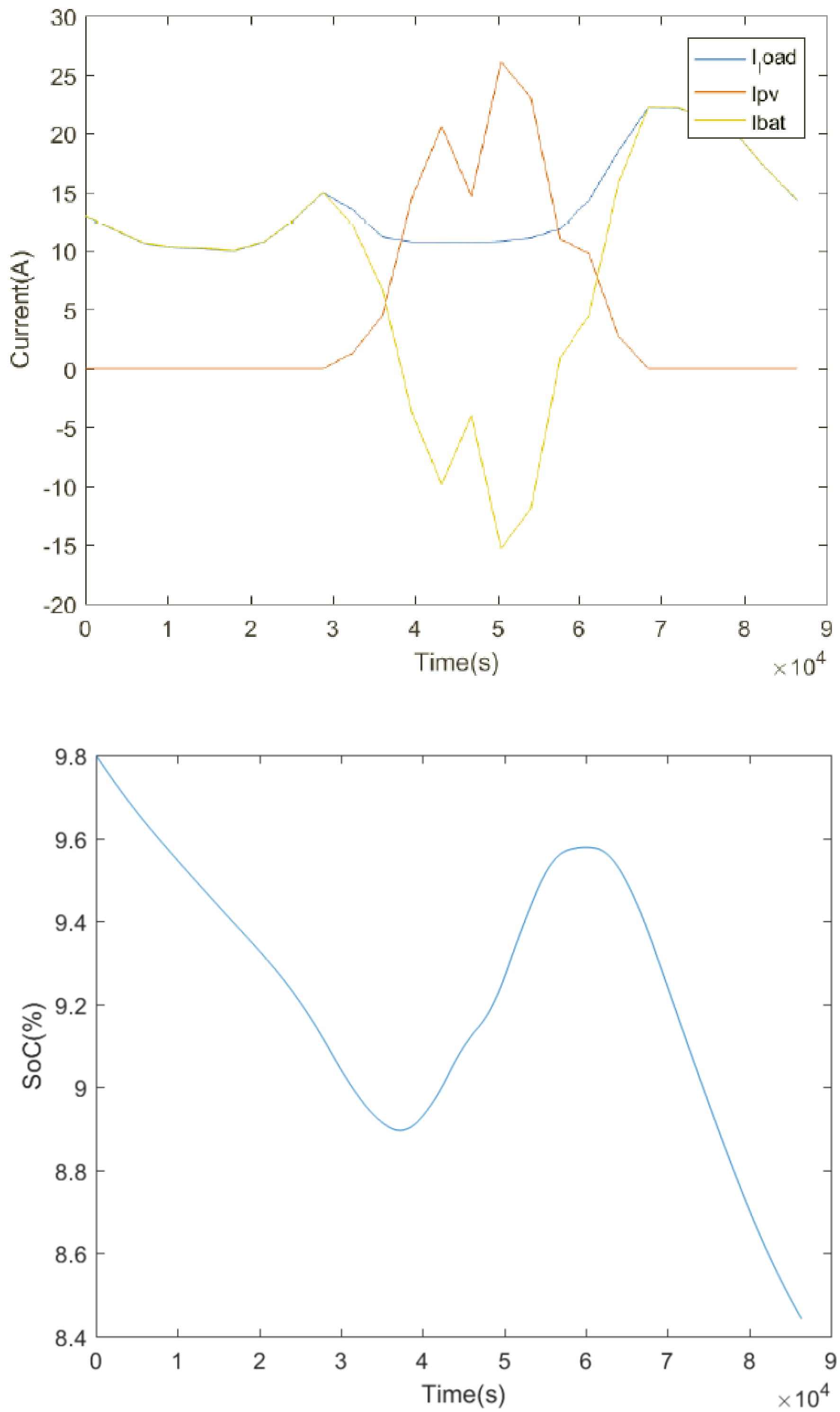

Figure 84-Current and SOC results for Houghton in January 29

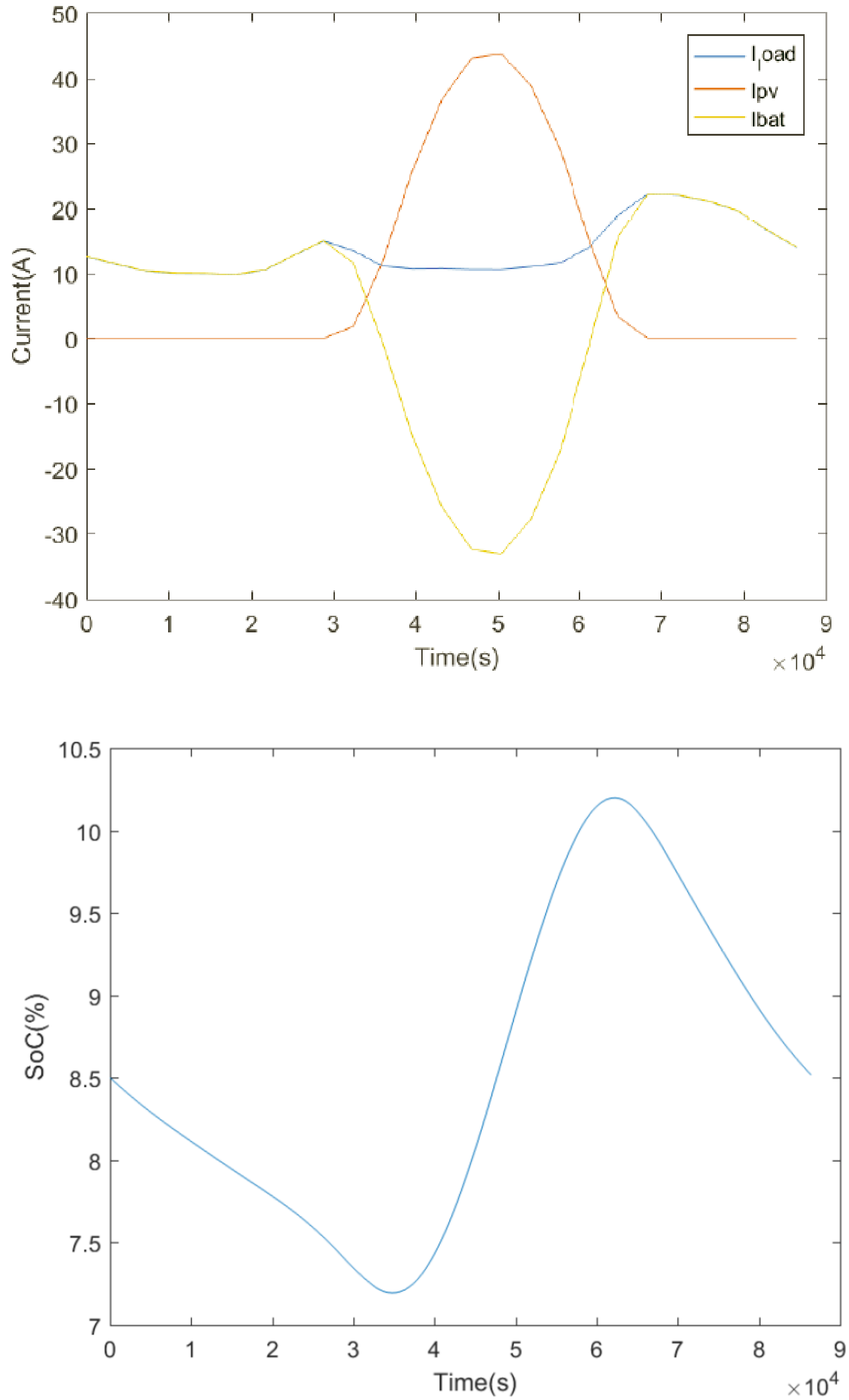

Figure 85-Current and SOC results for Houghton in January 30

Simulation Results for May in Tucson

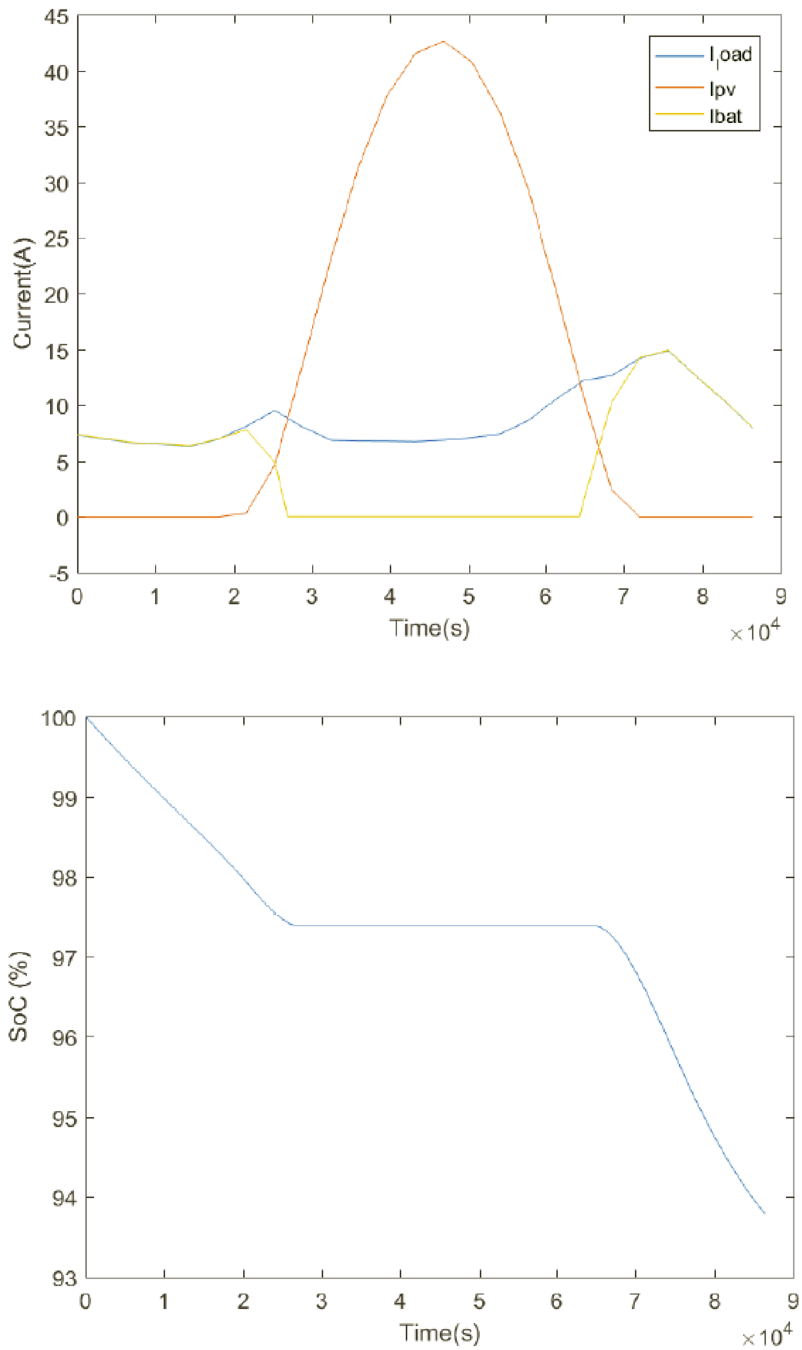

Figure 86-Current and SOC results for Tucson in May 1

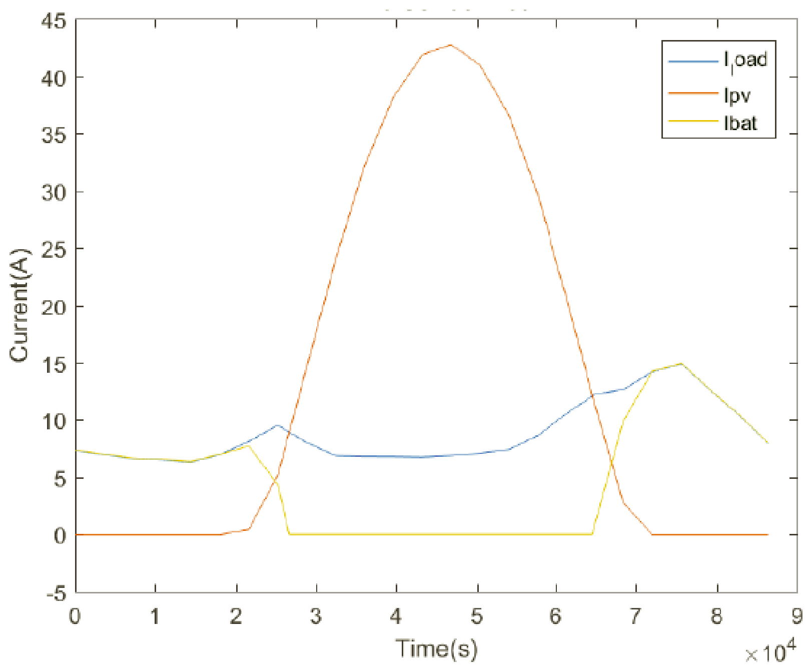

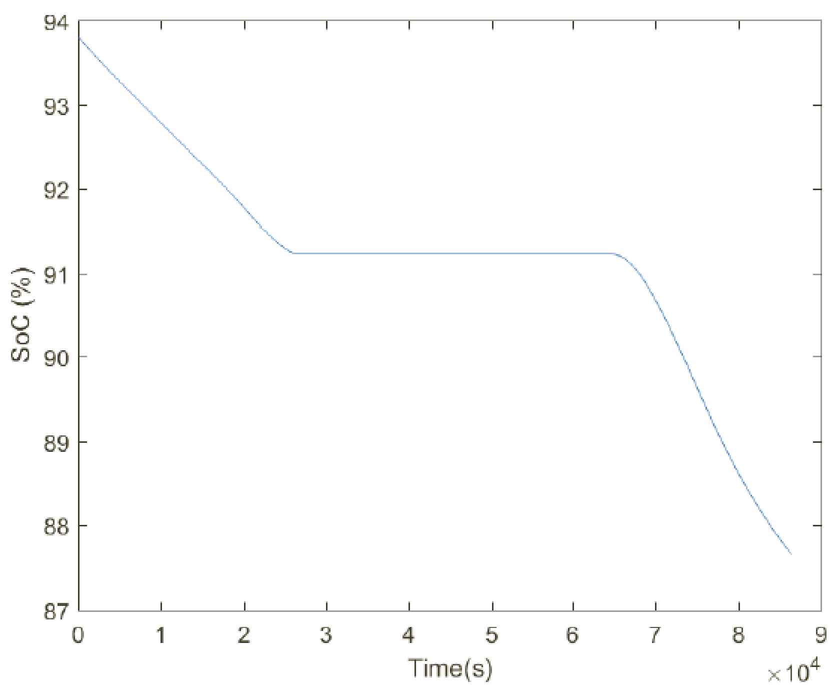

Figure 87-Current and SOC results for Tucson in May 2

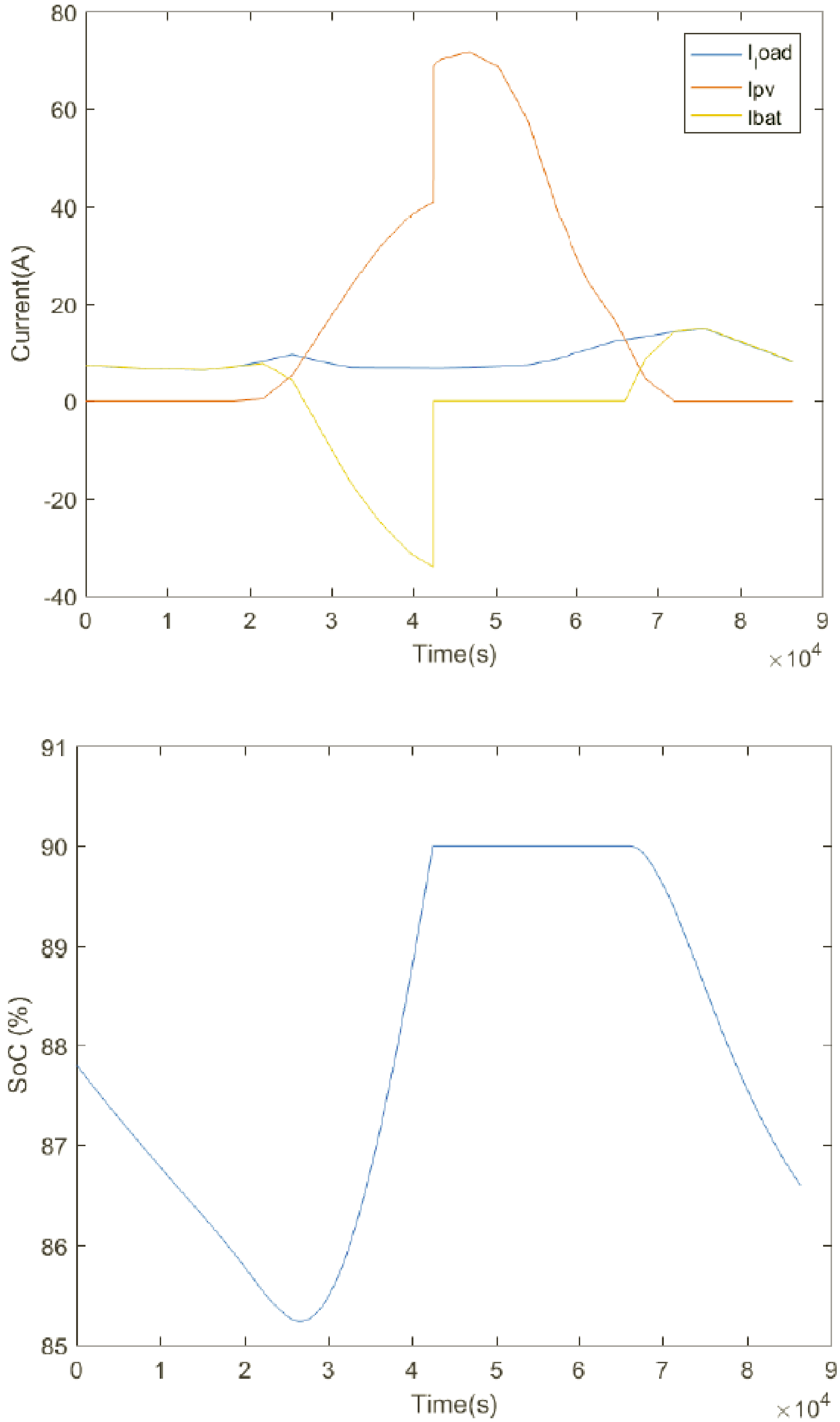

Figure 88-Current and SOC results for Tucson in May 3

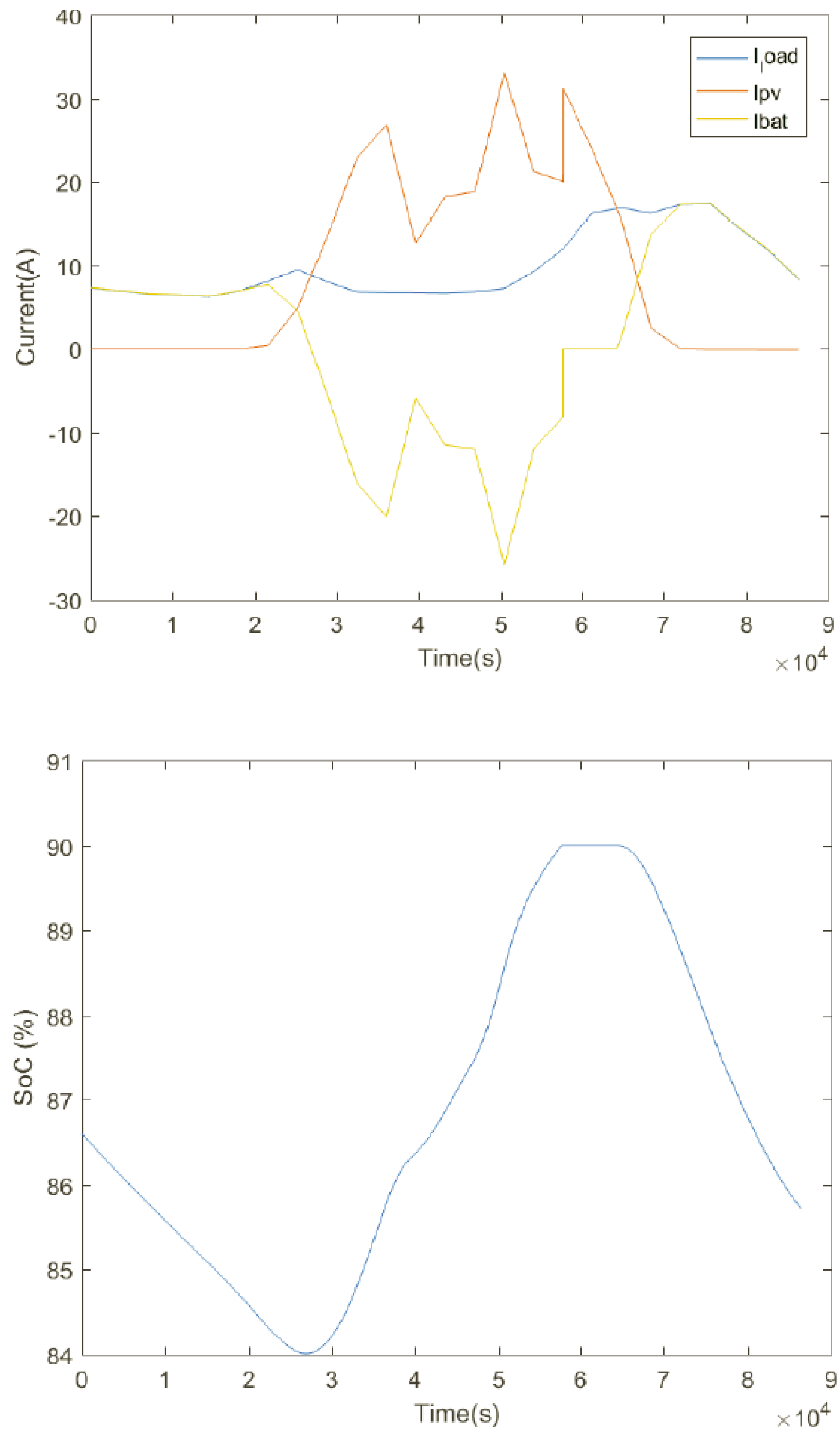

Figure 89-Current and SOC results for Tucson in May 4

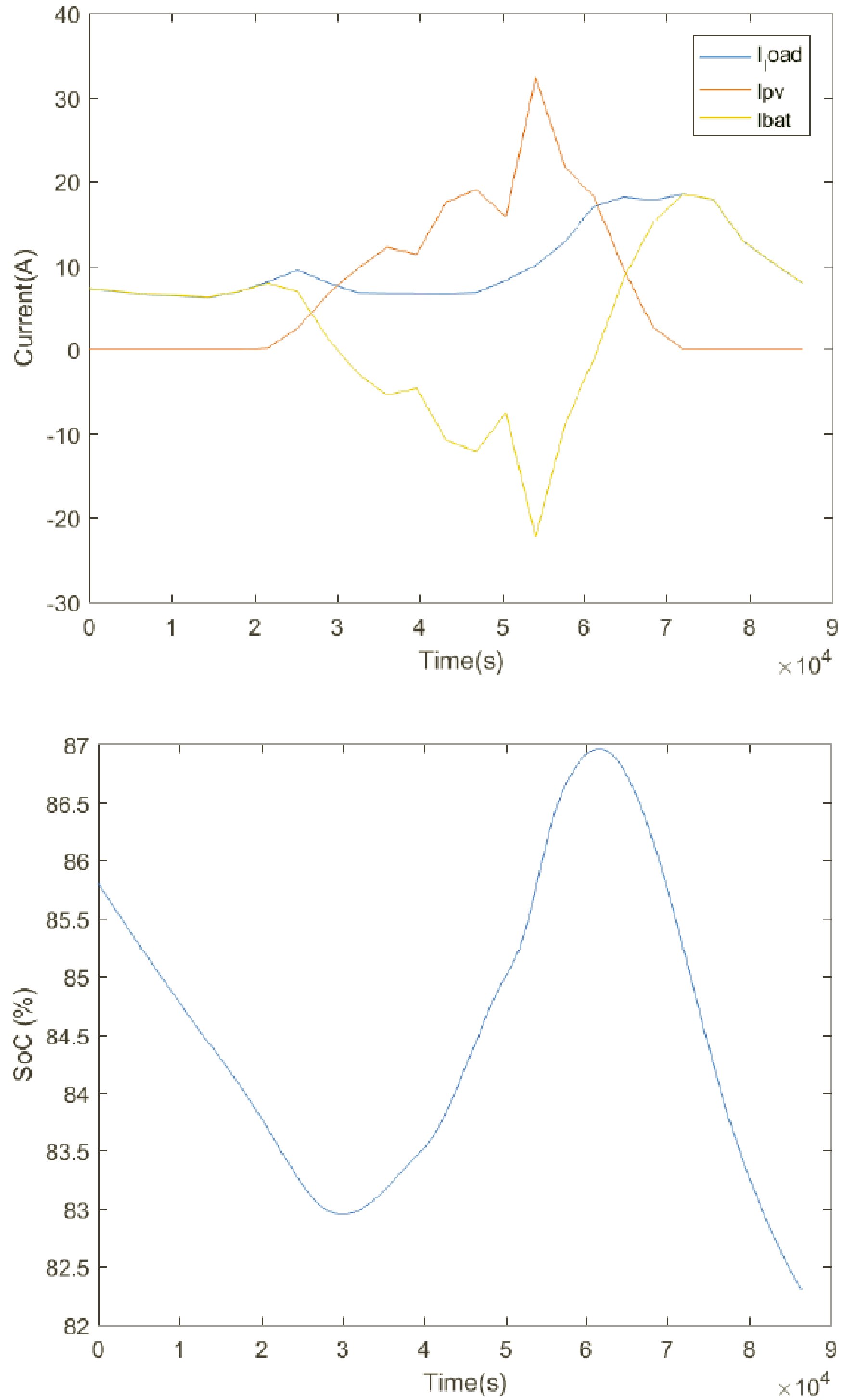

Figure 90-Current and SOC results for Tucson in May 5

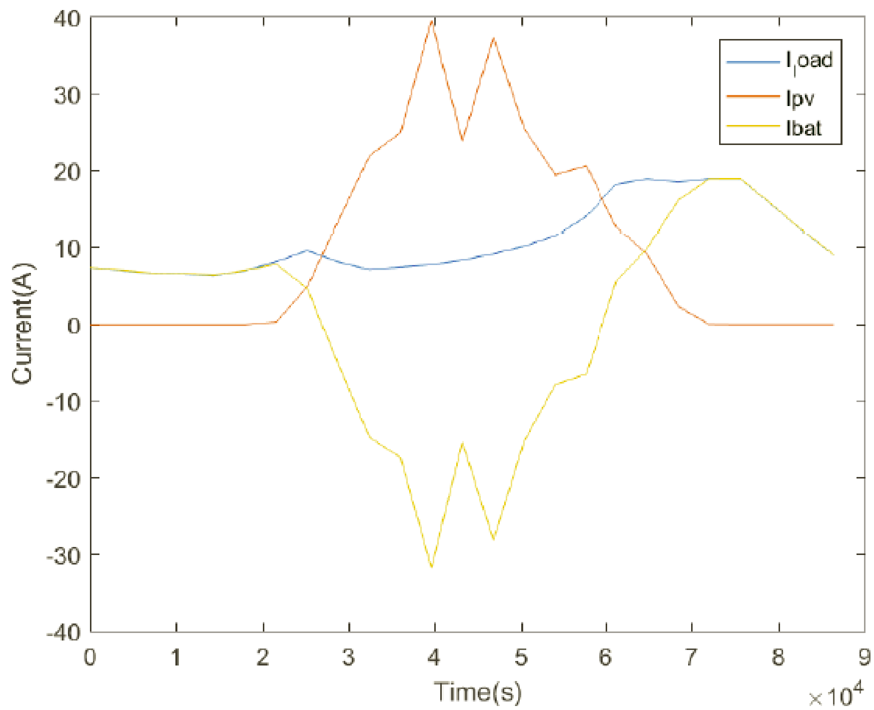

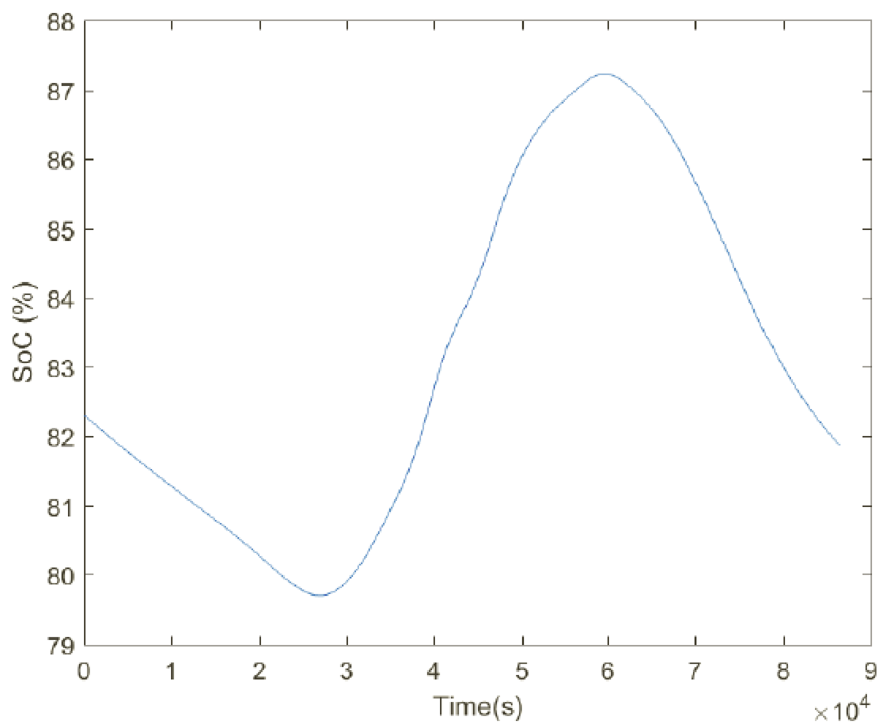

Figure 91-Current and SOC results for Tucson in May 6

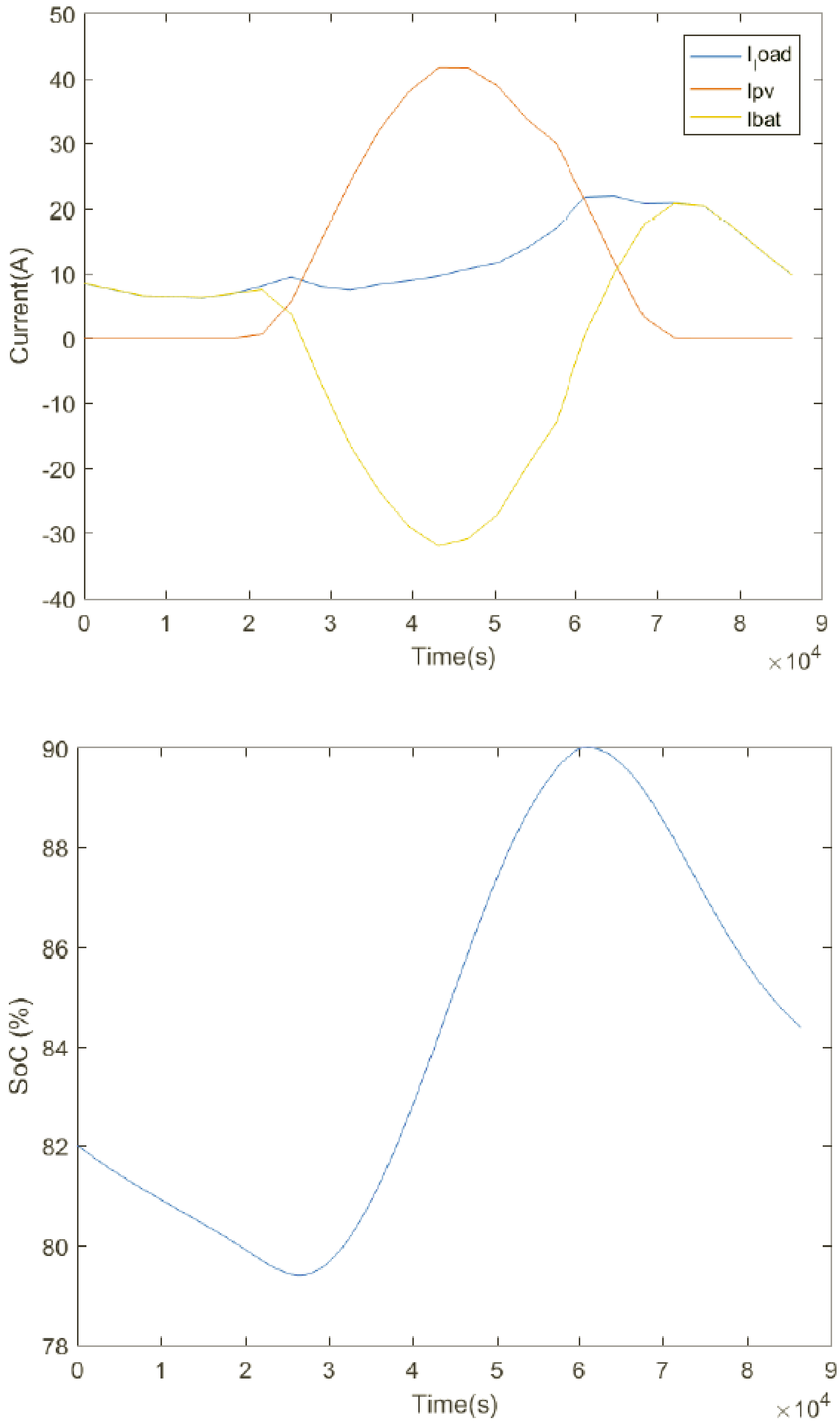

Figure 92-Current and SOC results for Tucson in May 7

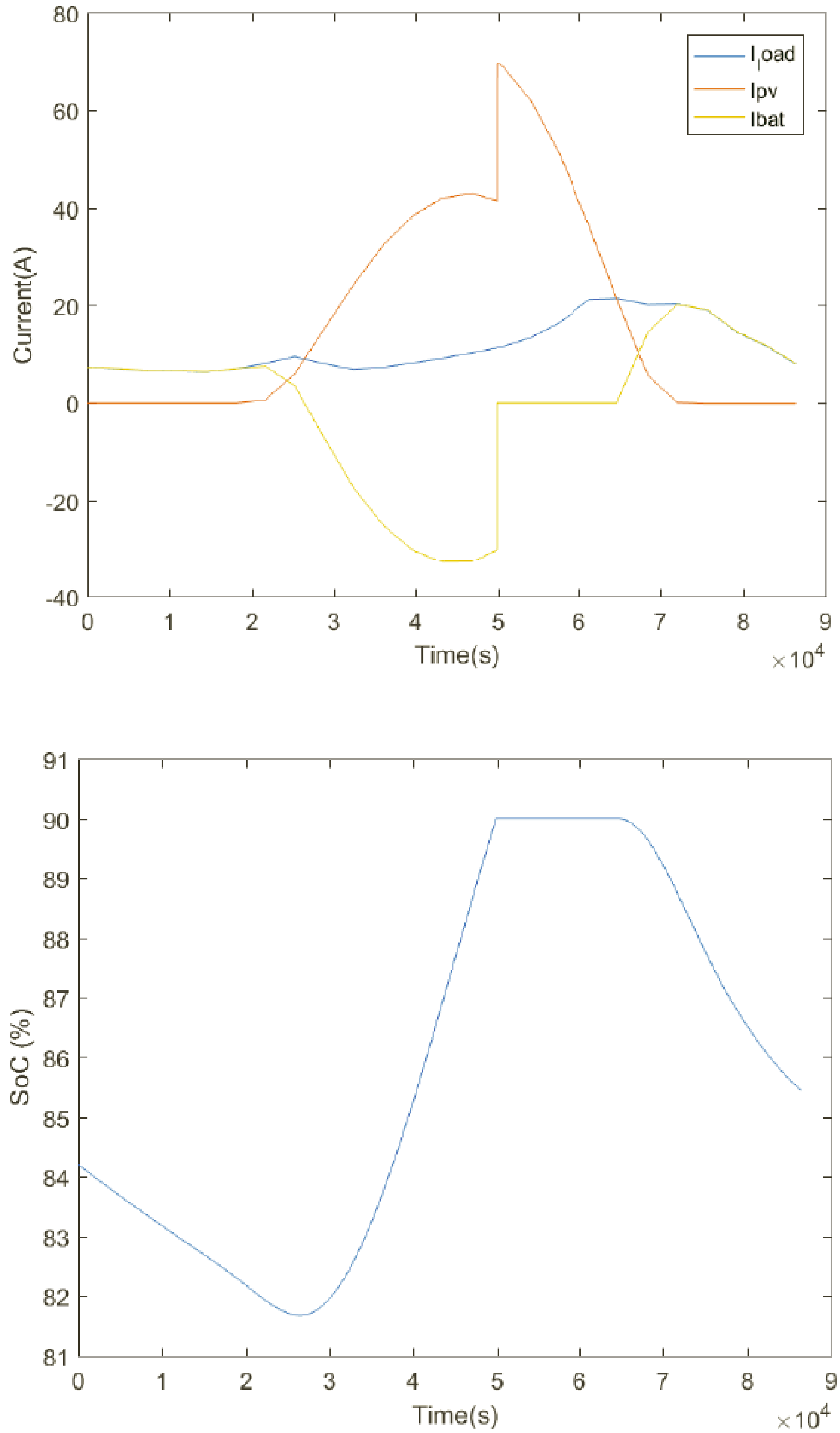

Figure 93-Current and SOC results for Tucson in May 8

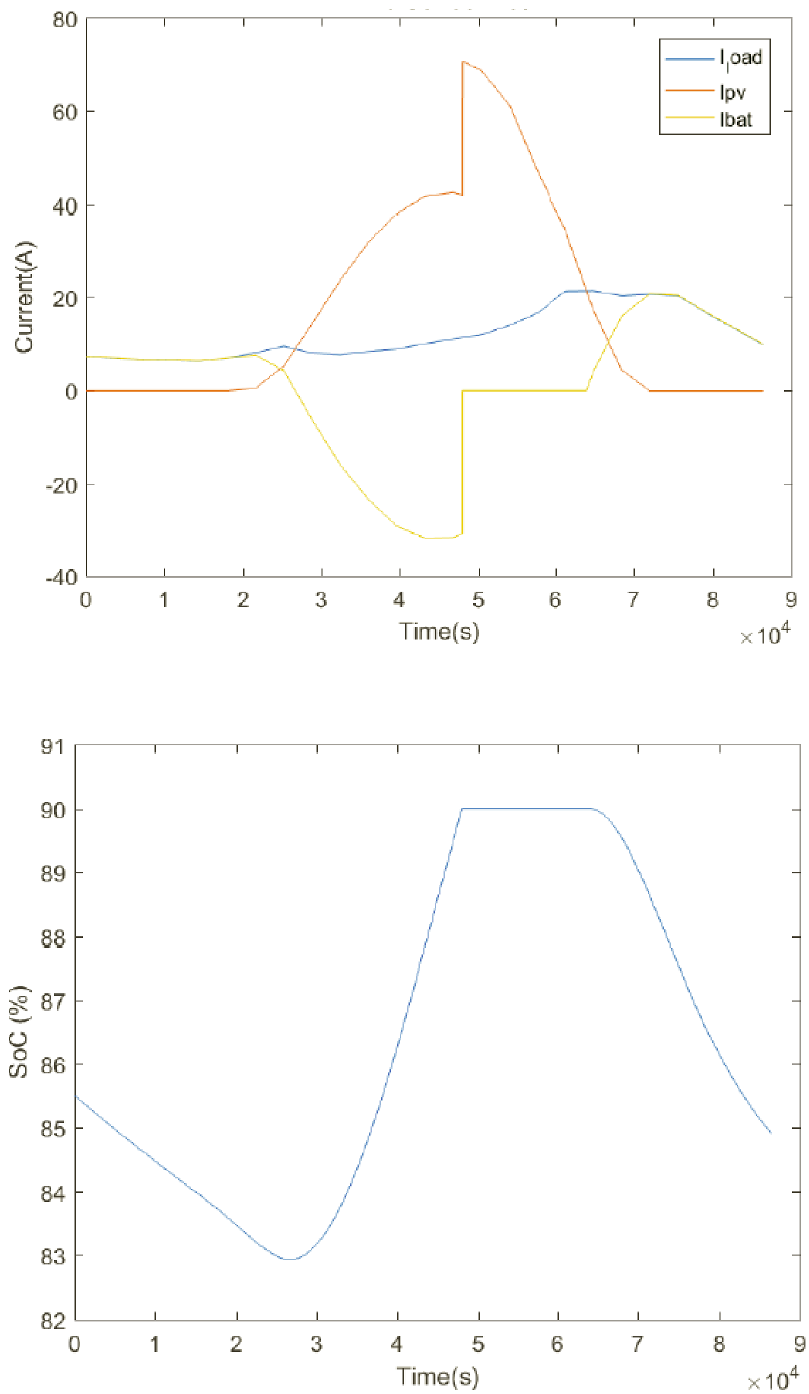

Figure 94-Current and SOC results for Tucson in May 9

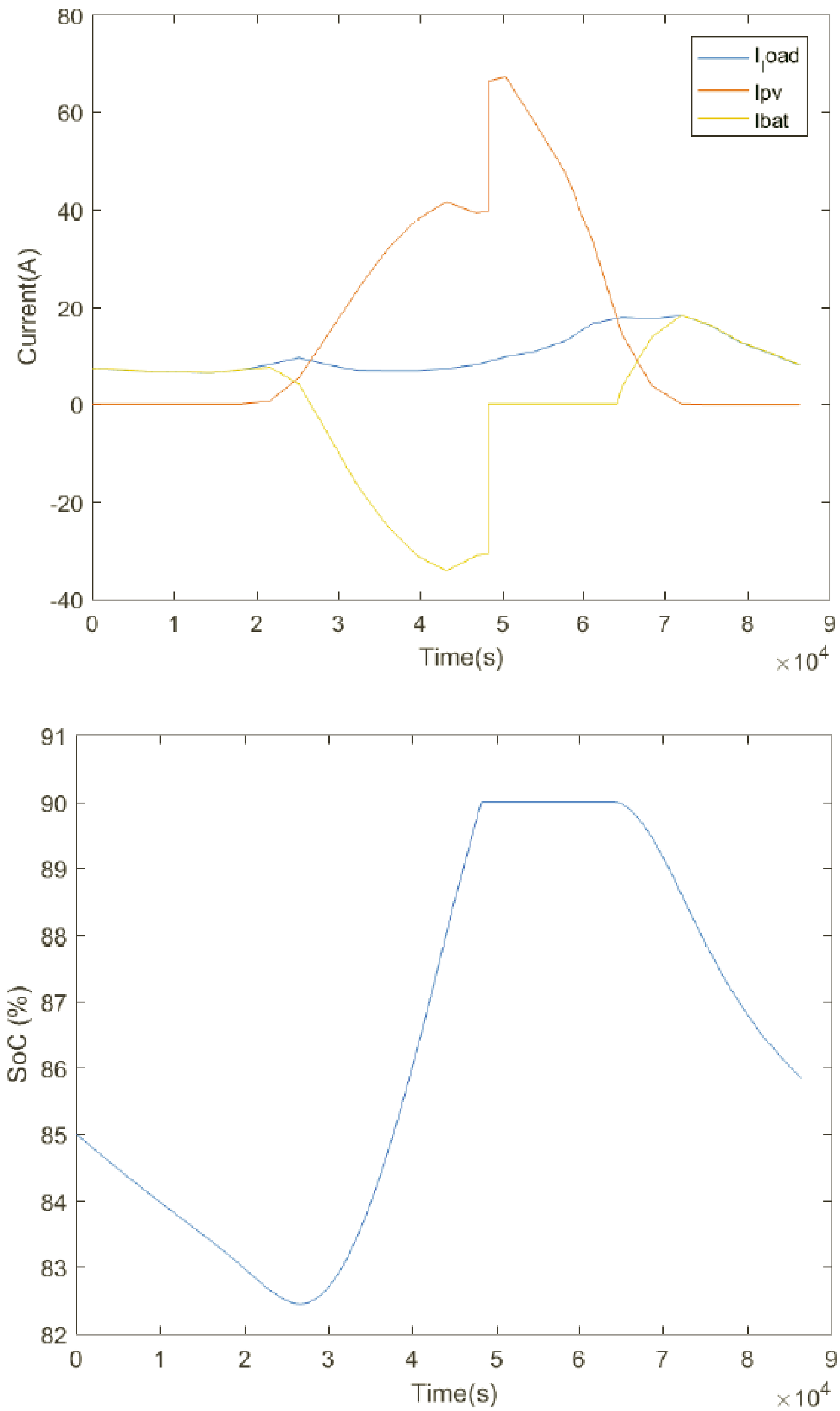

Figure 95-Current and SOC results for Tucson in May 10

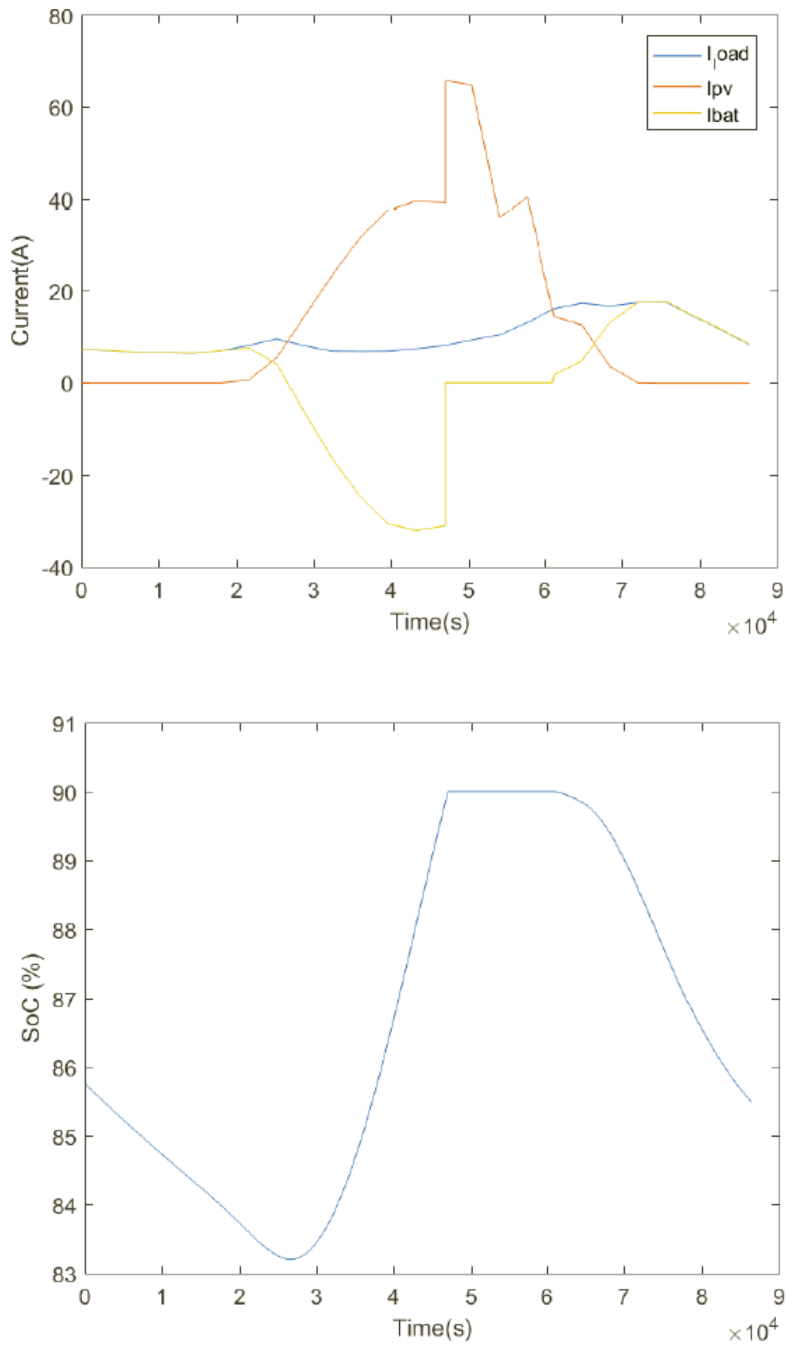

Figure 96-Current and SOC results for Tucson in May 11

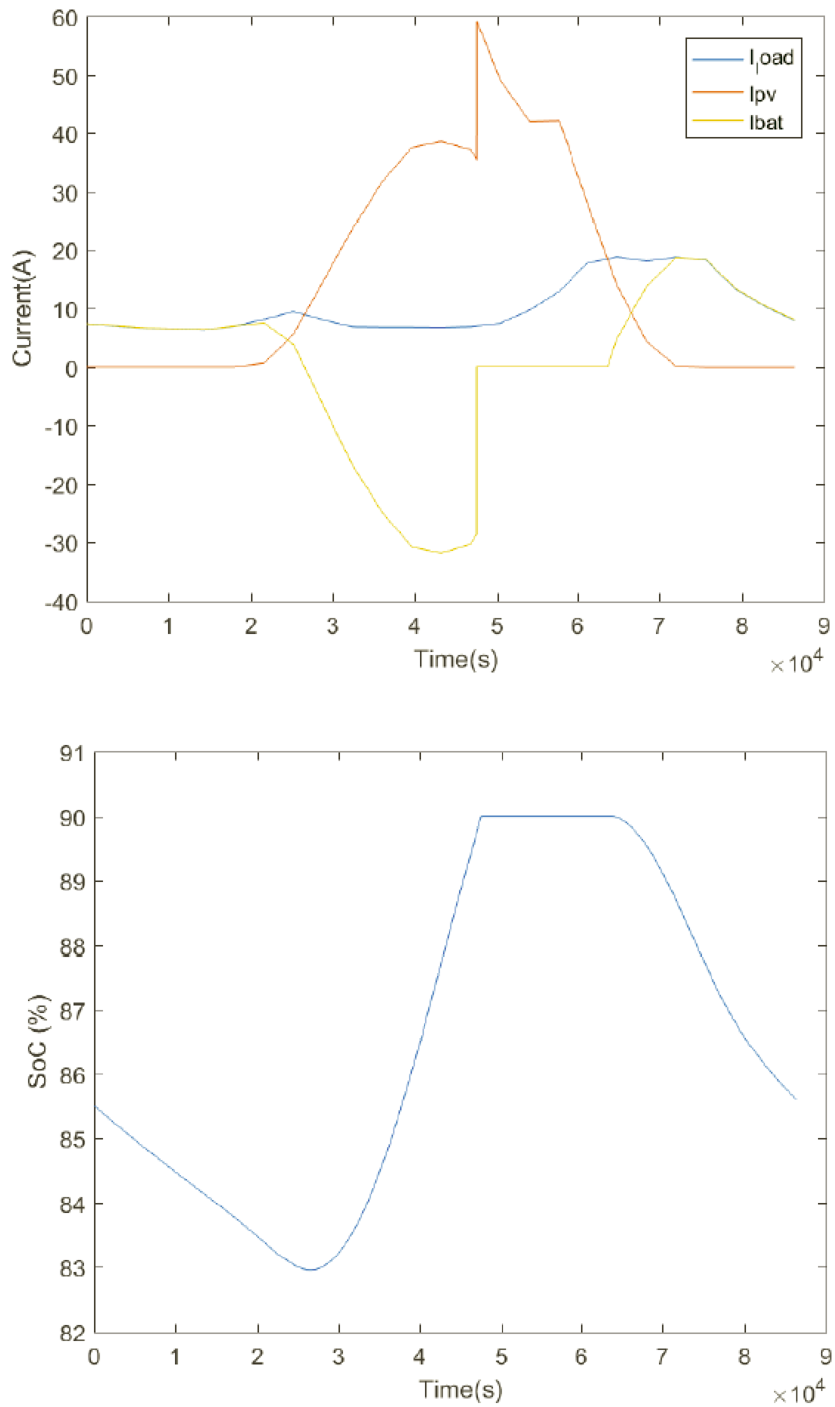

Figure 97-Current and SOC results for Tucson in May 12

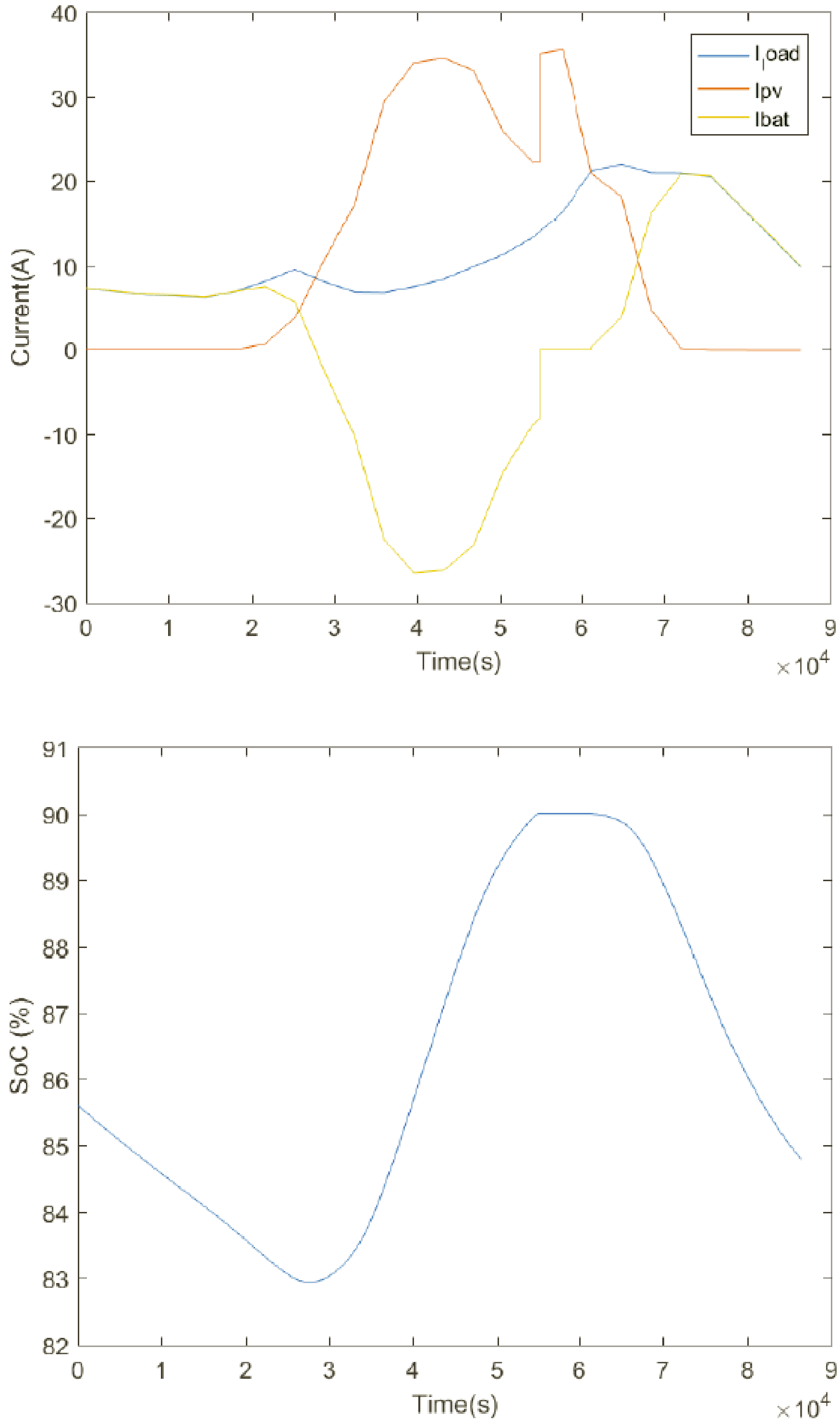

Figure 98-Current and SOC results for Tucson in May 13

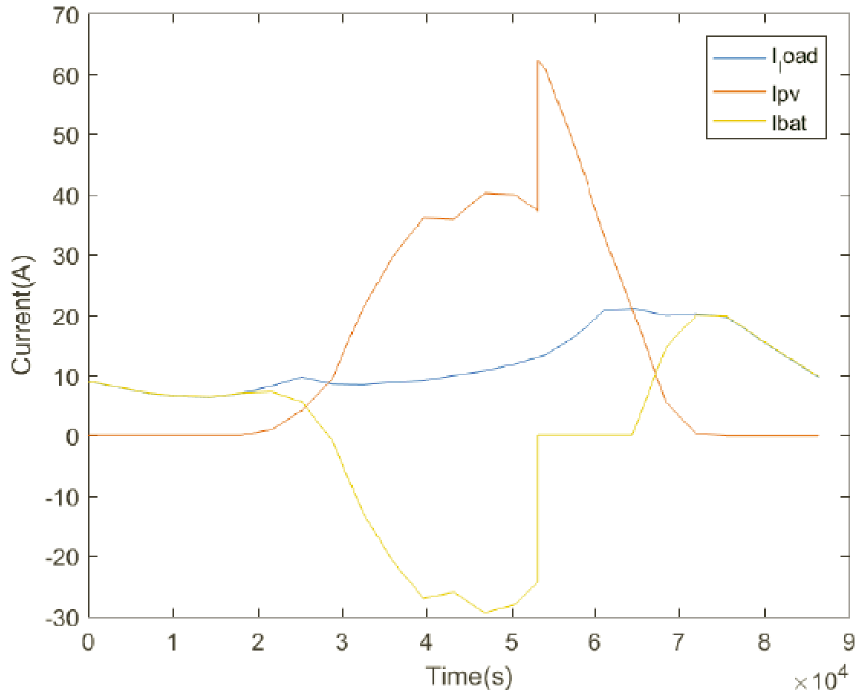

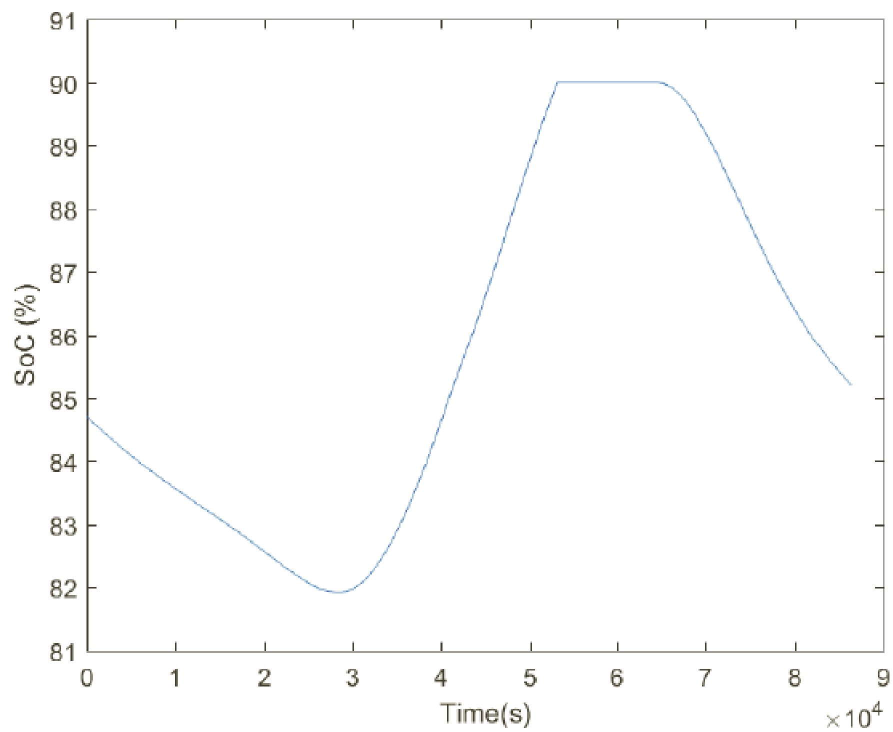

Figure 99-Current and SOC results for Tucson in May 14

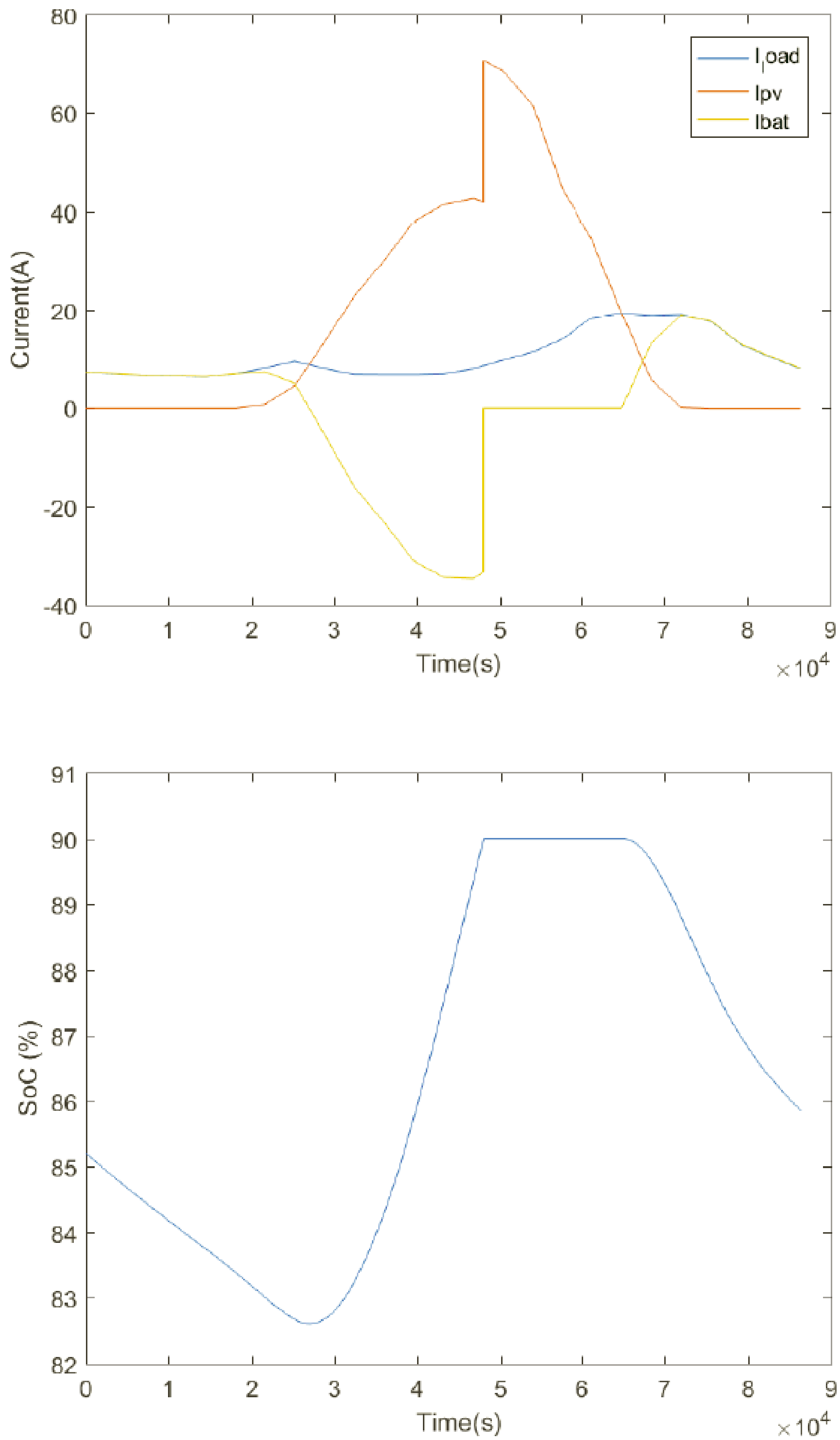

Figure 100-Current and SOC results for Tucson in May 15

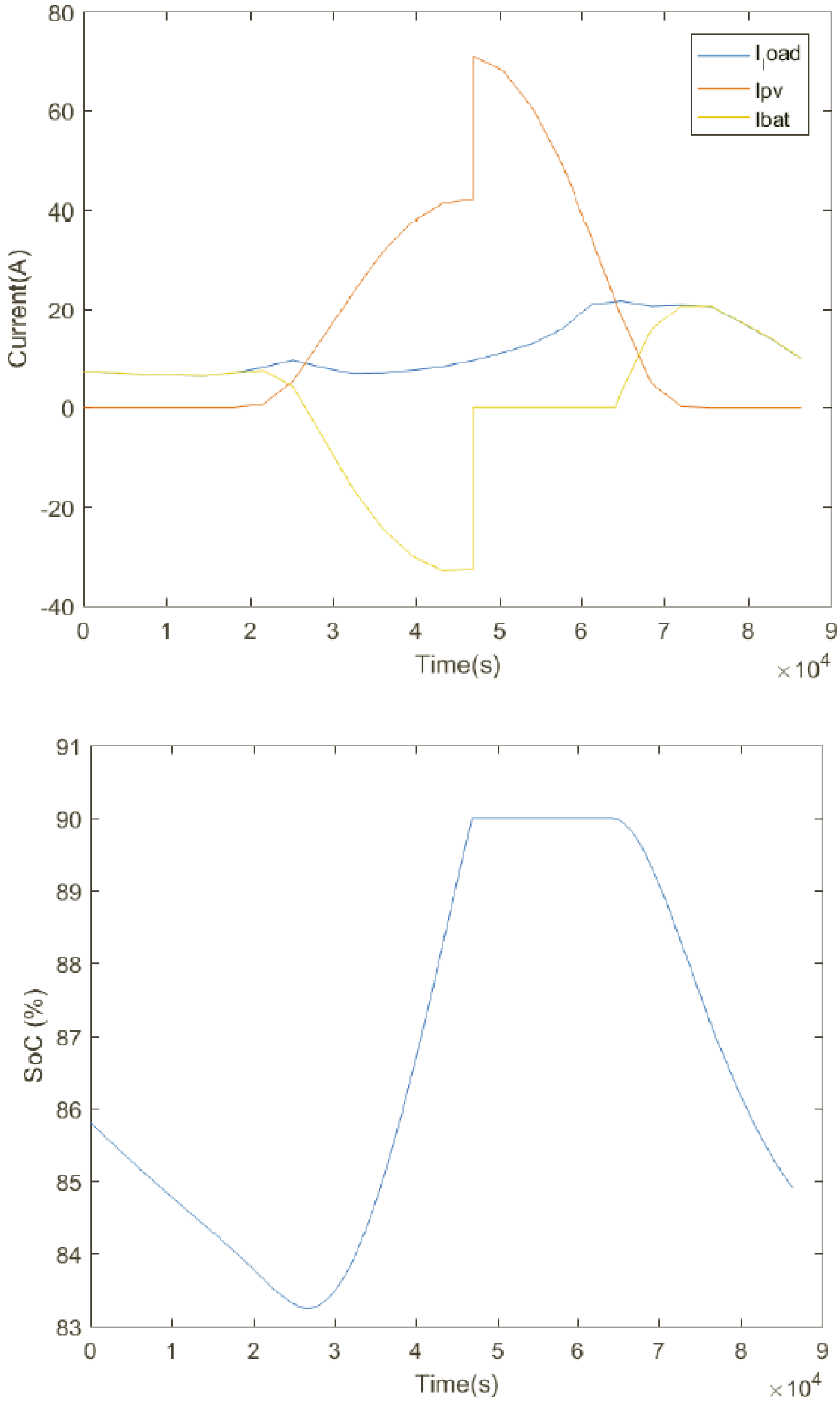

Figure 101-Current and SOC results for Tucson in May 16

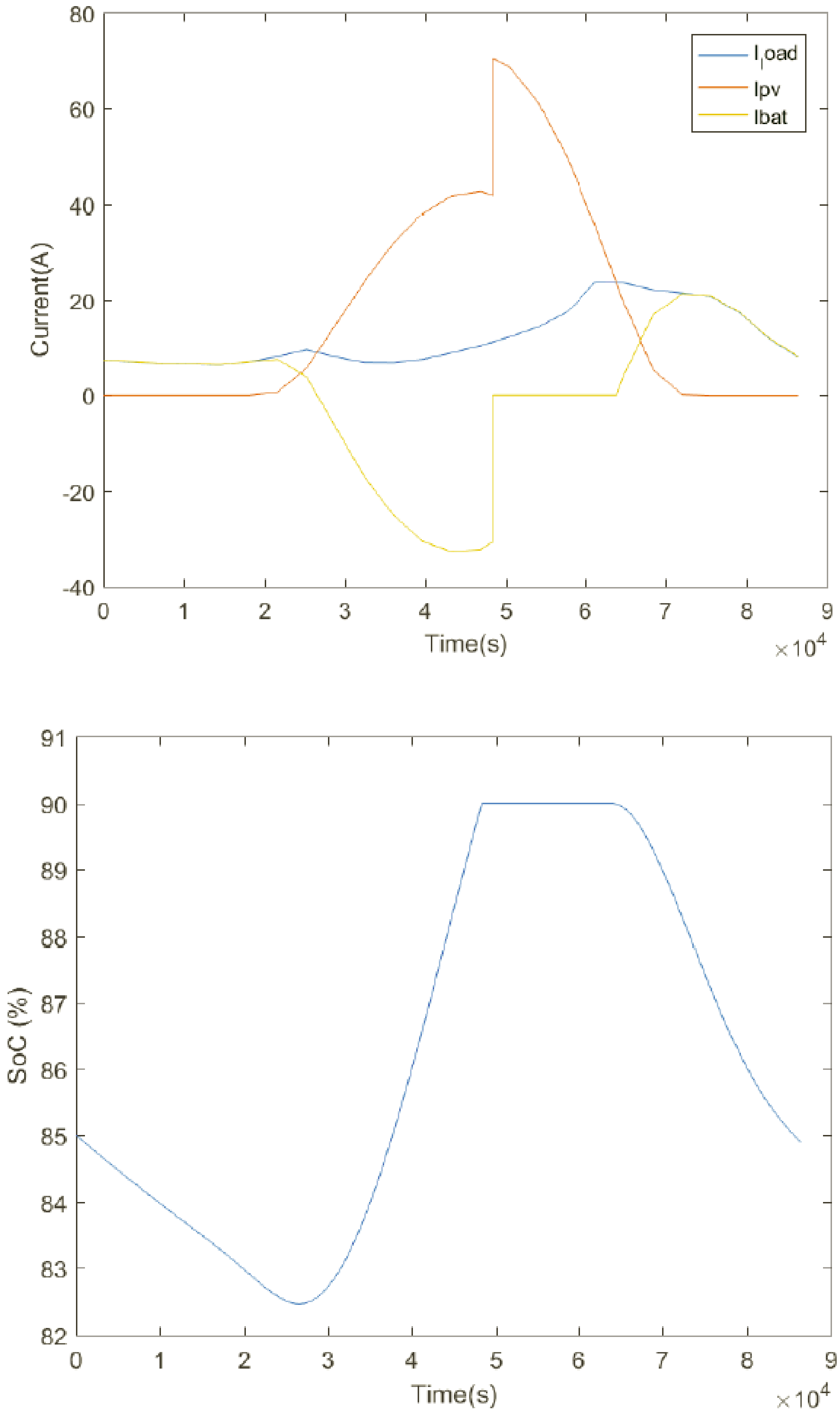

Figure 102-Current and SOC results for Tucson in May 17

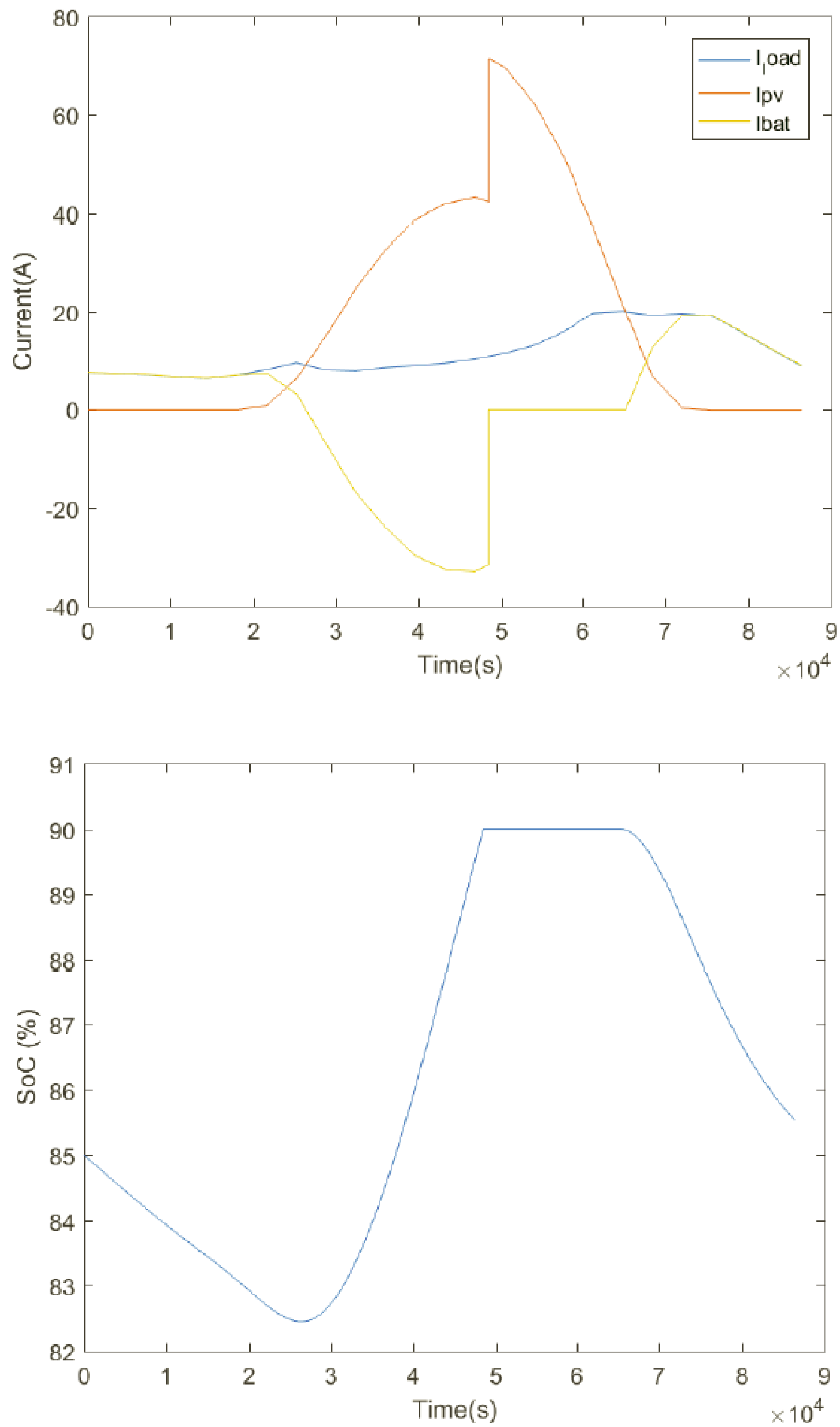

Figure 103-Current and SOC results for Tucson in May 18

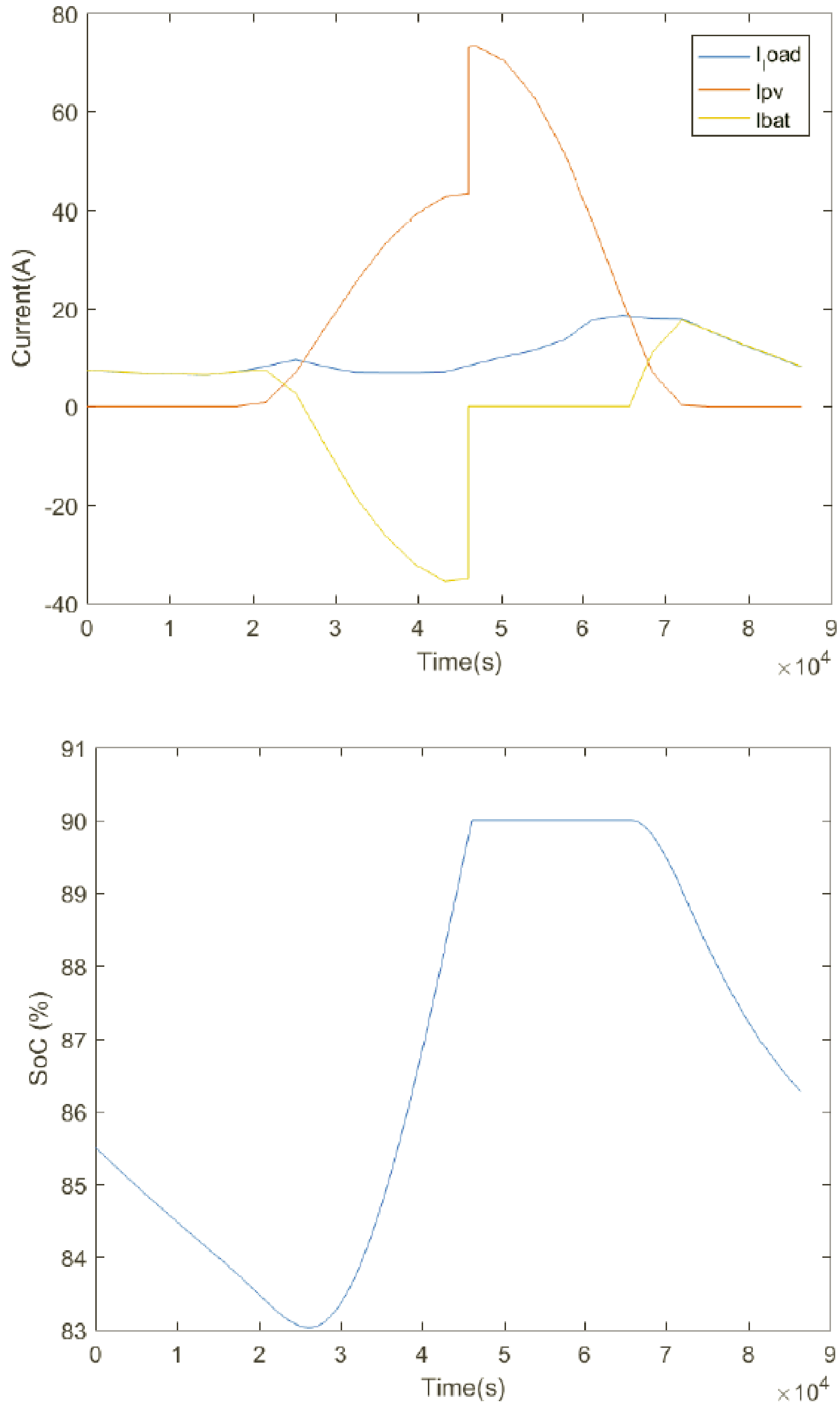

Figure 104-Current and SOC results for Tucson in May 19

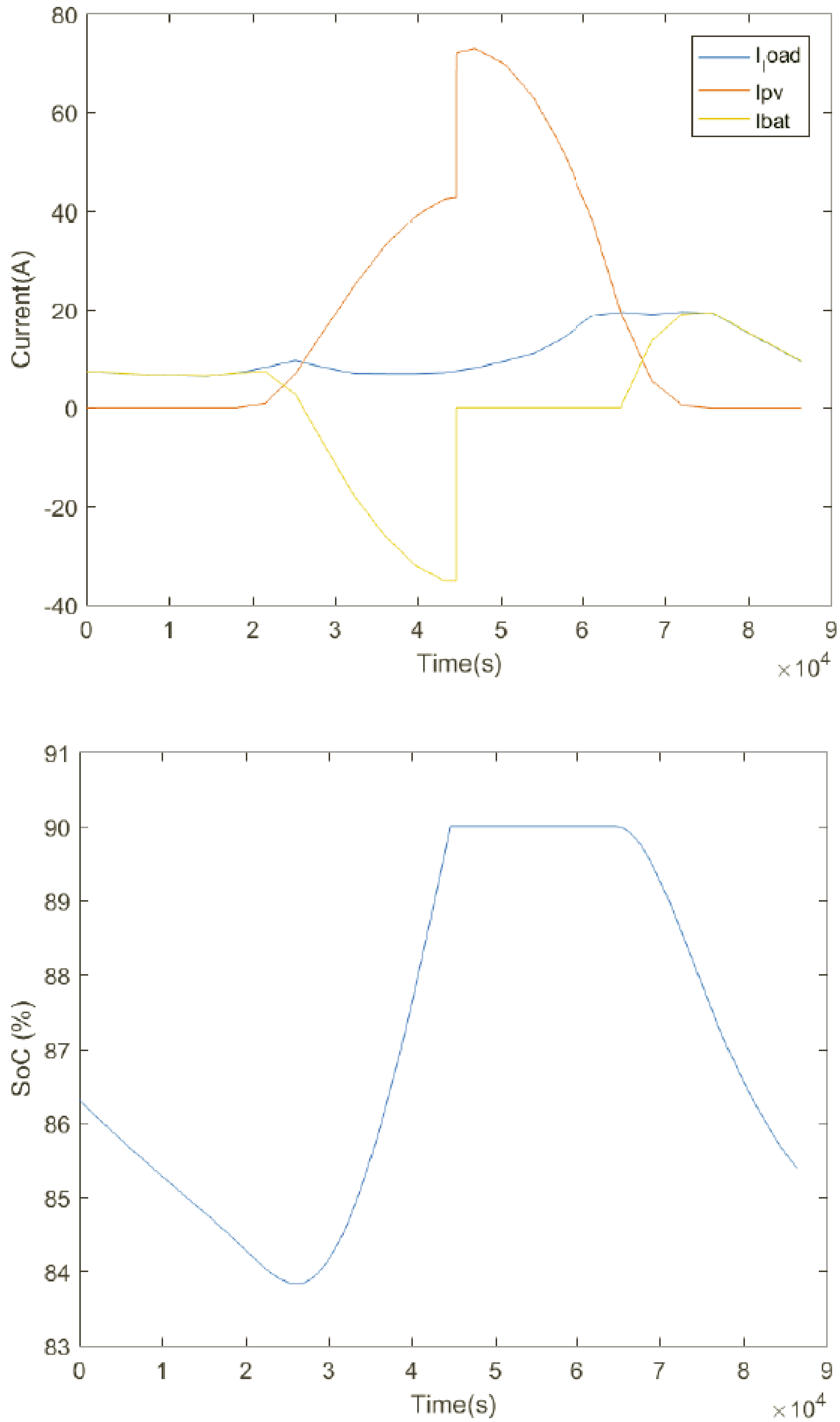

Figure 105-Current and SOC results for Tucson in May 20

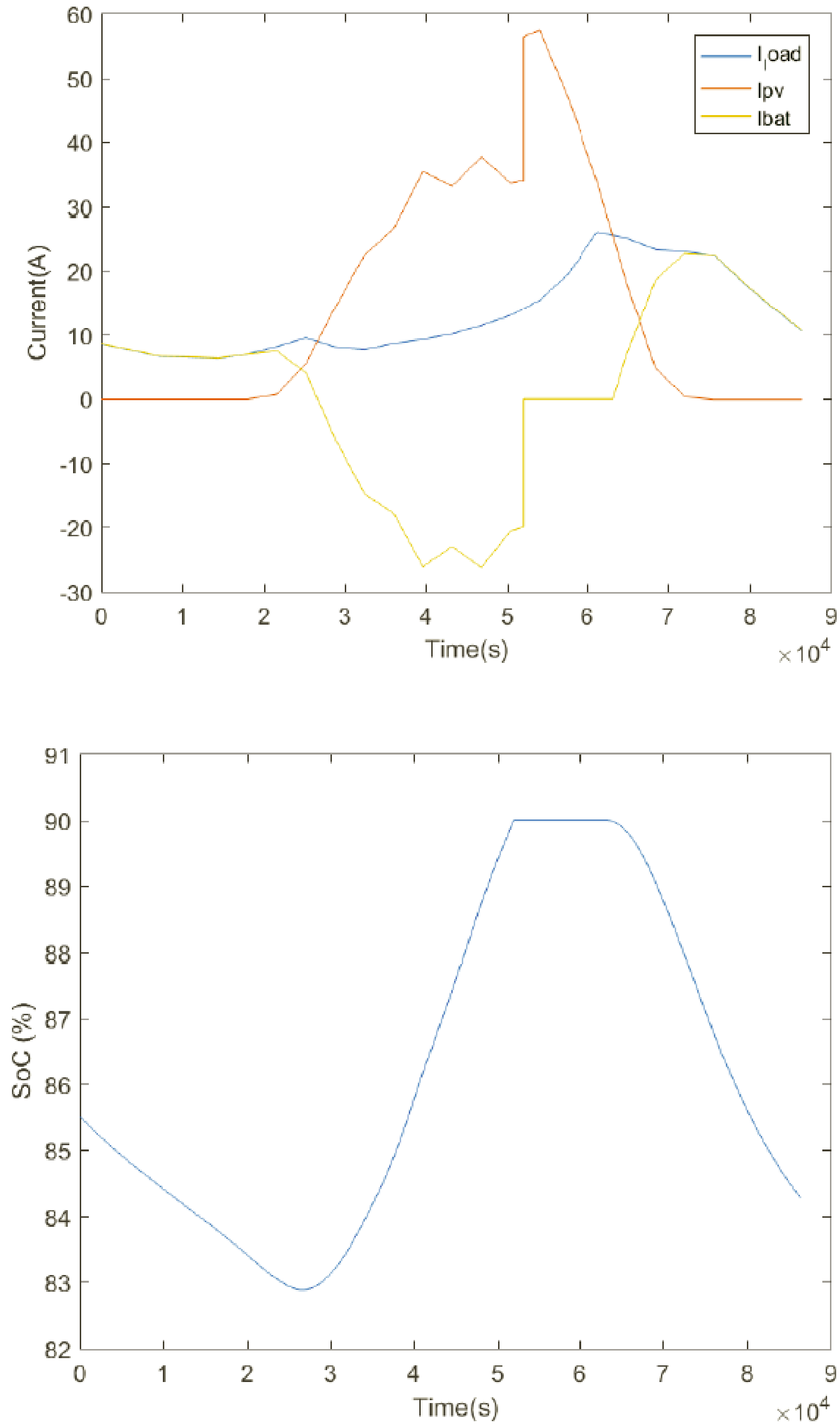

Figure 106-Current and SOC results for Tucson in May 21

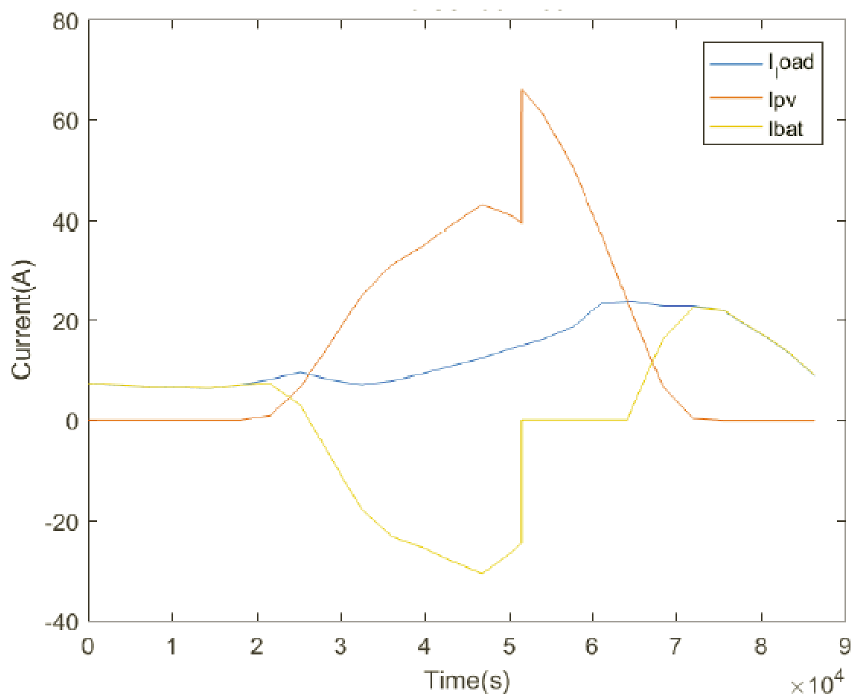

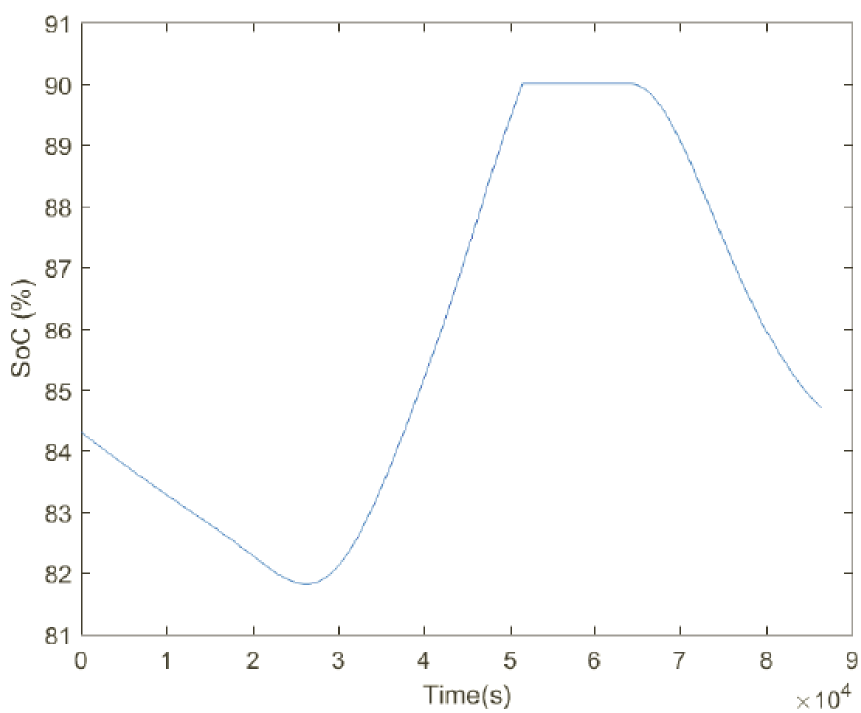

Figure 107-Current and SOC results for Tucson in May 22

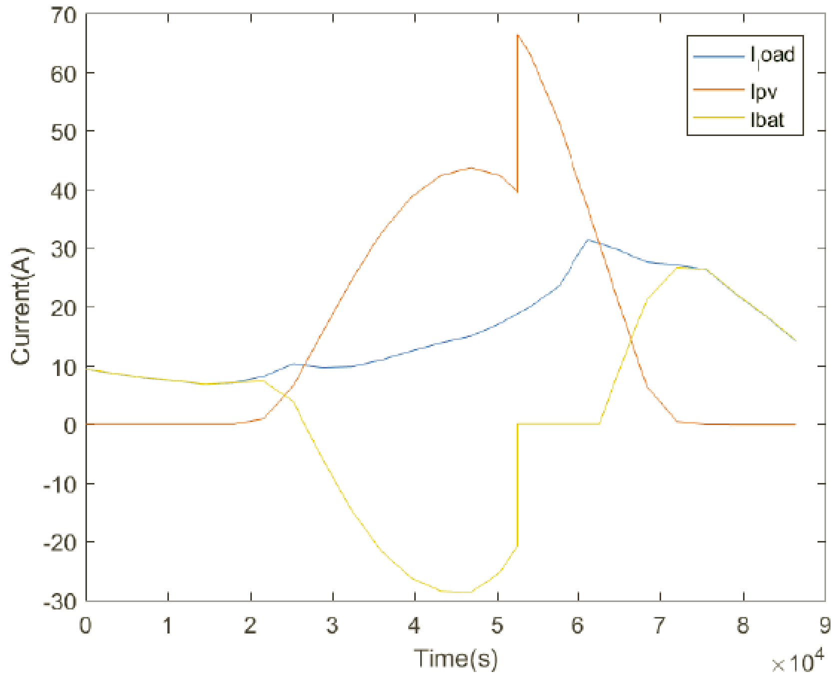

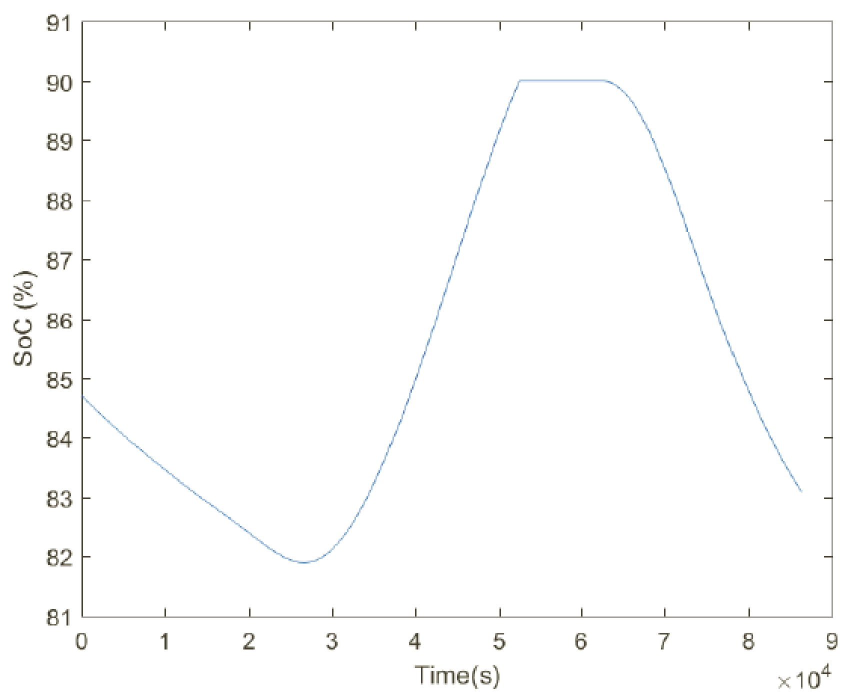

Figure 108-Current and SOC results for Tucson in May 23

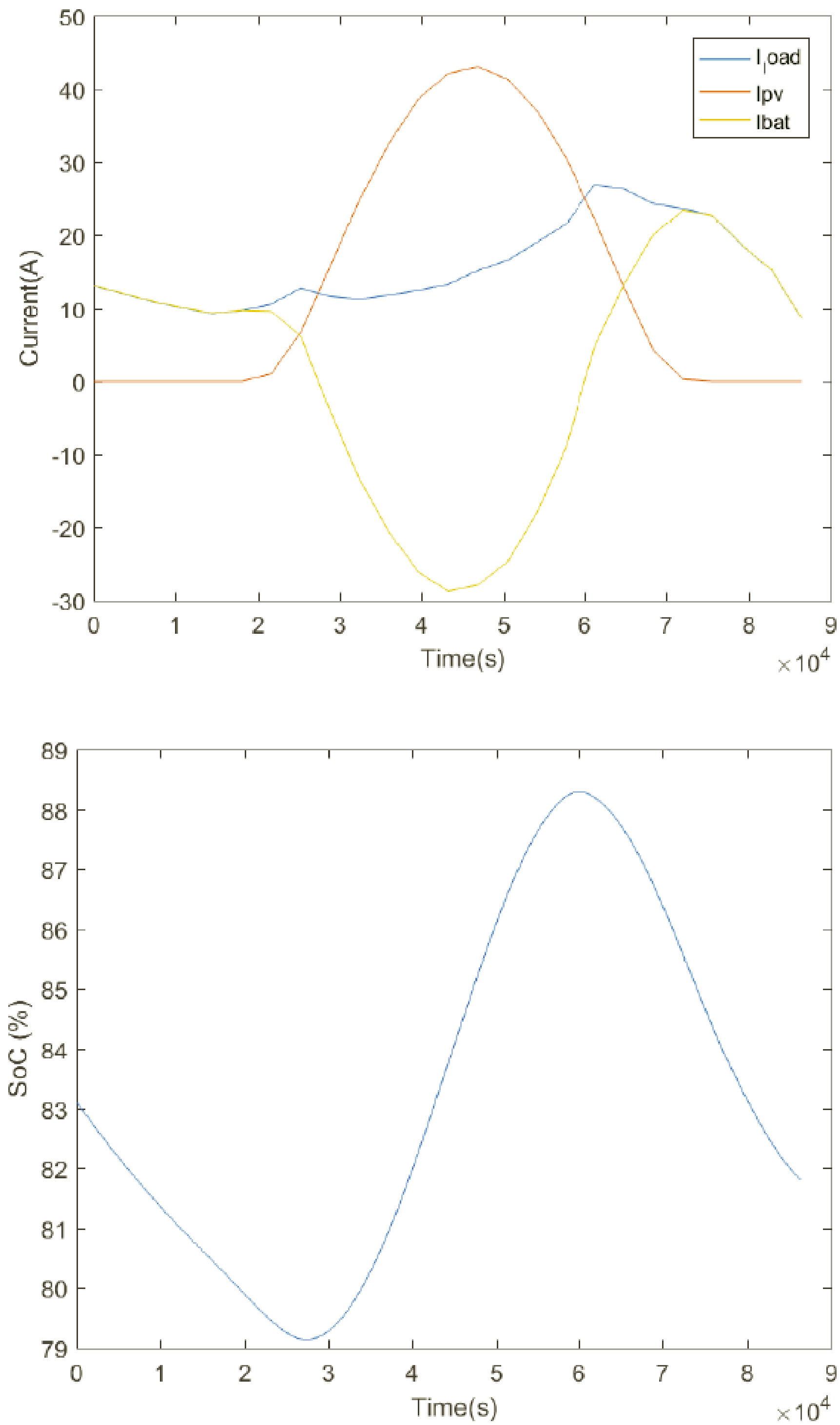

Figure 109-Current and SOC results for Tucson in May 24

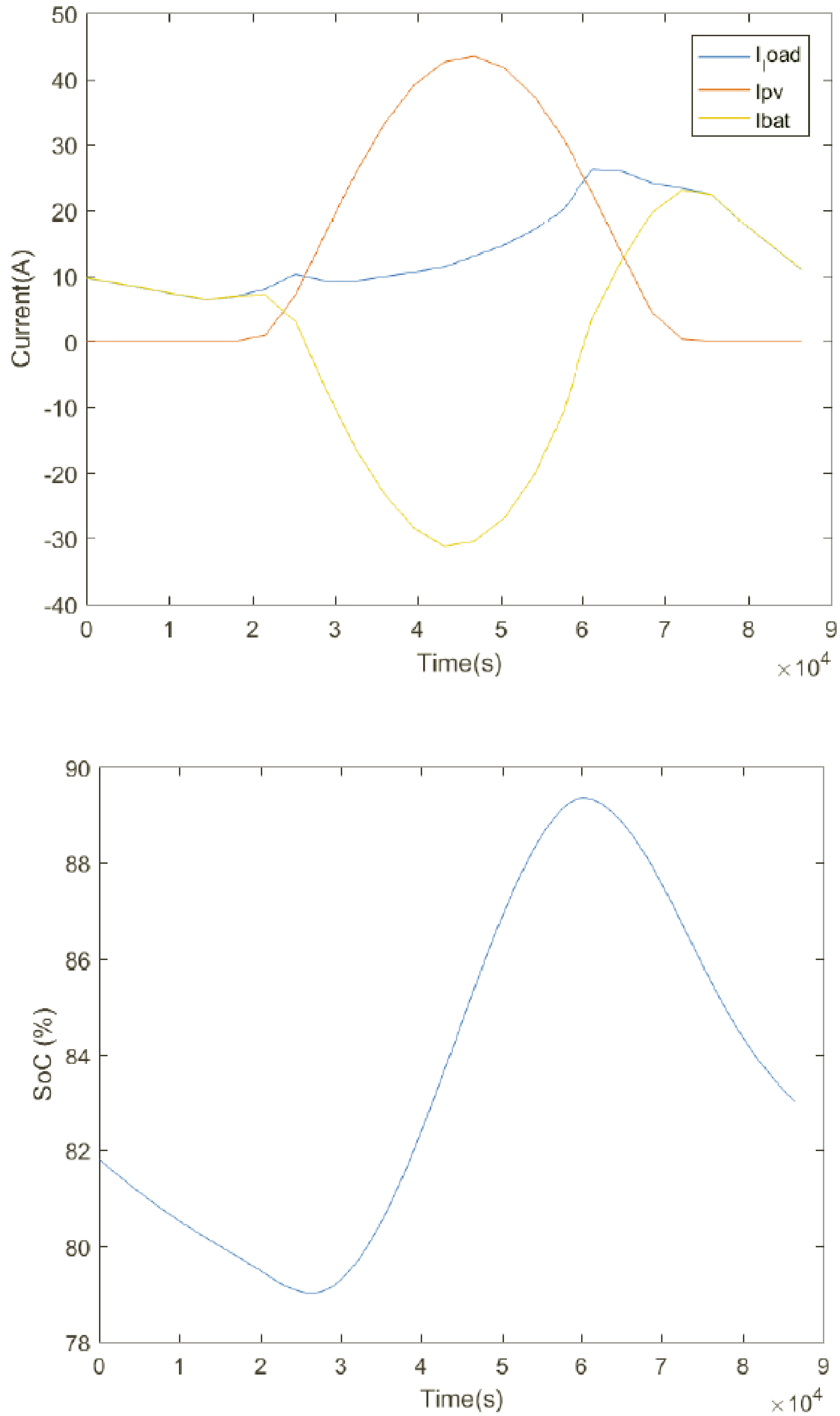

Figure 110-Current and SOC results for Tucson in May 25

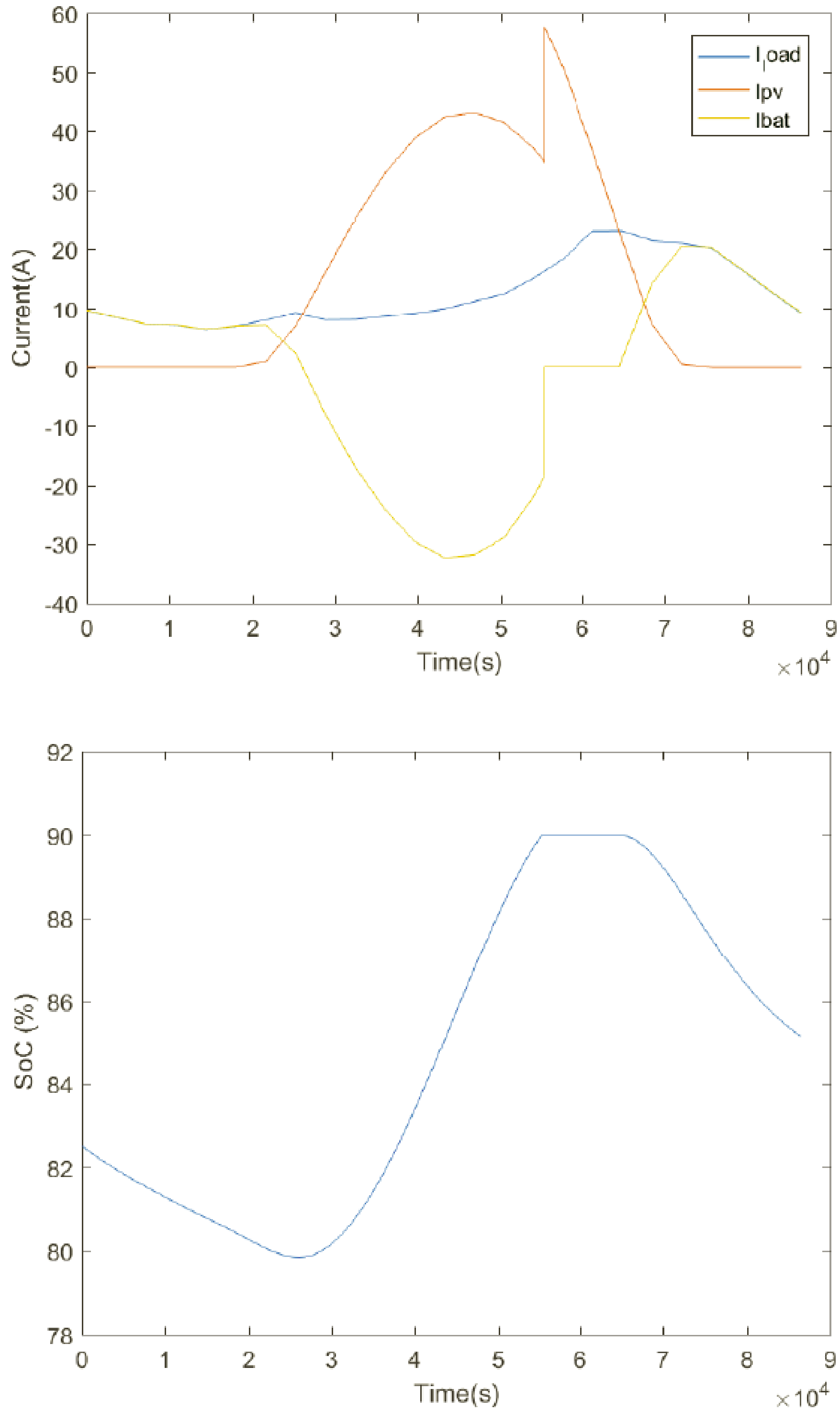

Figure 111-Current and SOC results for Tucson in May 26

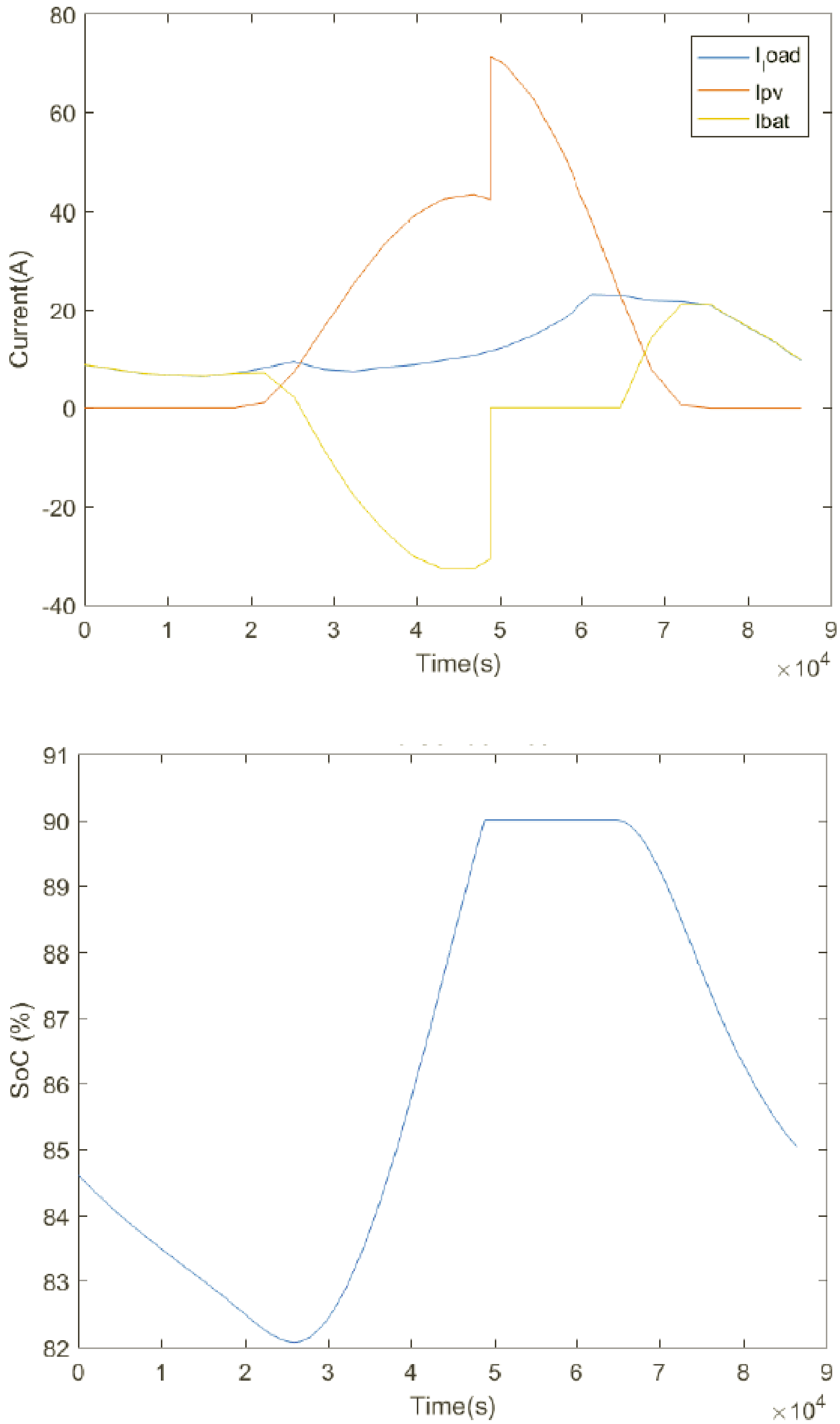

Figure 112-Current and SOC results for Tucson in May 27

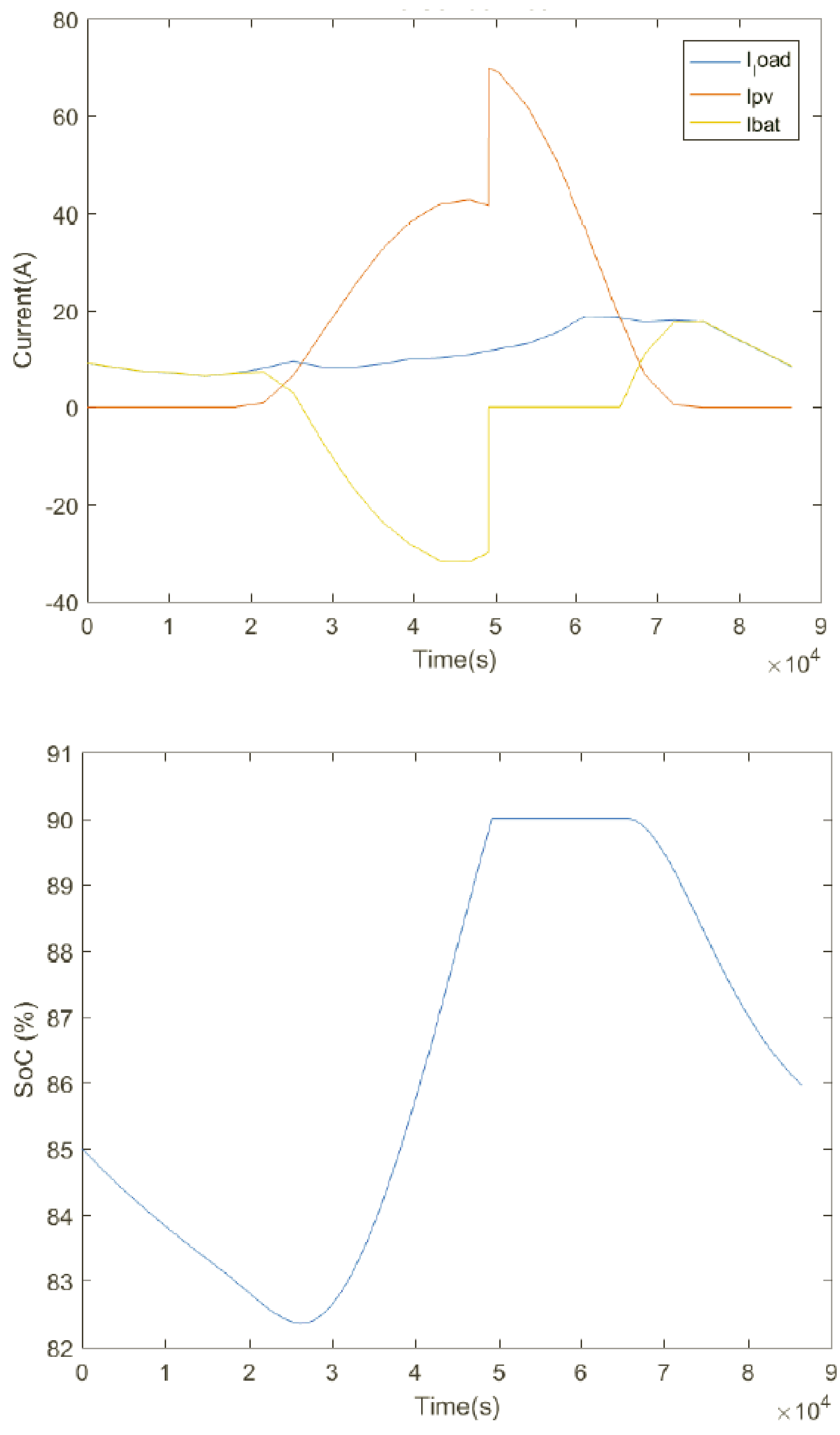

Figure 113-Current and SOC results for Tucson in May 28

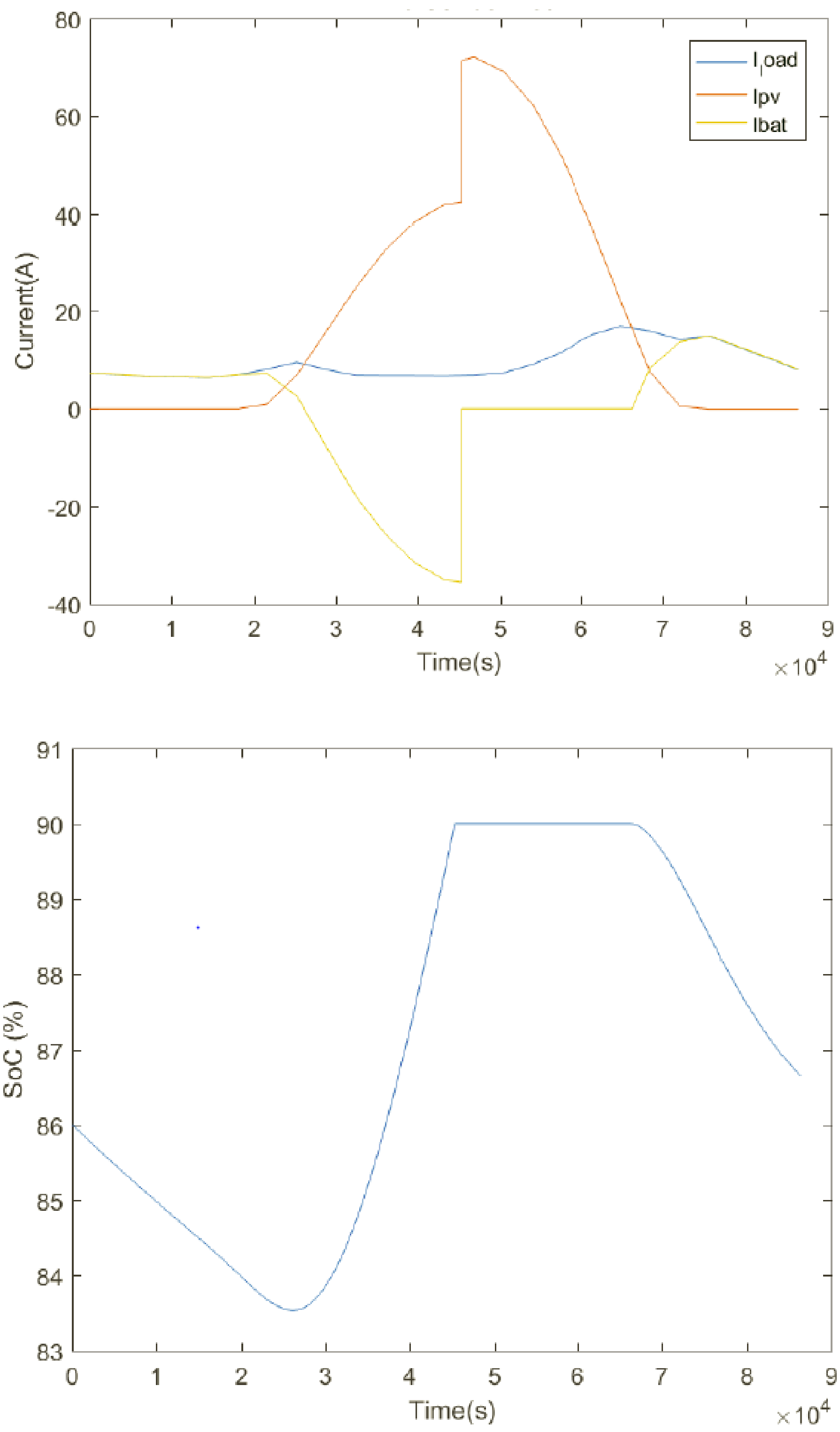

Figure 114-Current and SOC results for Tucson in May 29

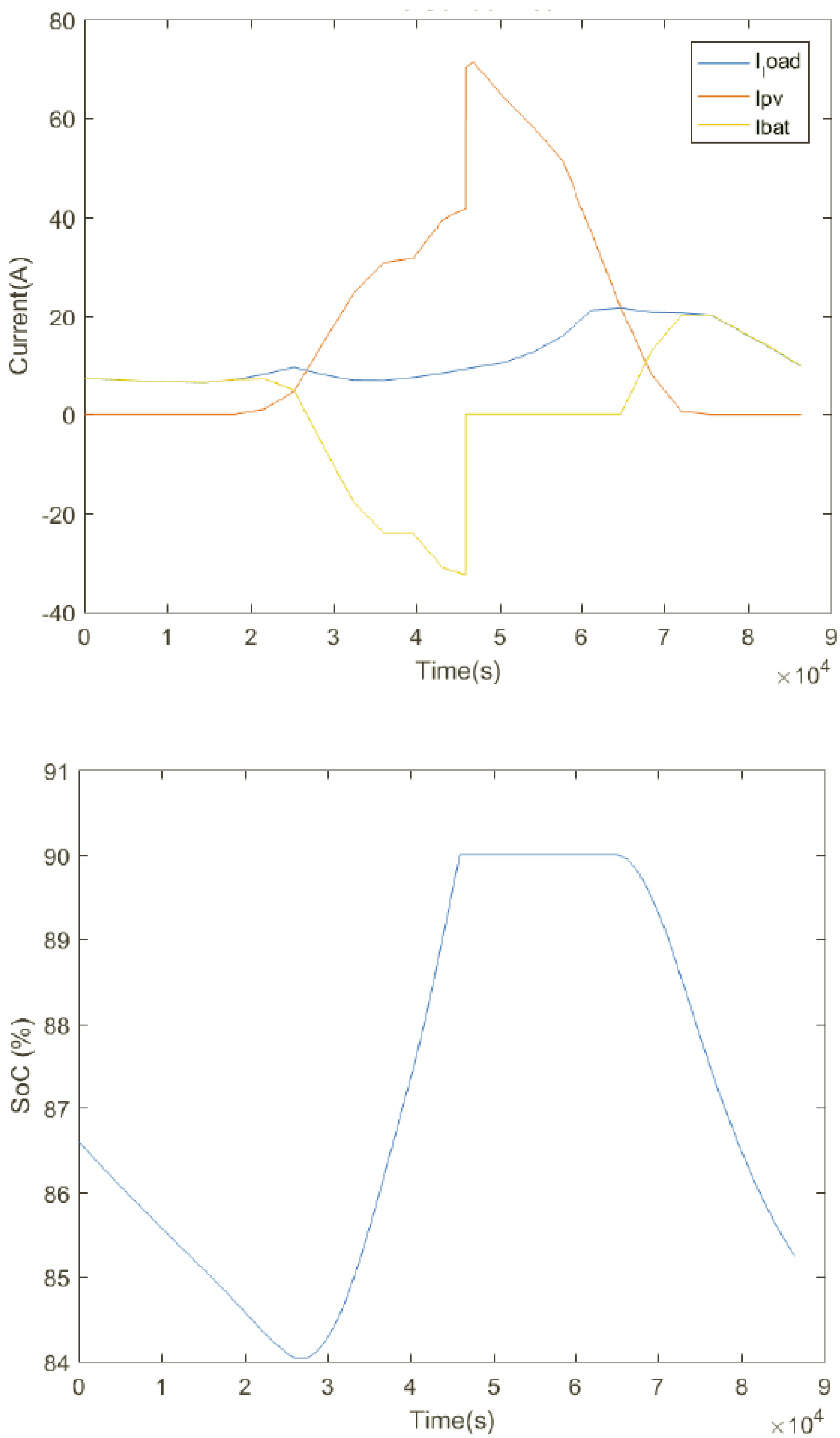

Figure 115-Current and SOC results for Tucson in May 30

12 References

[1] D. Mills, "technology, Advances in solar thermal electricity," *Science Direct ,* p. 19–31, 2004.

[2] *. C. L. b. Z. L. a. L. L. a. H. Y. a. Wei Zhou a, "Current status of research on optimum sizing of stand-alone hybrid," *Applied Energy,* p. 380–389, 2010.

[3] G. Y. Z. J. Islam MR, "11-kV series-connected H-bridge multilevel converter for direct grid connection of renewable energy systems.," *Int Conf Elec Mach Syst,* pp. 211-219, 2012.

[4] "Eco Watch," 5 Reasons Solar is Beating Fossil Fuels, [Online]. Available: http://ecowatch.com/2013/09/06/5-reasons-solar-beating-fossil-fuels/.

[5] "Solar Industry Data," [Online]. Available: http://www.seia.org/research-resources/solar-industry-data.

[6] E. A. G. Onokerhoraye, "TRANSITIONING TO SUSTAINABLE," Centre for Population and Environmental Development (CPED), Benin City, Nigeria, 2014.

[7] S. M. I. Jeyraj Selvaraj and Nasrudin A. Rahim, "Multilevel Inverter For Grid-Connected PV System," *IEEE TRANSACTIONS ON INDUSTRIAL ELECTRONICS,* vol. 56, pp. 149-158, 2009.

[8] J. Dunlop, Photovoltaic Systems, Orland Park : American Technical Publisher , 2010.

[9] T. S. W. Ivan Penn, "Solar energy positioned to boom in Florida," [Online]. Available: http://www.tampabay.com/news/business/energy/solar-energy-positioned-to-boom-in-florida/2136868.

[10] P. Gilman, "Weather Data," 4 April 2014. [Online]. Available: https://sam.nrel.gov/weather.

[11] "Open EI," [Online]. Available: http://en.openei.org/datasets/files/961/pub/.

[12] "Photovoltaic (Solar Electric)," [Online]. Available: http://www.seia.org/policy/solar-technology/photovoltaic-solar-electric.

[13] "What's inside a solar panel?," 12 April 2012. [Online]. Available: http://solarphotovoltaic.blogspot.com/.

[14] A. A. M. U. YAGMUR KIRCICEK, "Modeling and Analysis of a Battery Energy Storage System," in *7th International Ege Energy Symposium & Exhibition*, Usak , 2014.

[15] R. G. A. Savita Nema, "Matlab / simulink based study of photovoltaic," *ENERGY AND ENVIRONMENT,* pp. 487-500, 2010.

[16] F. Z. L. M. T. O. A. Amatoul, "Design Control of DC/AC Converter for a Grid Connected PV Systems with Maximum Power Tracking Using

MATLAB/SIMULINK,," in *International Conference on Multimedia Computing and Systems*, Ouarzazate, 2011.

[17] K. S. W. R. W. D. M. A. A. A. Z. TJUKUP MARNOTO, "Mathematical Model for Determining the Performance Characteristics of Multi-Crystalline Photovoltaic Modules," in *Int. Conf. on Mathematical and Computational Methods in Science and Engineering,*, Trinidad and Tobago, 2007.

[18] S. Z. S. Kashif Ishaque, "A comprehensive MATLAB Simulink PV system simulator with partial shading capability based on two- diode model," *Solar Energy,* pp. 2217-2227, 2011.

[19] S. S. Z. Ishaque K., "A comprehensive MATLAB Simulink PV system simulator with partial shading capability based on two- diode model," *Sol. Energy 85,* p. 2217–2227, 2011.

[20] R. A. Cullen, "What is Maximum Power Point Tracking (MPPT) and How Does it Work?," [Online]. Available: http://www.blueskyenergyinc.com/uploads/pdf/BSE_What_is_MPPT.pdf.

[21] "Leonics," [Online]. Available: http://www.leonics.com/support/article2_14j/articles2_14j_en.php.

[22] M. a. M. R. G. A. Chen, "Accurate electrical battery model capable of predicting runtime and I-V performance," *IEEE Transaction on Energy Conversion,* vol. 21, pp. 504-511, 2006.

[23] F. S.M.A., "Model of Grid Connected Photovoltaic System Using MATLAB/SIMULINK," *Journal of Electrical Engineering.*

[24] H. S. M. B. A. S. Kolsi1*, "Design Analysis of DC-DC Converters Connected to a Photovoltaic Generator and Controlled by MPPT for Optimal Energy Transfer throughout a Clear Day," *Journal of Power and Energy Engineering,* pp. 27-34, 2014.

[25] A. R. S. Dhananjay Choudhary1, "DC-DC Buck Converter for MPPT of PV system," *International Journal of Emerging Technology and Advanced Engineering,* vol. 4, pp. 813-821, 2014.

[26] P. a. V. K. Garg[2], "To Perform Matlab Simulation of Battery Charging Using Solar Power With Maximum Power Point Tracking(MPPT)," *International Journal of Electronic and Electrical Engineering,* vol. 7, pp. 511-516, 2014.

[27] z. a. J. R. A. Yuriy V. Mikhaylik*, "Polysulfide Shuttle Study in the Li/S Battery System," *J. Electrochem. Soc,* pp. A1969-A1976, 2004.

[28] A. J. A. K. P. N. R. N. I. Yao L.W., "Modeling of Lithium-Ion Battery Using MATLAB/Simulink," *IEEE,* pp. 4799-0224, 2013.

[29] W.-Y. Chang, "The State of Charge Estimating Methods for Battery: A Review," *ISRN Applied Mathematics,* vol. 2013, p. 7, 2013.

[30] C. K. L. C. Z. a. W. G. H. M. Coleman, "State-of-charge determination from EMF voltage estimation: using impedance, terminal voltage, and current for lead-acid and lithium-ion batteries," *IEEE Transactions on Industrial Electronics,* vol. 54, p. 2550–2557, 2007.

[31] "LITHIUM ION TECHNICAL DATA," [Online]. Available: http://www.ibt-power.com/Battery_packs/Li_Ion/Lithium_ion_tech.html.

[32] M. Zeman, "Photovoltaic System," in *SOLAR CELLS*, 2010, p. 91.

[33] "Autonomy and battery sizing," [Online]. Available: http://files.pvsyst.com/help/dimensisole_autonomy.htm.

[34] "Battery Sizing," [Online]. Available: http://www.sunxtender.com/battery_sizing.php.

[35] "Lithium-ion battery," [Online]. Available: https://en.wikipedia.org/wiki/Lithium-ion_battery.

[36] "Where to find Solar Resource Data to Use with SAM," [Online]. Available: https://sam.nrel.gov/weather.

[37] R.-Y. D. Rong-Jong Wai, "High-Efficiency Power Conversion for Low Power," *IEEE TRANSACTIONS ON POWER ELECTRONICS,* vol. 20, pp. 847-856, 2005.

[38] M. a. R.-M. G. A. Chen, "Accurate electrical battery model capable of predicting runtime and I-V performance," *IEEE Transaction on Energy Conversion,* vol. 21, pp. 504-511, 2006.

[39] "Basics about PV off-grid systems," [Online]. Available: http://pvshop.eu/offgrid.

[40] C. C. 1. B. X. 1. W. S. 2. Z. X. 2. a. W. Z. 2. Yong Tian 1, "An Adaptive Gain Nonlinear Observer for State of Charge Estimation of Lithium-Ion Batteries in Electric Vehicles," *Energies,* pp. 5995-6012, 2014.